Gordon Andrews (designer)
Gazelle chair (c. 1950) designed, 1957 manufactured
plywood, aluminium, wool
74.0 x 48.0 x 55.0 cm
Museum of Applied Arts and Sciences, Sydney
Purchased, 1989 (89/499)

Genome Visualization with Circos

INTRODUCTION TO CIRCOS +

VISUALIZATION GUIDELINES

MARTIN KRZYWINSKI
Genome Sciences Center
BC Cancer Agency
Vancouver, Canada

EMBO PRACTICAL COURSE:
BIOINFORMATICS GENOME ANALYSES
Centre for Research & Technology - Hellas, Thessalonica, Greece
June 5–17, 2017

COURSE RESOURCES

We have 4 sessions today. All material is available at

`/BGA2017/Course_material/June08`

including

—slides
—handouts (detailed explanation of the session)
—all session configuration and data files
—visualization articles (*pov.collection.pdf*)

Materials are also at

http://www.circos.ca/documentation/course

COURSE OUTLINE

theory

what is circos?
how does it work?
how and why would you use it?
are there any useful general rules for data visualization? (yes)

practical sessions

drawing data on one genome
comparing genomes
visualizing yeast genome analysis from yesterday

Circos is a tool

to solve problems—

it is not itself a solution

PERFECTLY USEFUL

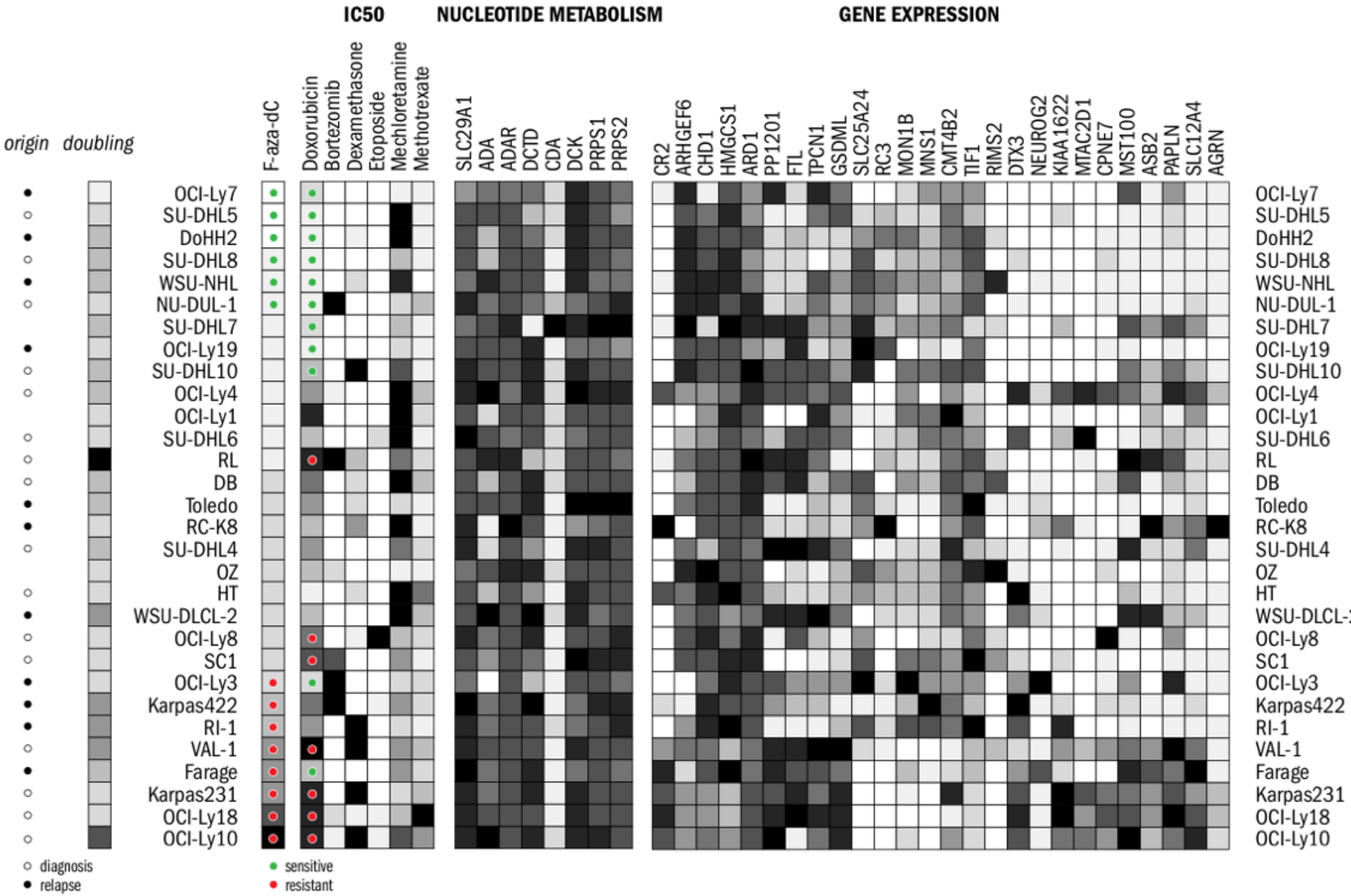

.

PERFECTLY OPAQUE

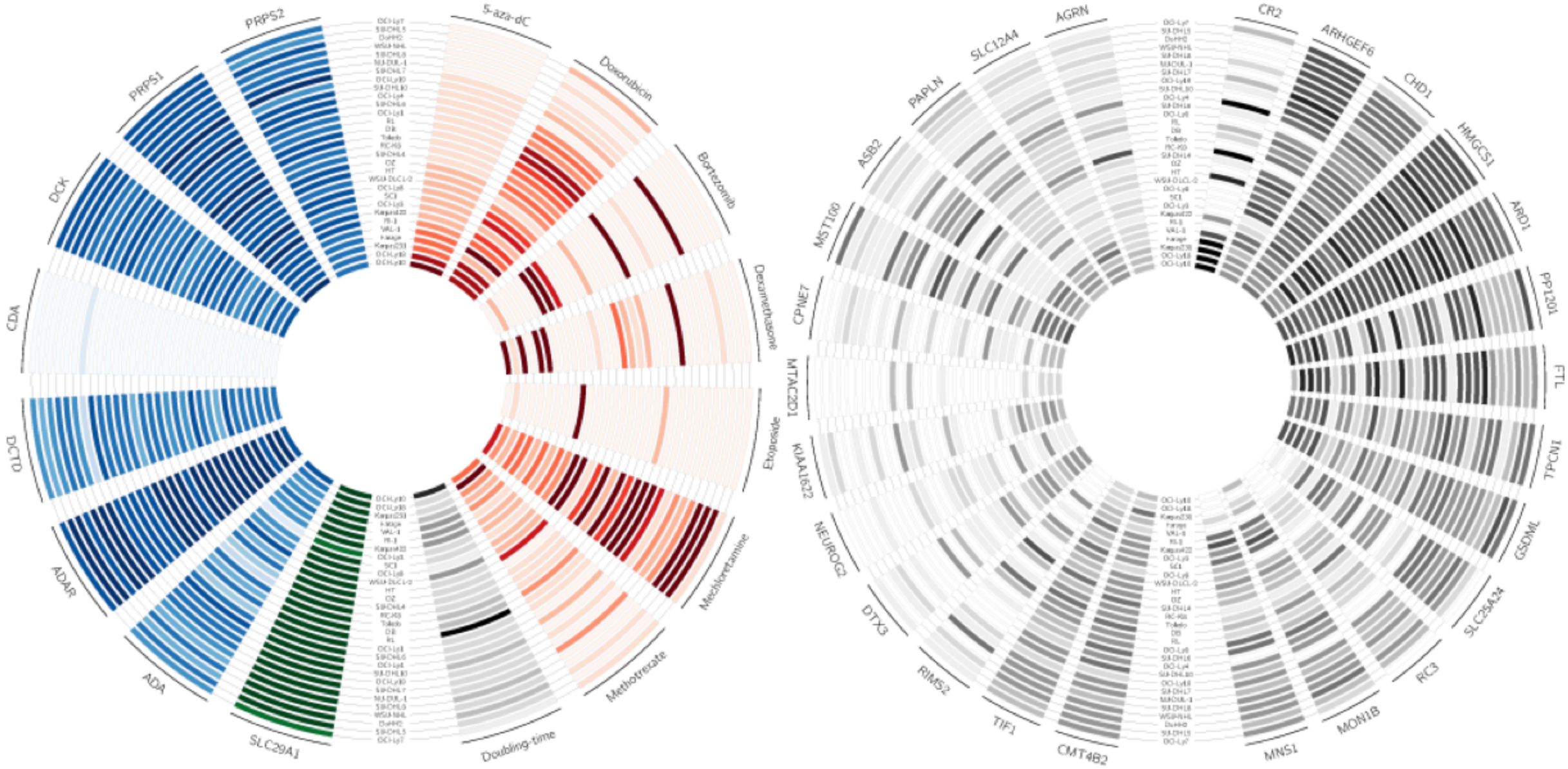

.

I want to use Circos...

I want to use a hammer...

I want to use Circos to demonstrate the differences in patterns of conservation across genome X.

(there are patterns to show)

I want to use a hammer to put a nail in the wall so that I can hang a picture.

(you have a picture to hang)

purpose of Circos

AVOID LINEAR LAYOUT COMPARISONS

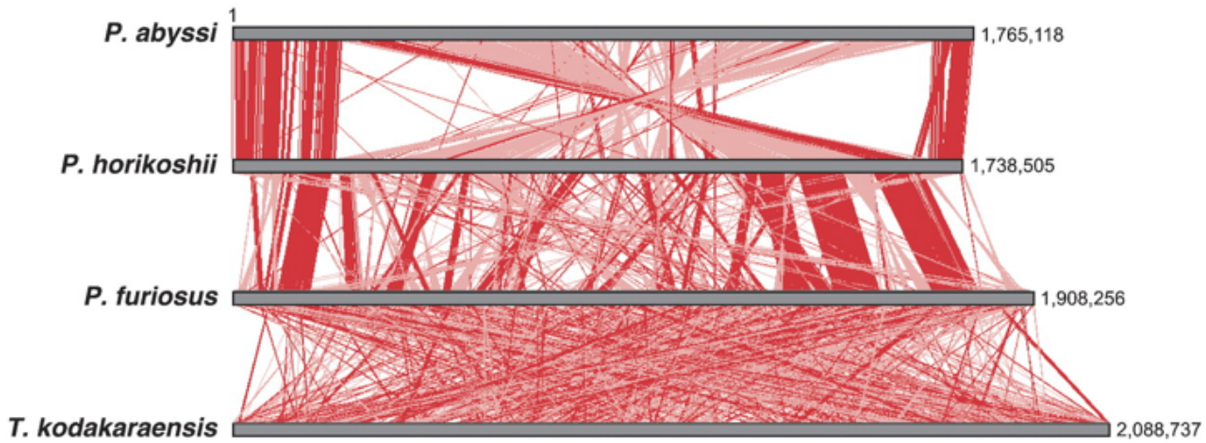

Thomson, N.R., et al., Comparative genome analysis of Salmonella Enteritidis PT4 and Salmonella Gallinarum 287/91 provides insights into evolutionary and host adaptation pathways. Genome Res, 2008. 18(10): p. 1624-37.

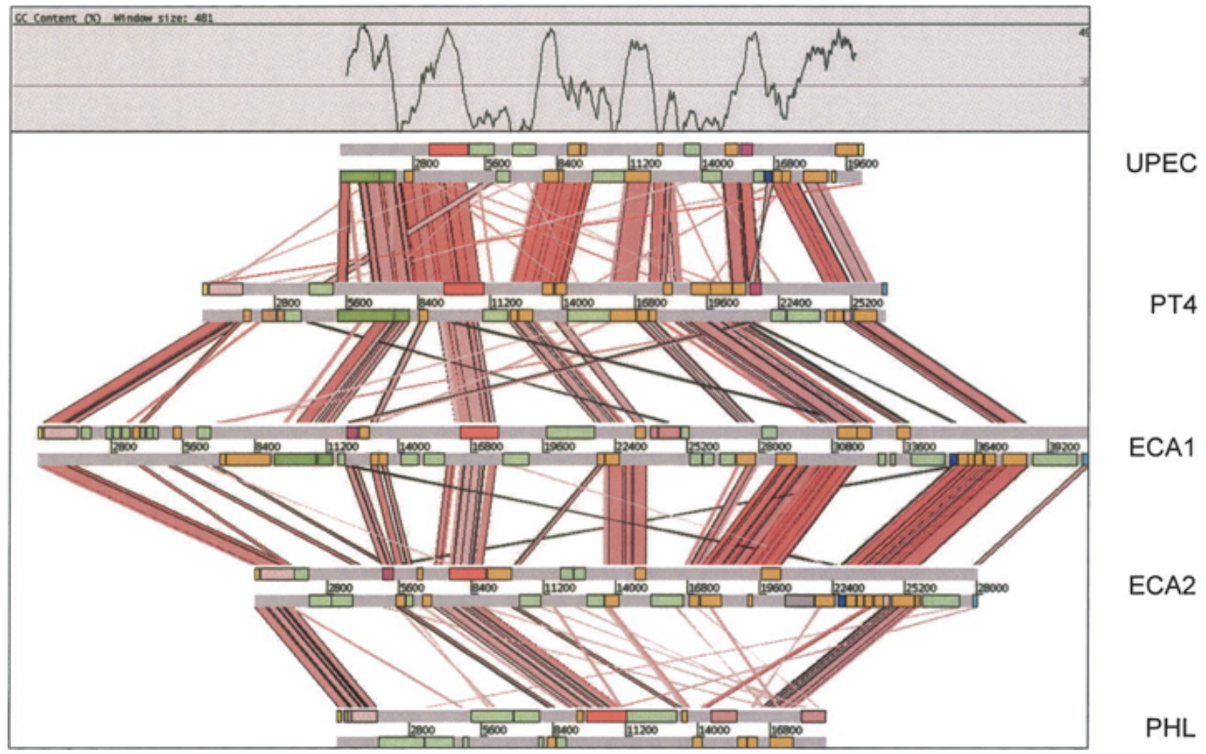

Thomson, N.R., et al., Comparative genome analysis of Salmonella Enteritidis PT4 and Salmonella Gallinarum 287/91 provides insights into evolutionary and host adaptation pathways. Genome Res, 2008. 18(10): p. 1624-37.

AVOID LINEAR LAYOUT COMPARISONS

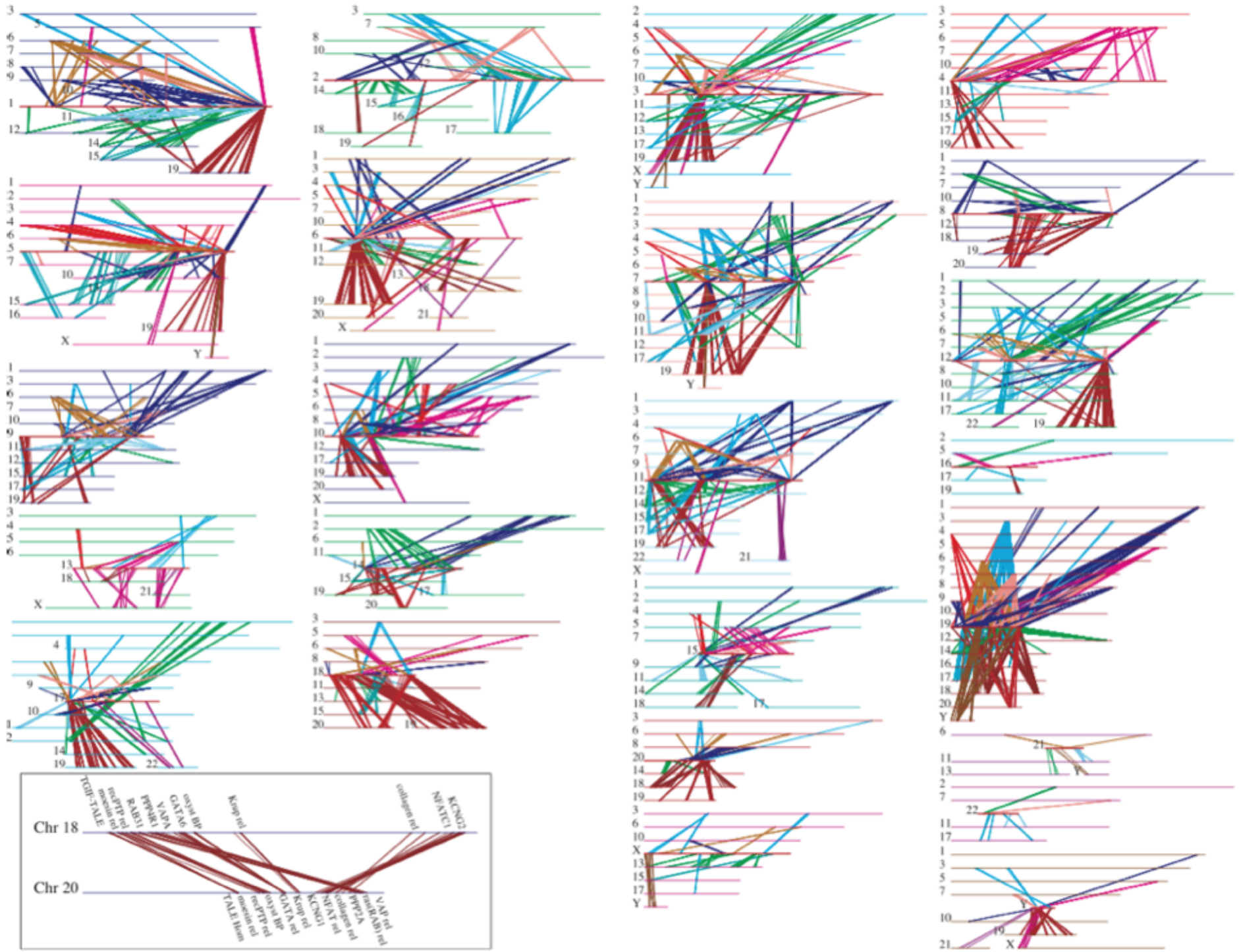

J. C. Venter, M. D. Adams, E. W. Myers et al., Science 291 (5507), 1304 (2001).

ENCODING SPATIAL RELATIONSHIPS

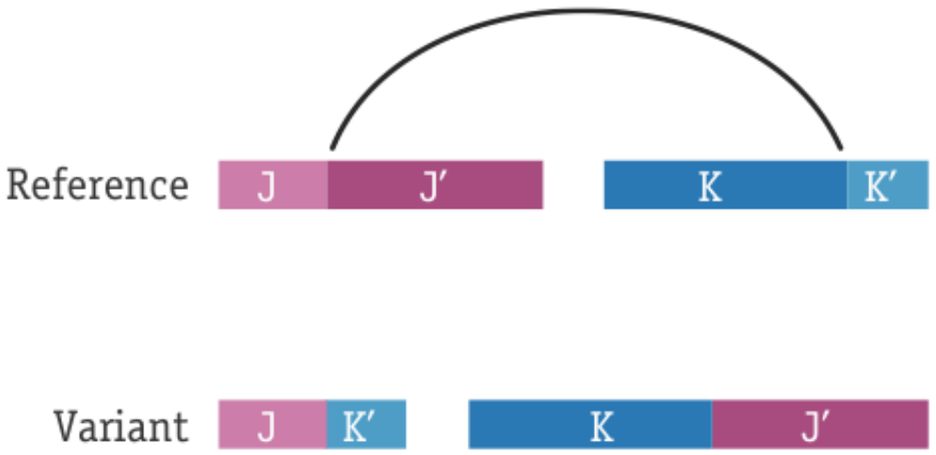

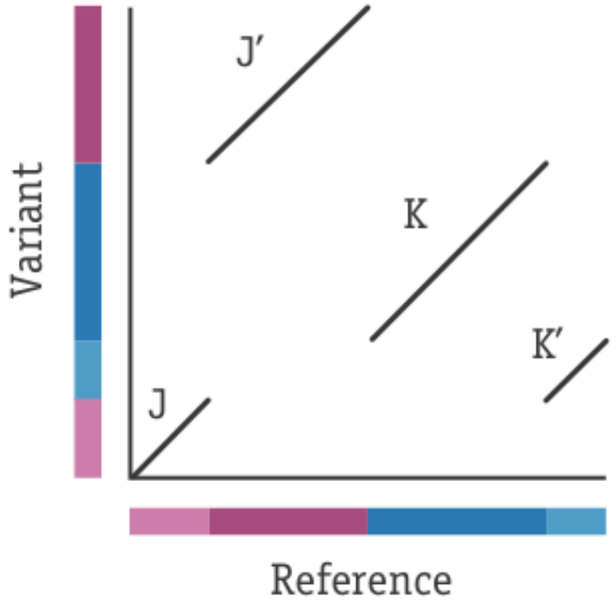

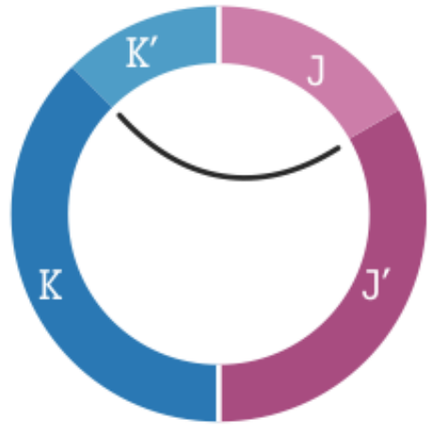

Nielsen C, Wong B (2012) Representing genomic structural variation. Nat Methods 9:631.

circos appearances

LITERATURE AND MEDIA

CIRCOS IN THE LITERATURE

Bioinformatics · Genome Biology · nature · Science · Nucleic Acids Research · American Scientist · Genome Research · Conde Nast Portfolio · WIRED · PNAS · PLoS Public Library of Science · The Plant Cell · The New York Times · Leukemia · SEED

>100 citations, 5 book covers

PRIMARY LITERATURE

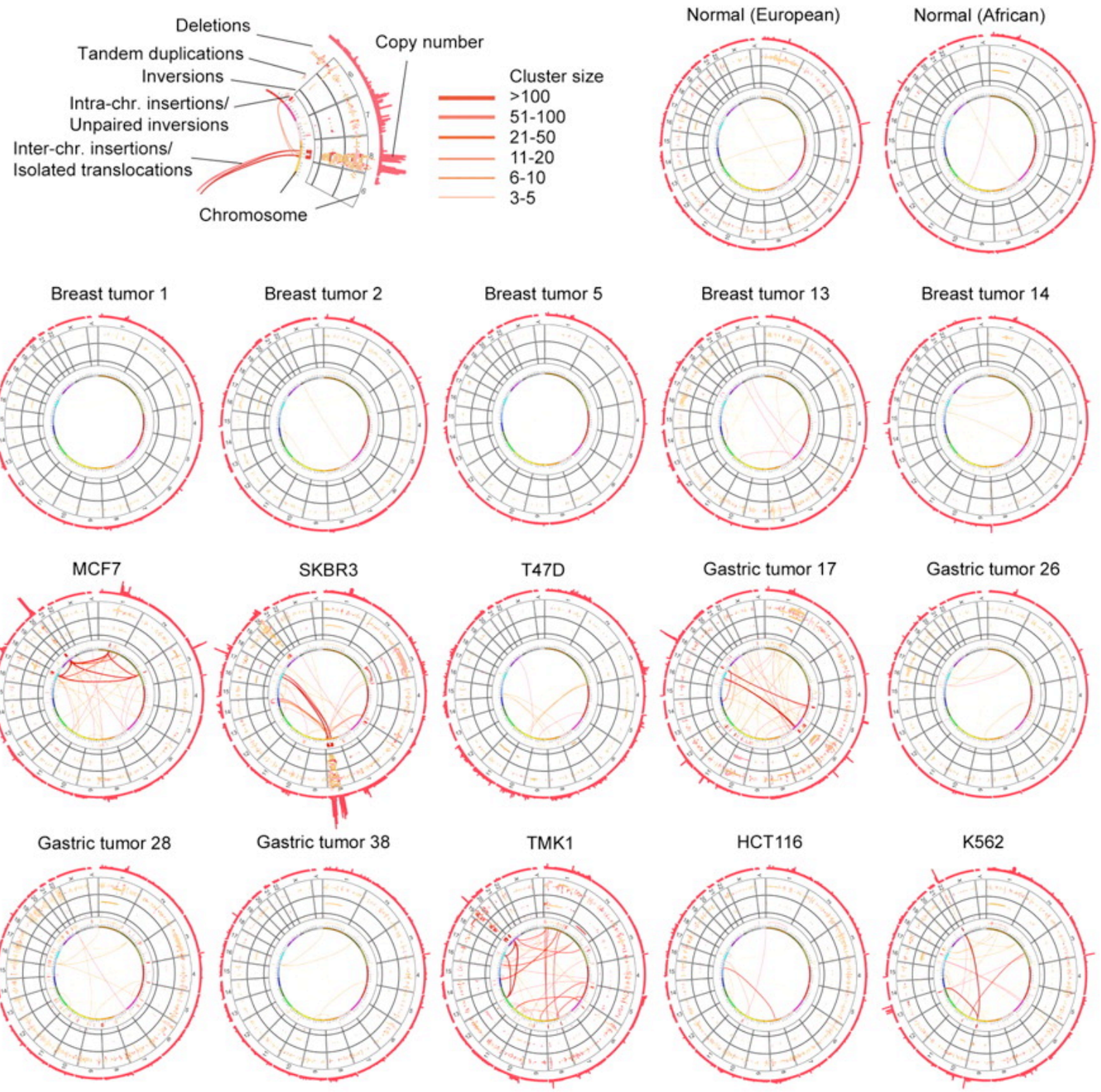

Hillmer AM, Yao F, Inaki K et al. 2011 Comprehensive long-span paired-end-tag mapping reveals characteristic patterns of structural variations in epithelial cancer genomes. Genome research 21:665-675.

NYT

The New York Times

Science

WORLD | U.S. | N.Y. / REGION | BUSINESS | TECHNOLOGY | SCIENCE | HEALTH | SPORTS | OPINION

ENVIRONMENT | SPACE & COSMOS

SIDE EFFECTS

‘Ome,’ the Sound of the Scientific Universe Expanding

Martin Krzywinski/Michael Smith Genome Sciences Center

Visualizations, in progressively greater detail, that show duplications within the human genome.

By JAMES GORMAN
Published: May 3, 2012

The age of “omes” is here. It began with the genome, continued with the proteome, branched out with the memome and reached full flowering with the notion of the omome.

This probably sounds like raw material for nonsense poetry, but it’s a real biological and linguistic trend that makes sense, once you get the idea of just what an “ome” is.

FACEBOOK
TWITTER
GOOGLE+
EMAIL
SHARE
PRINT
REPRINTS

Related

More Side Effects Columns

Connect With Us on Social

The New York Times

Health

WORLD | U.S. | N.Y. / REGION | BUSINESS | TECHNOLOGY | SCIENCE | HEAL

Search Health

Go

Genetic Gamble

New Approaches to Fighting Cancer

PART ONE
A Race to Leu
Source

A New Treatment’s Tantalizing Promise B
Heartbreaking Ups and Downs

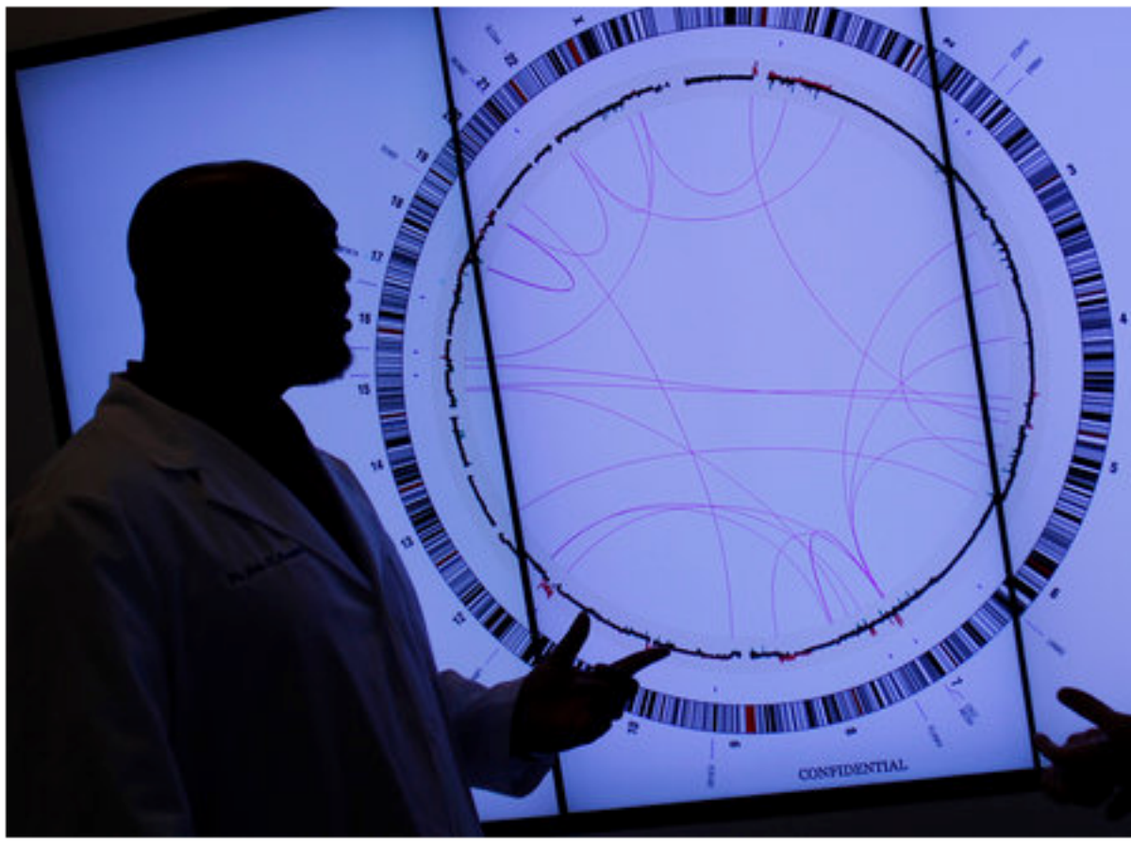

Dr. John Carpten, left, and Dr. David Craig with a cancer genome display. New strategies att

POPULAR SCIENCE

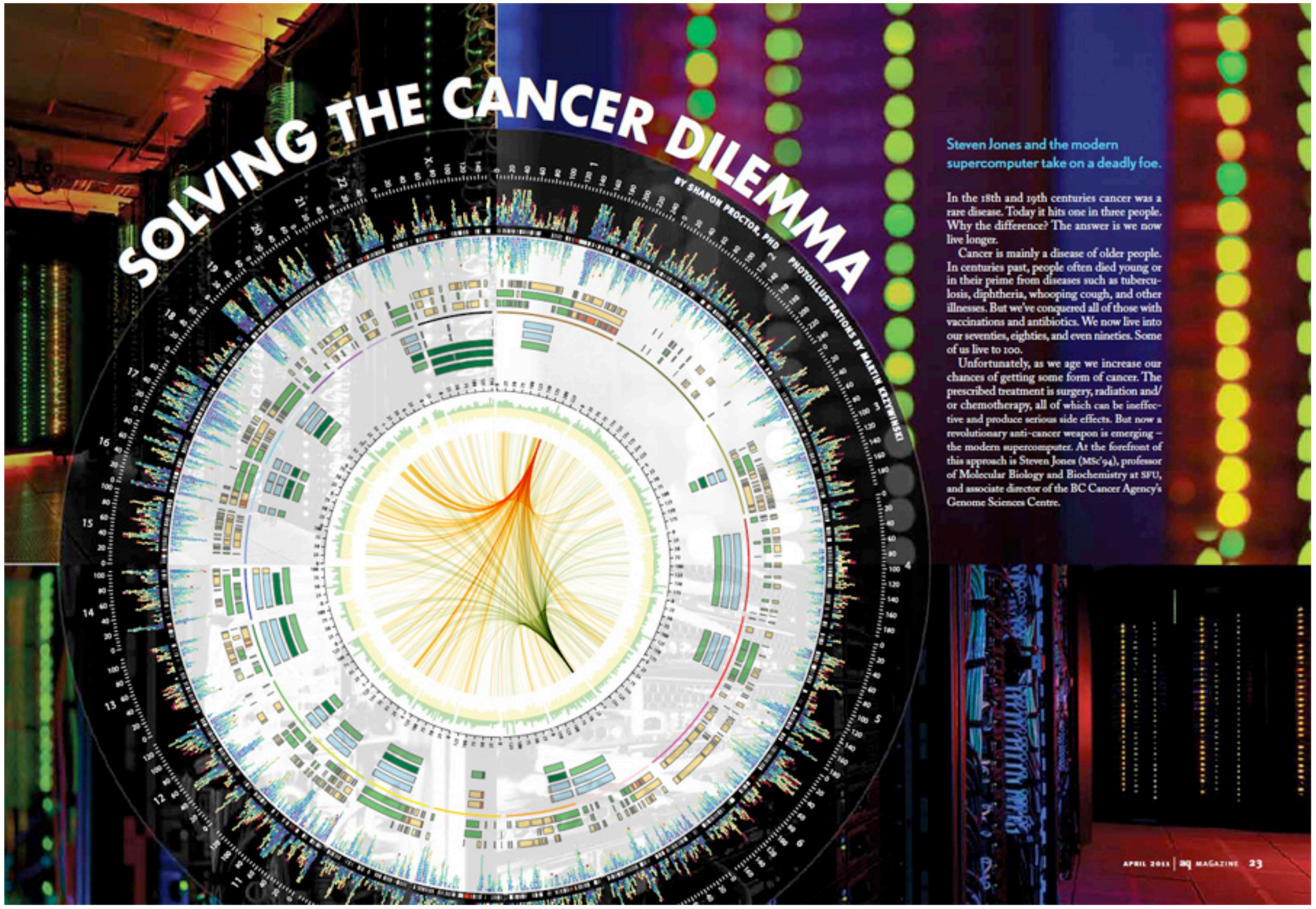

AQ Magazine, April 2011 (Simon Fraser University)

POPULAR CULTURE

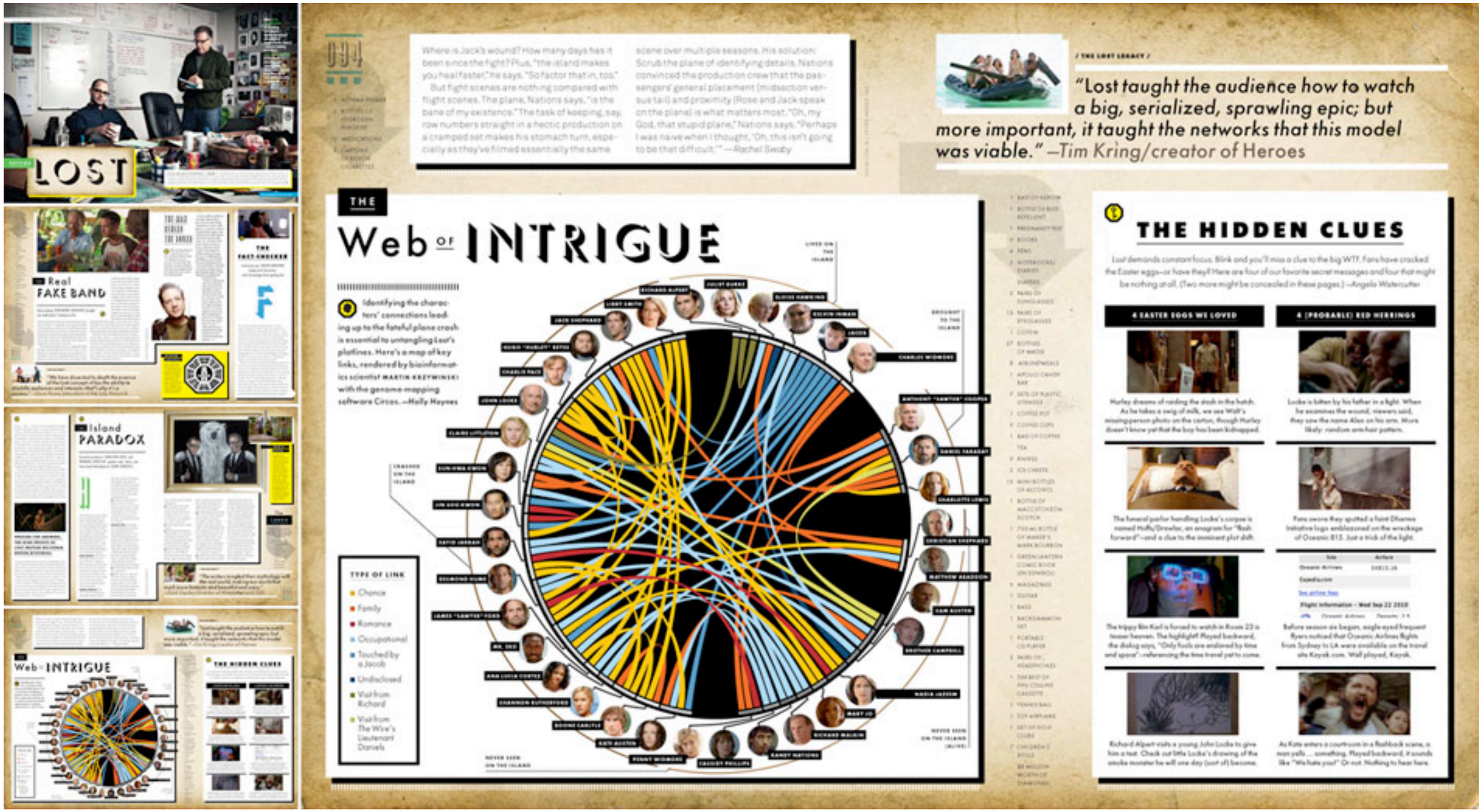

Wired, April 2010

URBAN PLANNING

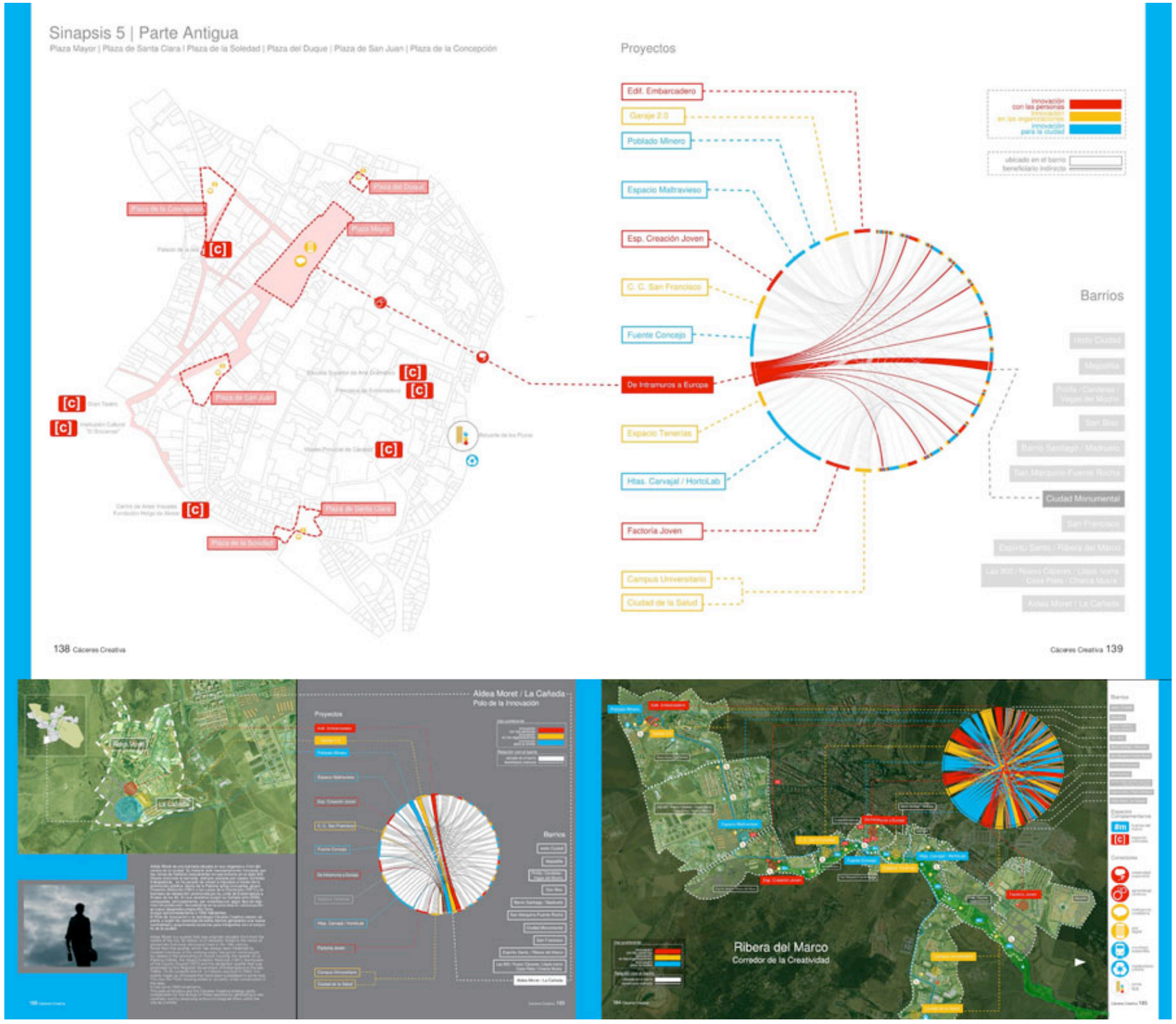

The town of Caceres, Spain, a UNESCO World Heritage Site, used Circos to illustrate the relationships between businesses in their urban planning strategy.

ADVERTISING

.

ACTUAL ART YOU CAN TOUCH

Julie Sperling Mosaics
http://sperlingmosaics.com/

ART EXHIBITS

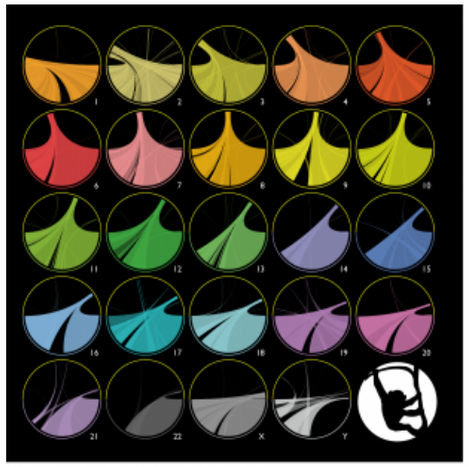

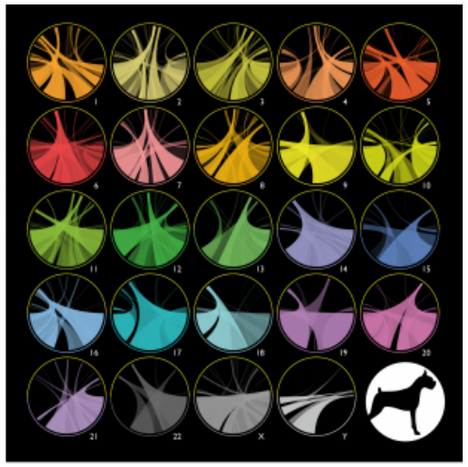

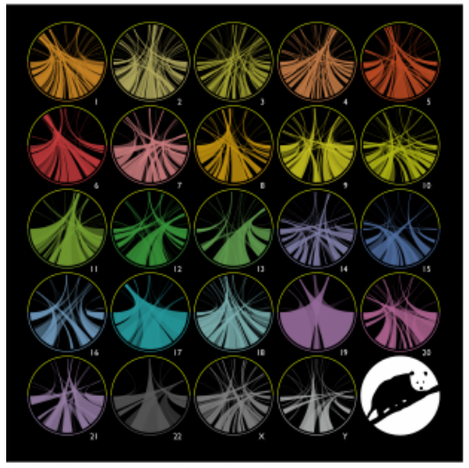

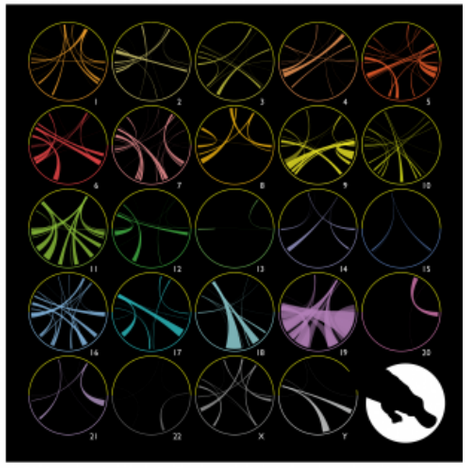

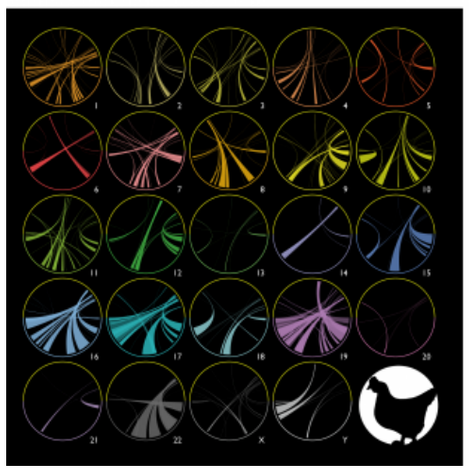

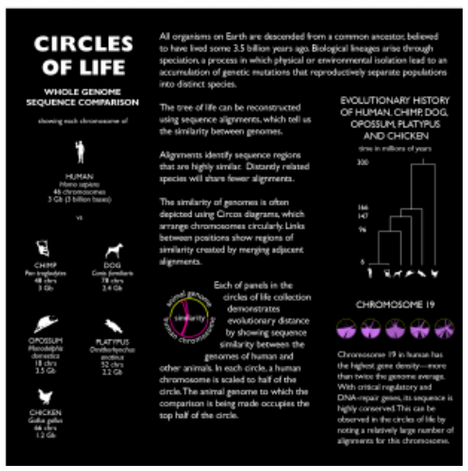

Beautiful Science, British Library
http://www.bl.uk/whatson/exhibitions/beautiful-science/

WWW.CIRCOS.CA

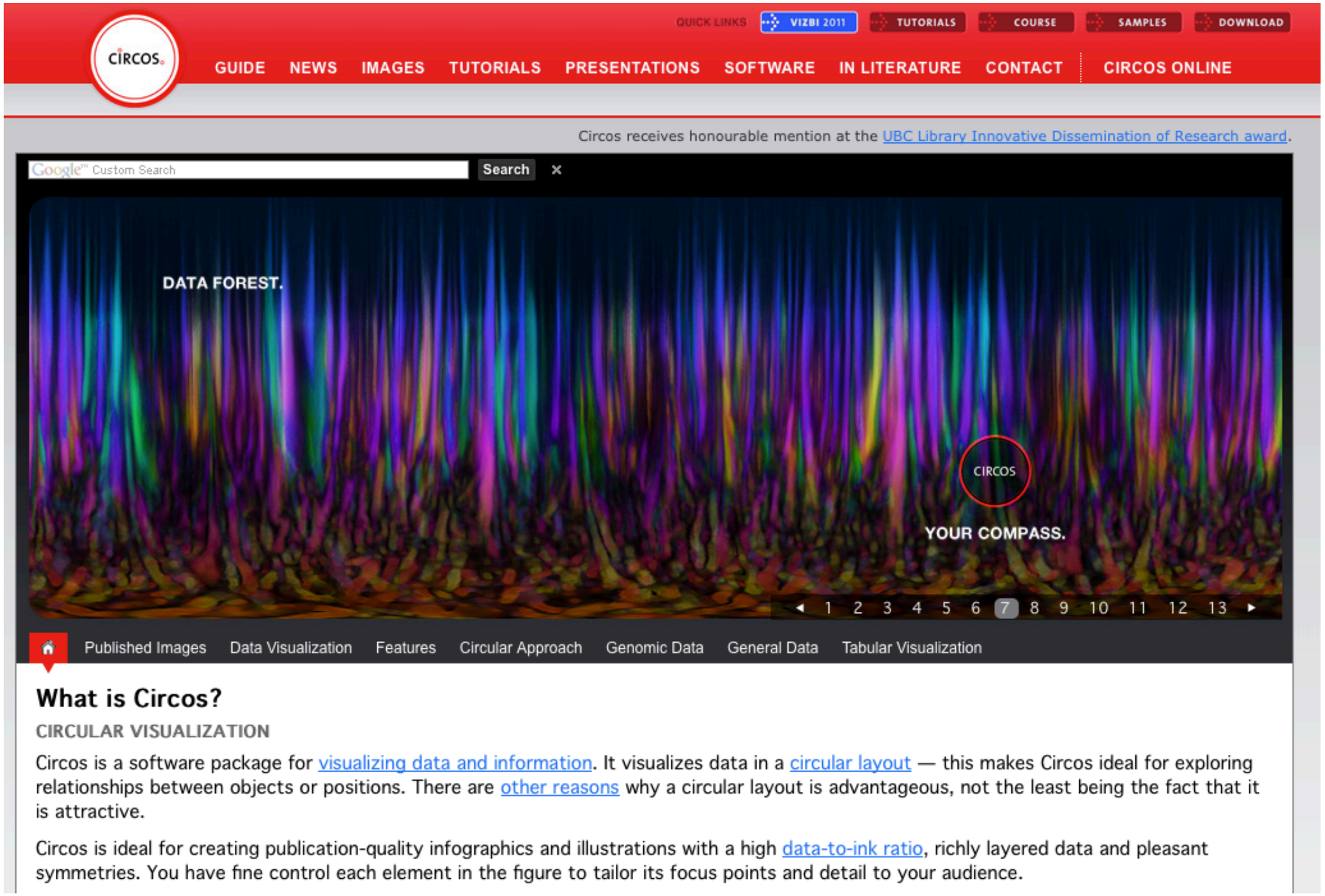

.

what makes circos useful?

CIRCULAR LAYOUT + FLEXIBLE IMPLEMENTATION

WHY IS CIRCOS USEFUL?

TIMELY + EFFECTIVE

Circos addresses the need to visualize differences in disease genomes and assess variation in genomic content across many samples.

Dynamic rules provide a way to adjust the format of figure elements based on data values.

SVG output is designed for publication-quality visualizations.

Perceptual color palettes and high quality fonts are built in.

COMPATIBLE

Driven entirely by plain-text configuration files.

Data agnostic.

Simple format for data input.

Highly automatable.

Fits naturally into any data pipeline.

Extended longevity: performs only visualization, not analysis.

SIMPLE + DEEP

Large number of data tracks, which can be stacked and layered.

Format of everything in the figure can be dynamically adjusted based on rules that react to data values.

Utility tools assist with manipulating data files (e.g. binning links and ordering ideograms to optimize layout).

TYPICAL CIRCOS IMAGE

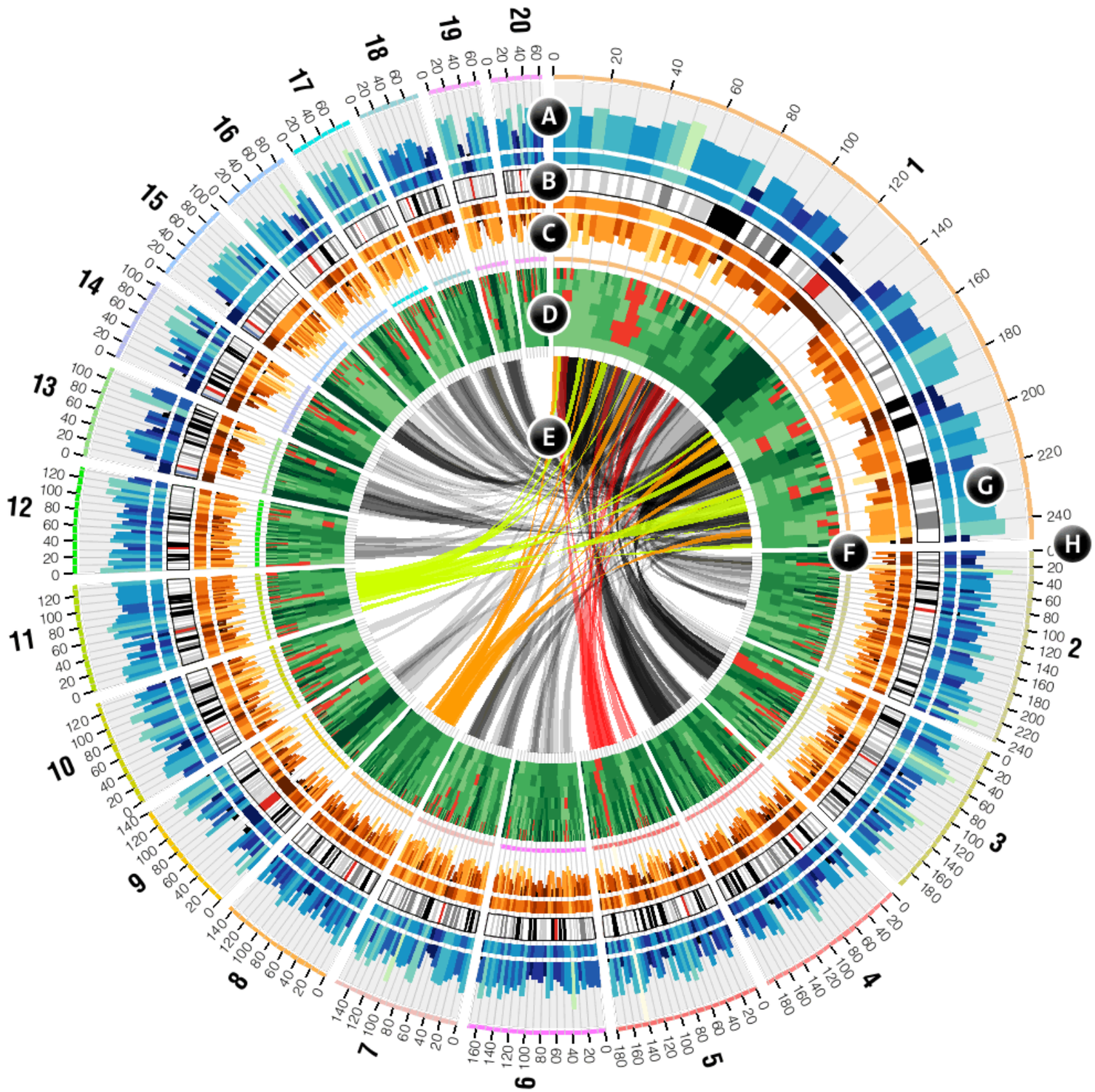

(A) histogram (B) ideograms (C) histogram (D) heat map (E) links (F) highlights (G) grid (H) ticks. Format of data in tracks A, C, D, E is adjusted by rules based on data values.

IMAGE PANELS

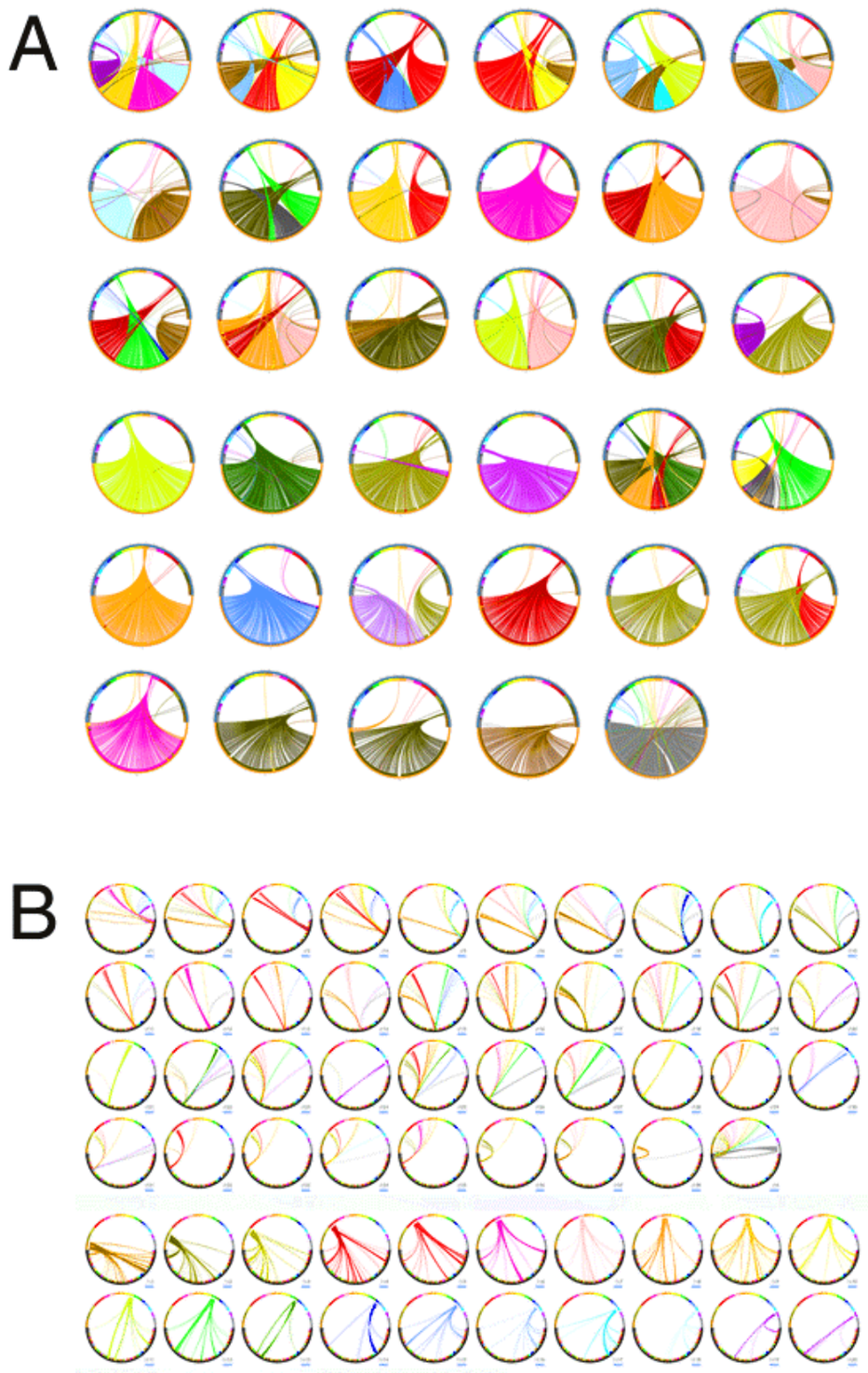

(A) Synteny between dog and human genomes. Each image represents the comparison of a single dog chromosome (bottom half of circle) with the entire human genome. Krzywinski, M. et al. (2009). "Circos: an information aesthetic for comparative genomics." Genome Res 19(9): 1639-1645. (B) Each image contains the entire dog and human genomes (bottom and top half of circle, respectively). Links shown are based on the same data as in (A), but limited to a single chromosome (dog or human) for each image in the panel. http://mkweb.bcgsc.ca/circos/presentations/articles/amsci_cover

drawing ideograms

LINEAR LAYOUT OF CHROMOSOMES

ORDER AND ORIENTATION

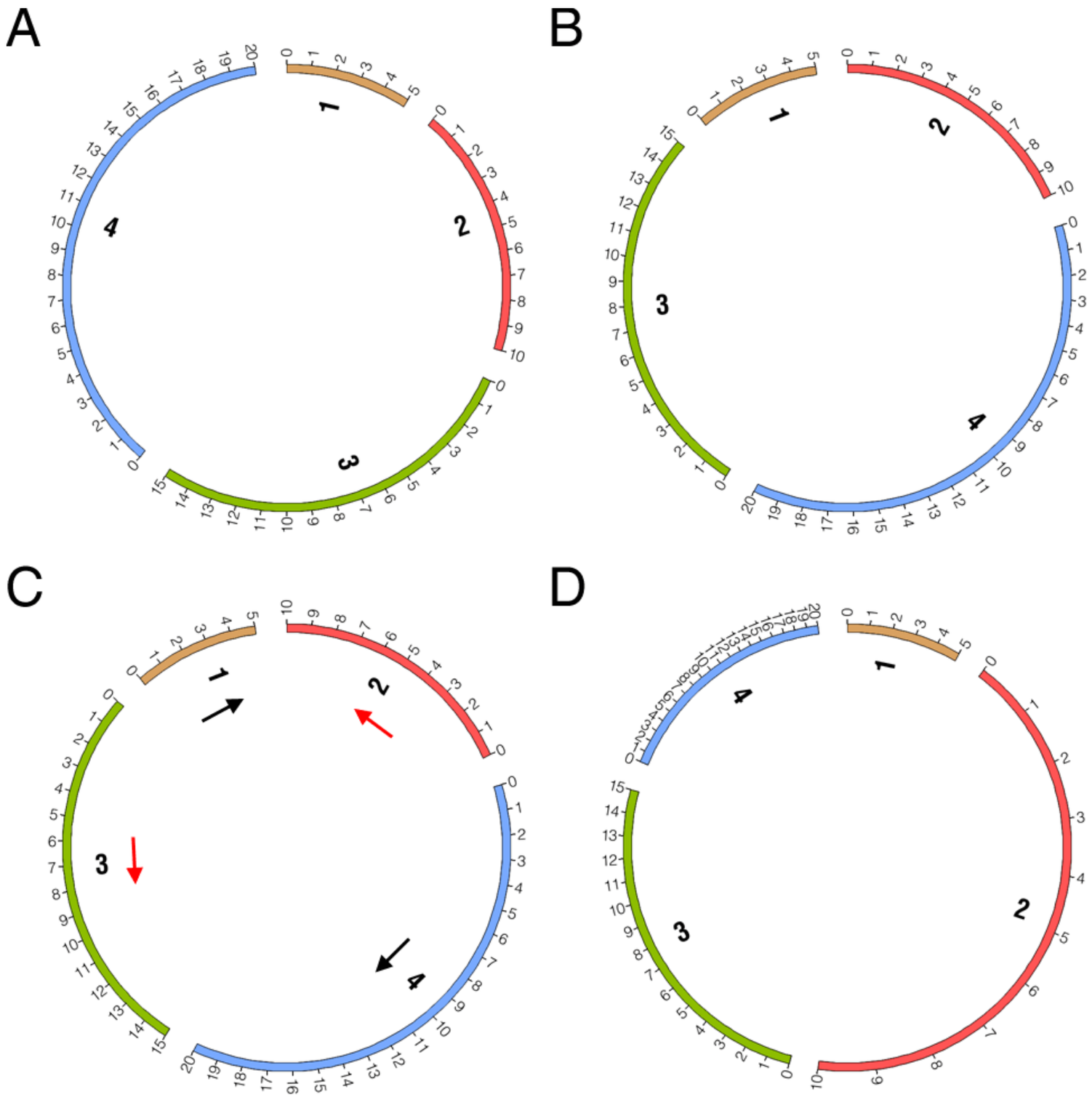

Ideogram order, scale and axis breaks help arrange ideograms to suit the data. (A) four chromosomes 5, 10, 15 and 20Mb in size. (B) ideograms can be reordered. (C) ideogram scale can be reversed. (D) global scale of ideograms can be changed – here, chr2 2.5x and chr4 0.5x

AXIS BREAKS

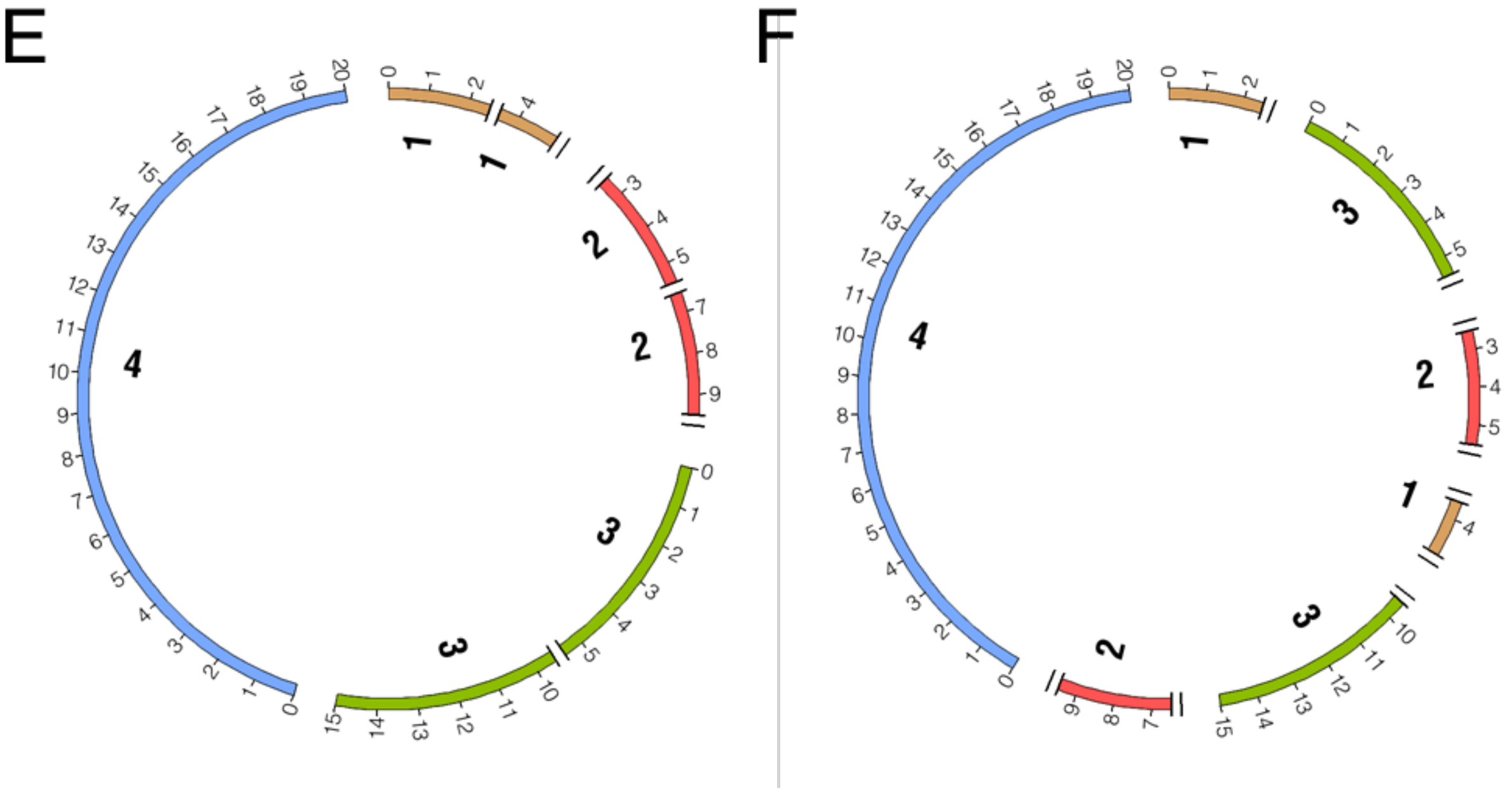

Cropped ideogram regions are treated as individual ideograms. (E) axis breaks are used to remove the following ideogram regions chr1:2.5-3.5Mb, chr1:4.5-5, chr2:0-2.5Mb, chr2:5.5-6.5Mb, chr2:9.5-10Mb, chr3:5.5-9.5Mb. (F) order of ideogram regions can be changed

EXAMPLE FROM LITERATURE

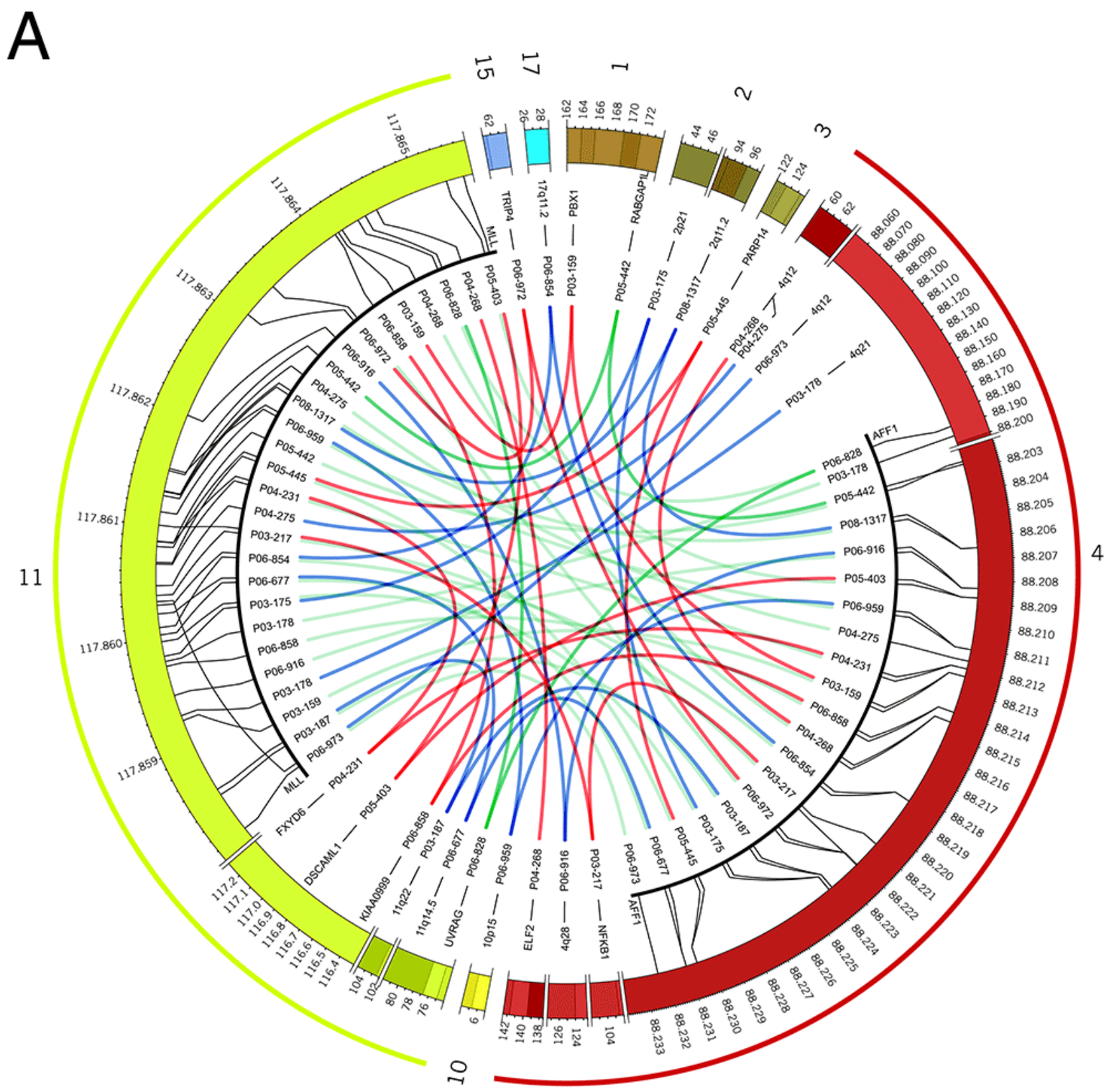

The most frequent complex rearrangements involving MLL and (A) AFF1/AF4. Localization of chromosomal breakpoints and UPN of individual patients are indicated. Colored lines indicate in-frame fusions (green), out-of-frame fusions (red), no partner gene present at the recombination site (blue). Meyer, C., E. Kowarz, et al. (2009). "New insights to the MLL recombinome of acute leukemias." Leukemia 23(8): 1490-1499. Figure by M Krzywinski.

data tracks

PLACEMENT AND FORMATTING

DATA IN CONCENTRIC RINGS

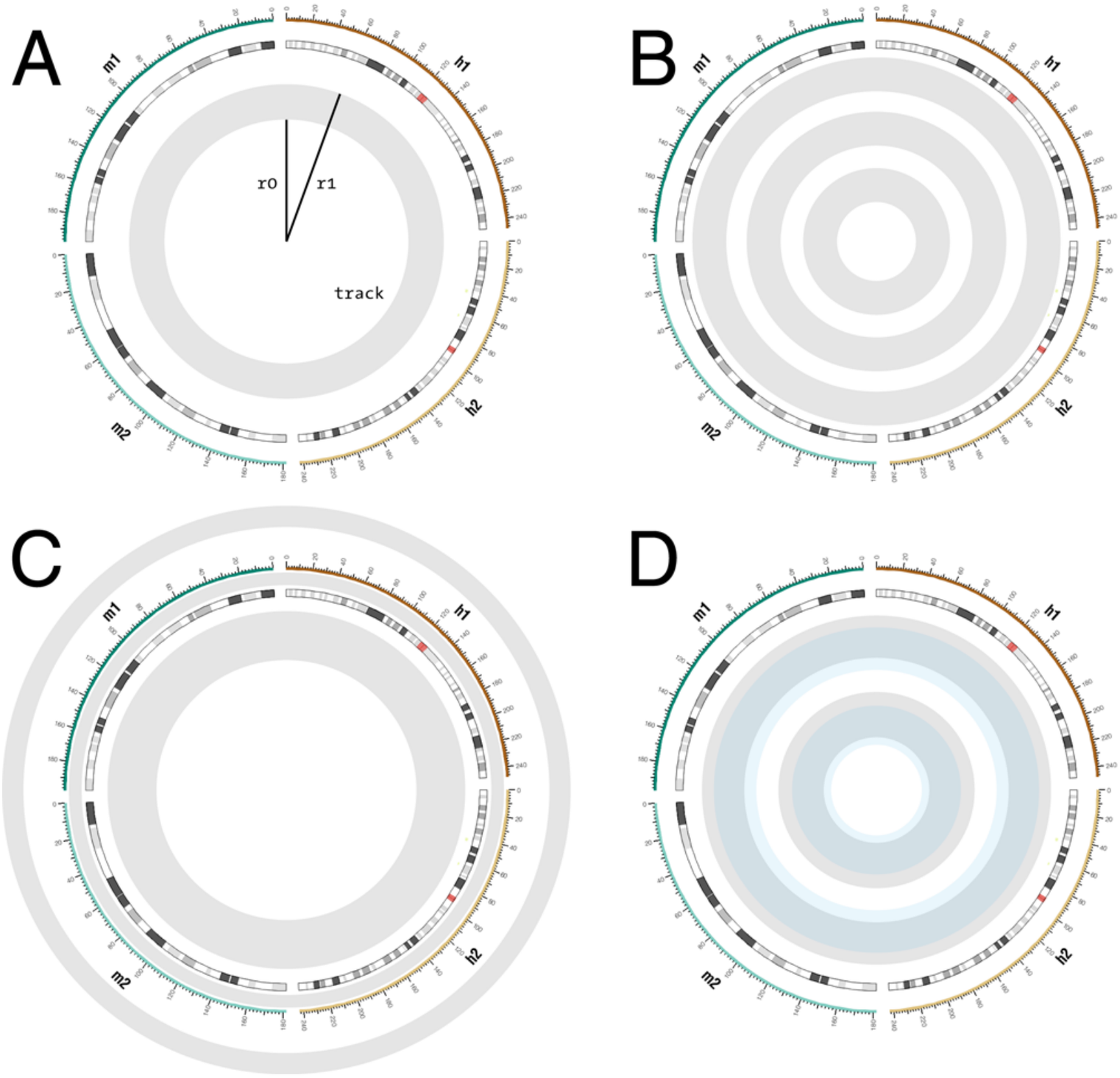

(A) each data track confined to an annulus bounded by radii r0 and r1. (B) any number of tracks can be placed on the figure. (C) tracks can be placed at any radial position, including inside/outside ideogram circle and inside/outside ticks. (D) tracks can be made to overlap and can be drawn in any order.

COMPOUND TRACKS POSSIBLE

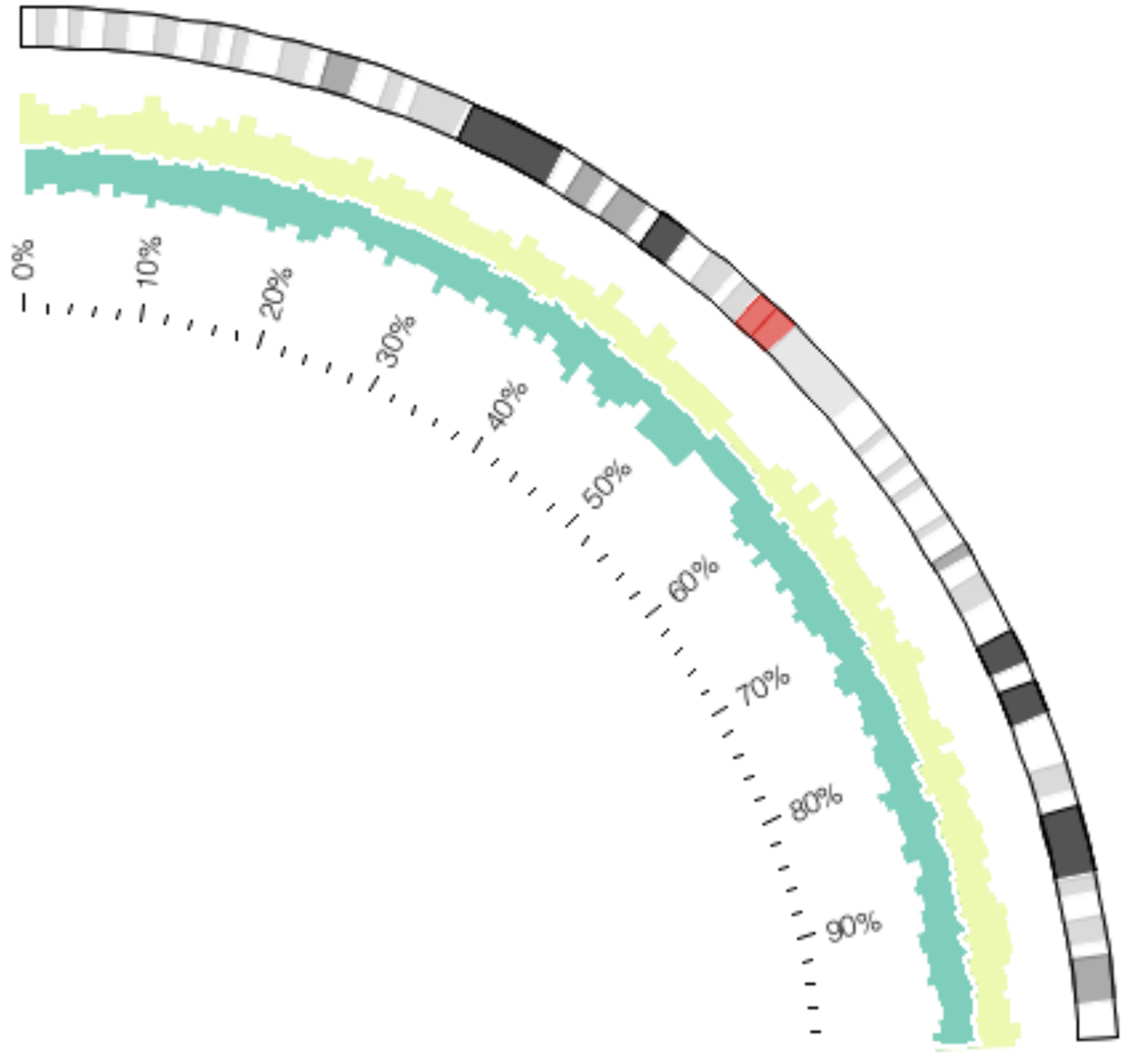

By defining three histogram tracks within the same radial region, and drawing the data in a specific order, a compound track can be created. In this example, three histograms were used.

EXAMPLE FROM LITERATURE

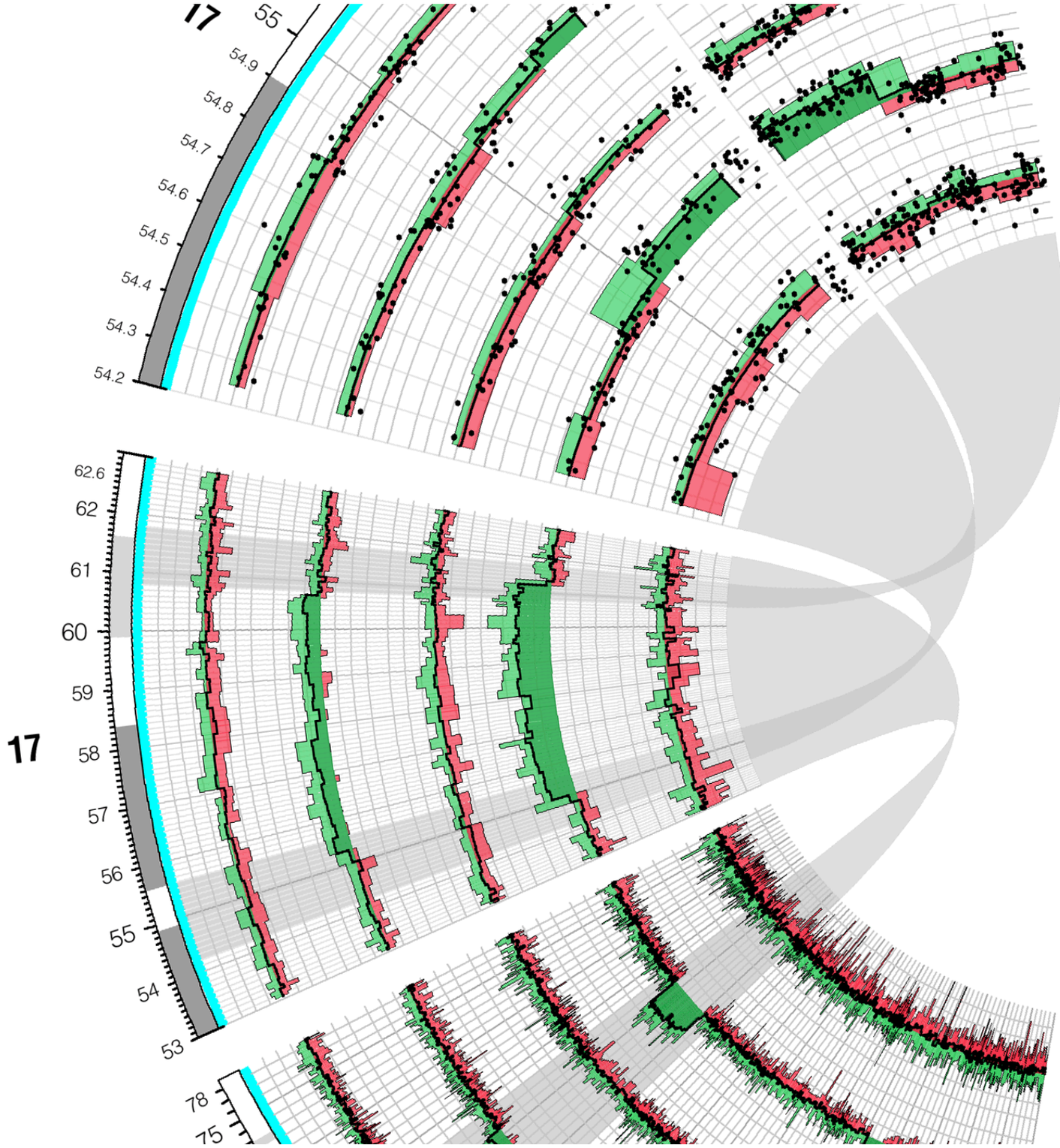

Various types of data tracks can be stacked. Five instances of a compound track each represent copy number information from a different sample. Two histograms, a line plot and a scatter plot are used to form a compound track. Using links and highlights, attention is drawn to the progression of scale increase within chr17:53-63Mb. This region is magnified at 5x and smaller subregions are further magnified to 40x.
Krzywinski, M., J. Schein, et al. (2009). "Circos: an information aesthetic for comparative genomics." Genome Res 19(9): 1639-1645.

EXAMPLE FROM LITERATURE

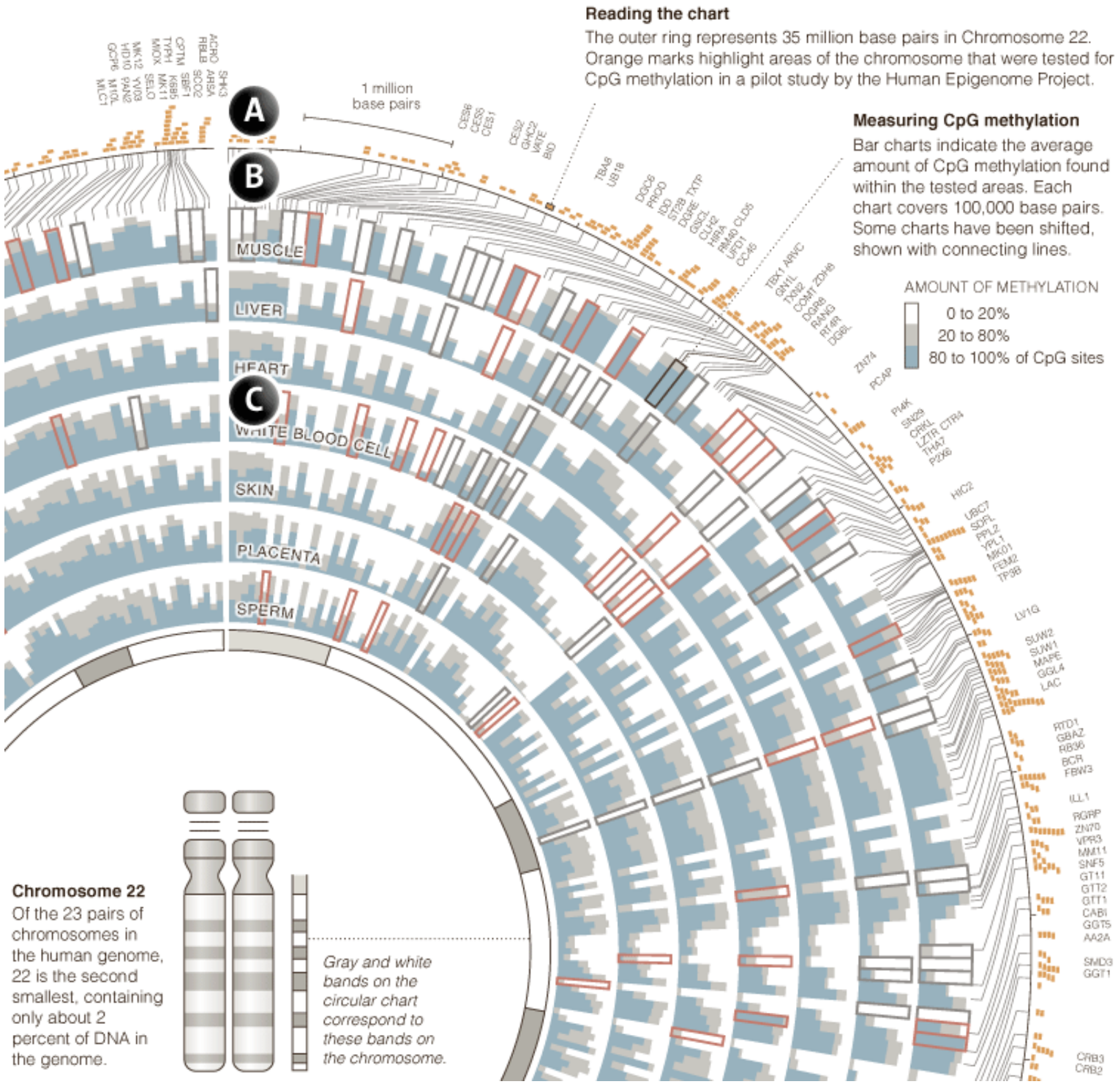

Data sets which do not sample the genome uniformly (A) can be effectively shown by using a connector track (B) to show the remapping onto an index scale (C). Shown in the figure are methylation values (A) for 7 tissues are summarized using stacked histograms (C), whose bins represent statistics for remapped methylation probe positions. Zimmer, C. (2008). Now: The Rest of the Genome. New York Times. Figure by M Krzywinski.

links

DISPLAYING RELATIONSHIPS

LINK GEOMETRY

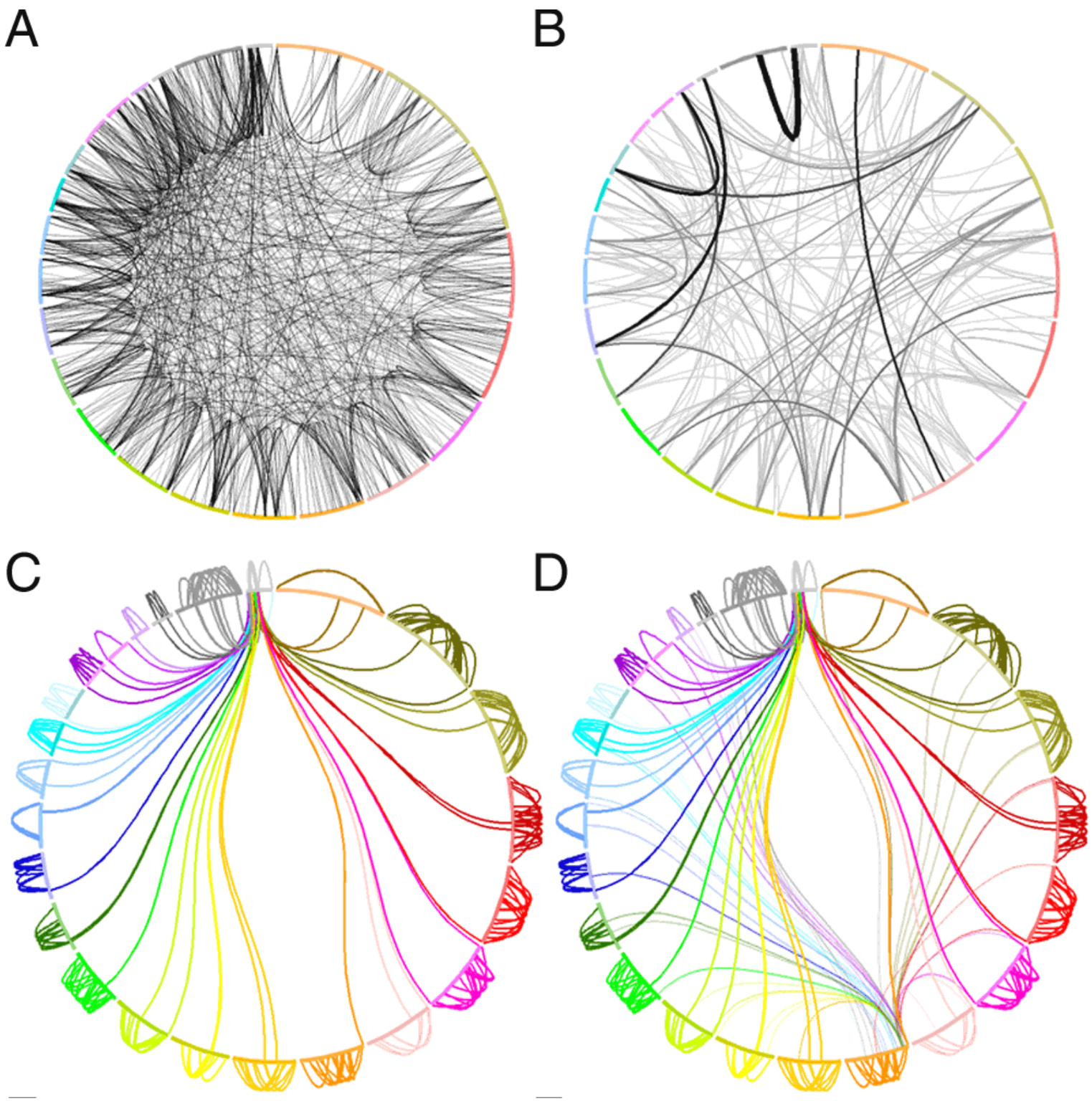

The same data set is shown in all panels. (A) each link represents one of a subset of 2,500 segmental duplications within the human genome. (B) rules are used to change link color and thickness. (C) rules are used to show only links to chrY. (D) in addition to rules in (C), other rules add a second layer of links from chr8.

BUNDLES

E

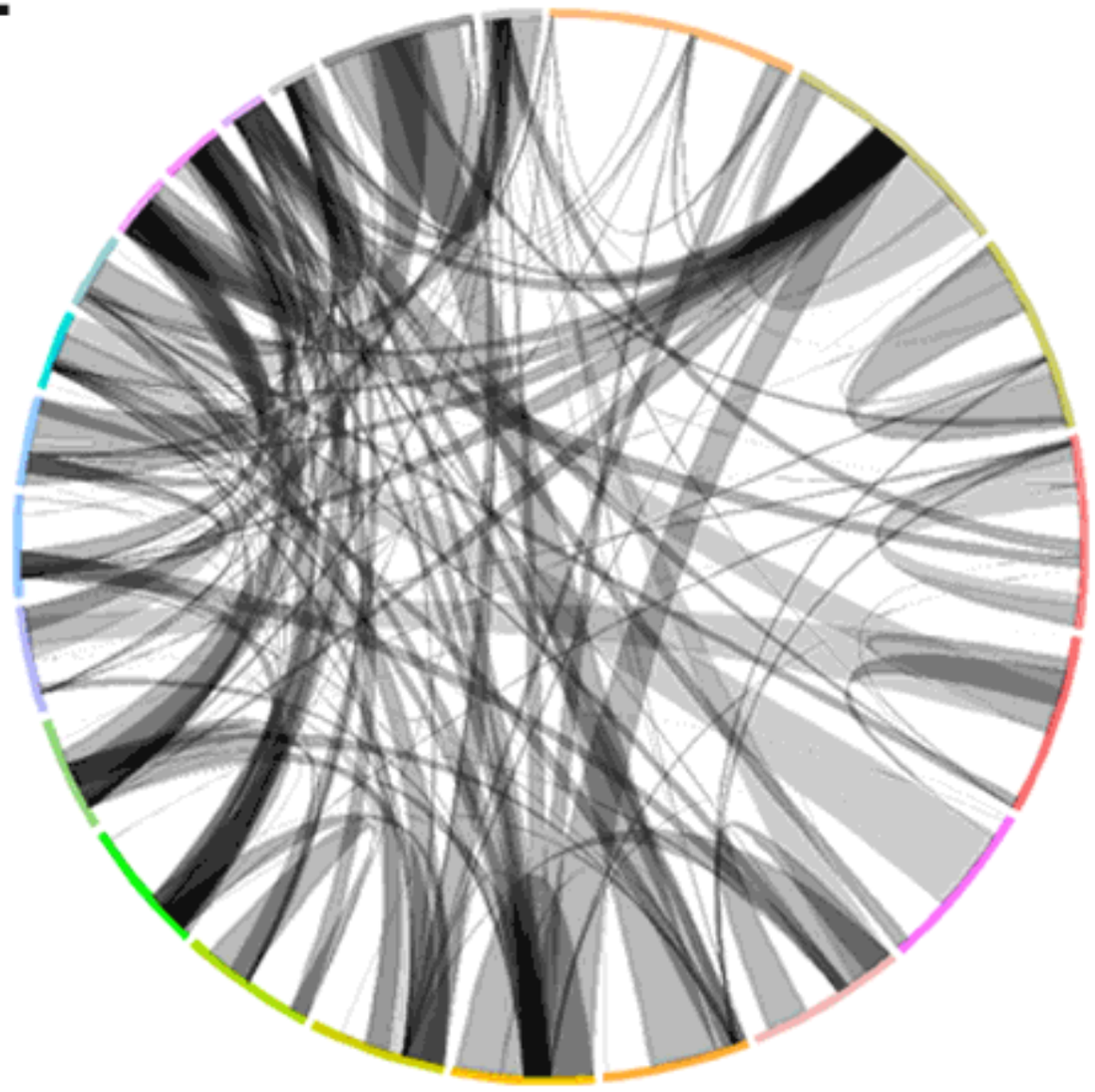

F

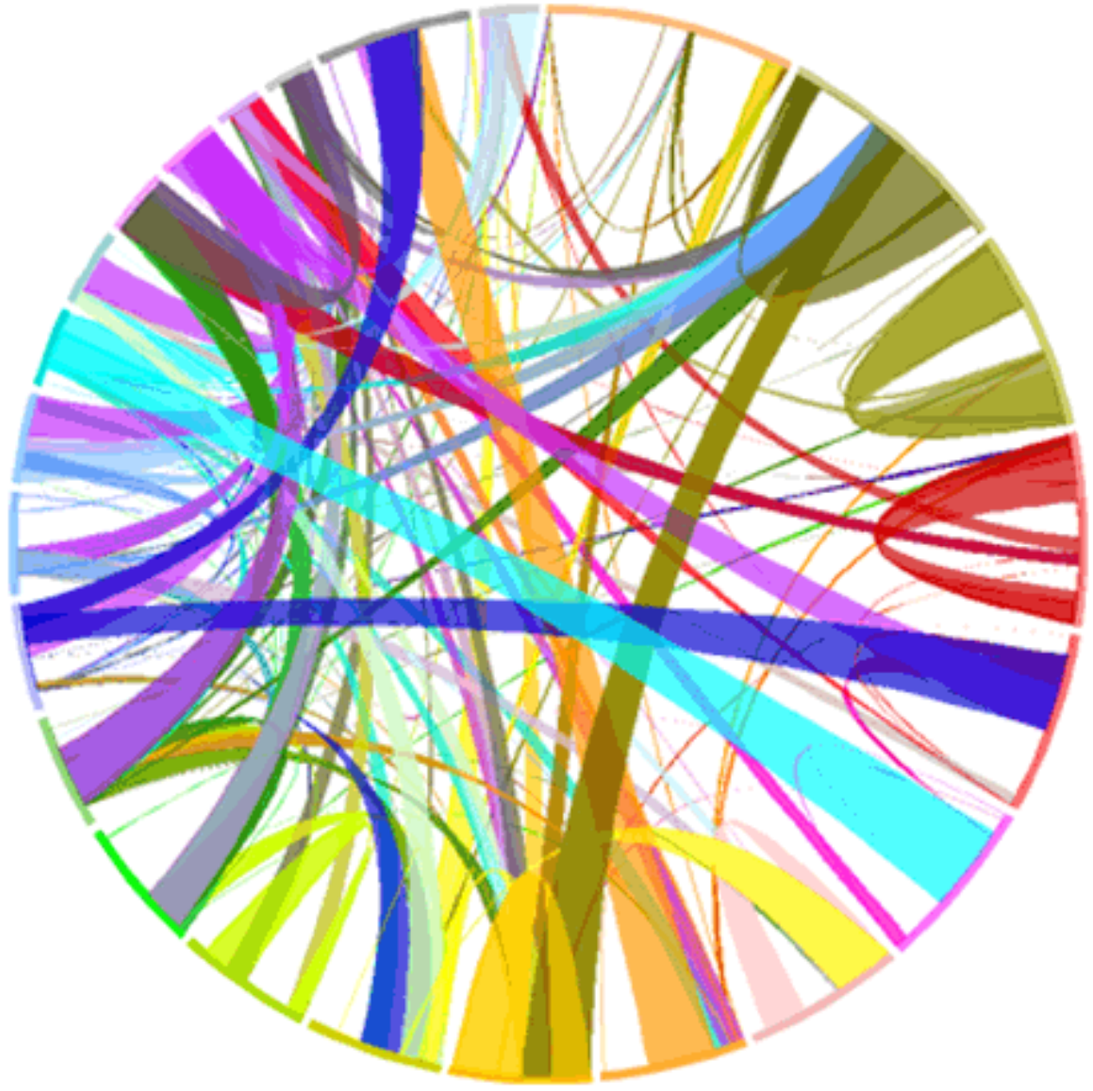

(E,F) adjacent links are grouped into thicker links (bundles) to reduce the complexity of the figure.

EXAMPLE FROM LITERATURE

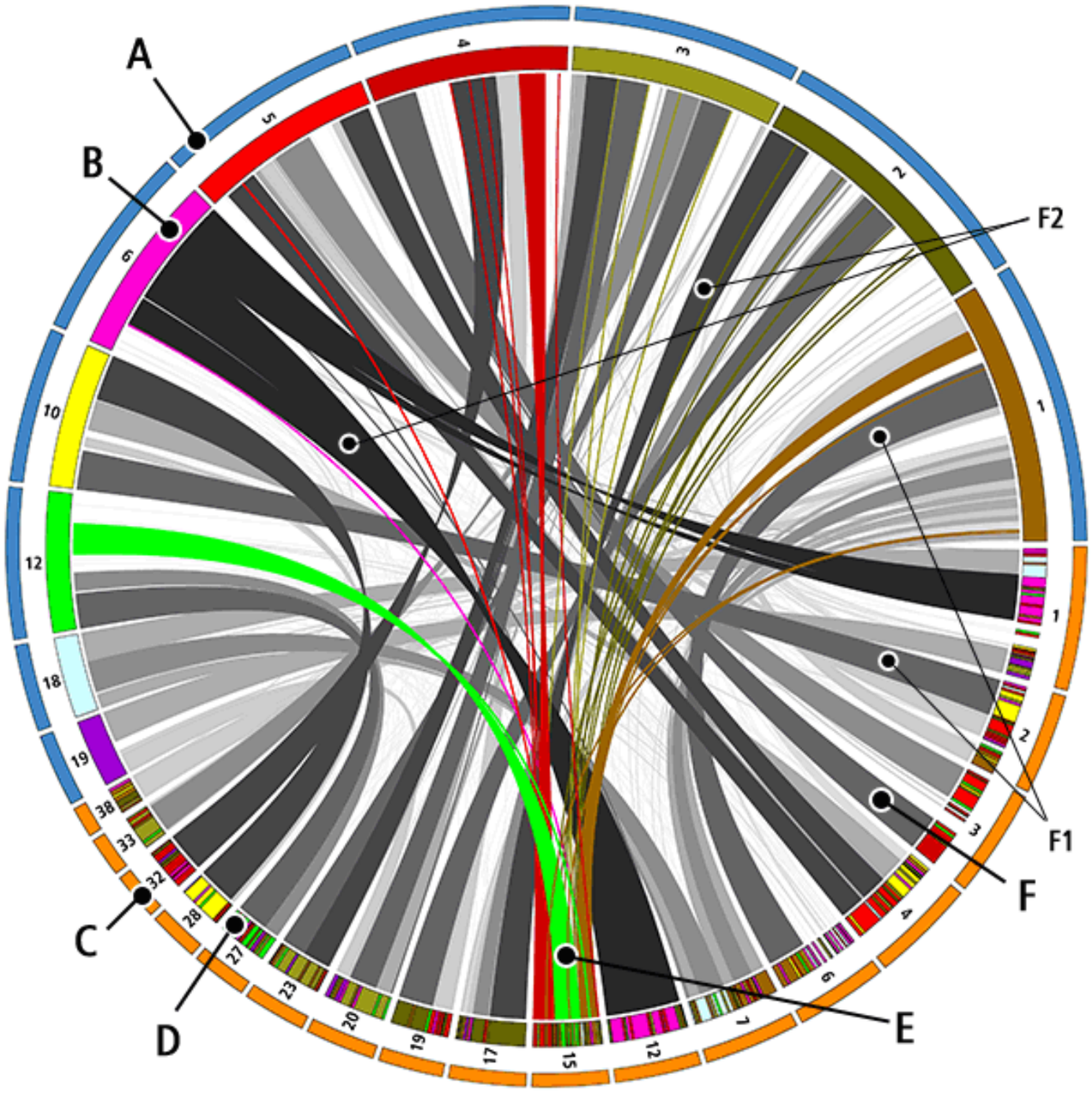

Regions of similarity between human and dog genomes. (A) human genome. (B) human ideograms. (C) dog genome. (D) dog ideograms, coded by most similar human chromosome. (E,F) link bundles connect similar regions. (F1) rules are used to color bundles by size. (F2) bundles twist when similarity involves opposite strands. American Scientist, Sept-Oct 2007. Cover figure by M Krzywinski.

dynamic rules

DATA-BASED FILTERING AND FORMATTING

RULES CAN CHANGE LINK GEOMETRY

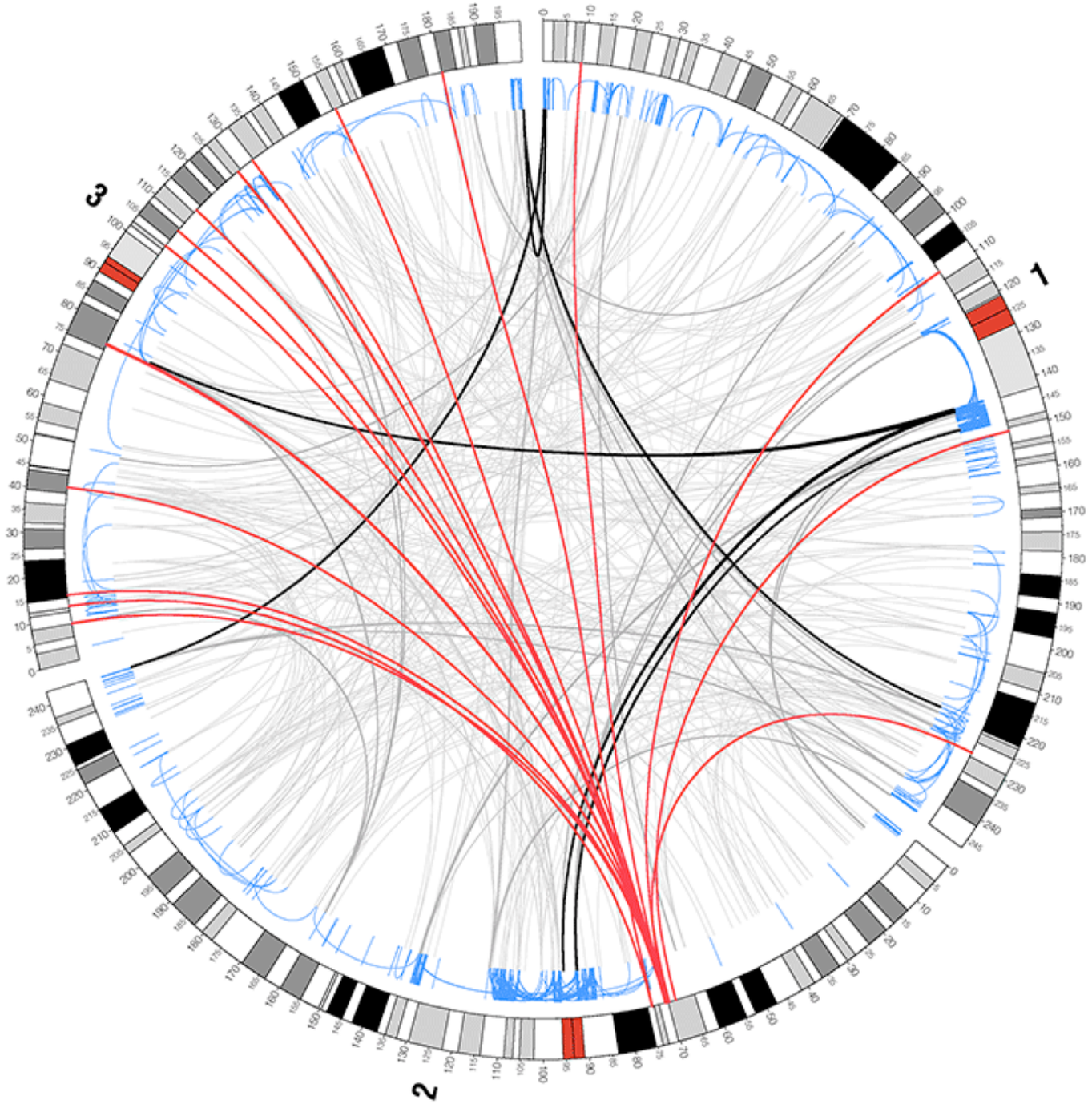

Link color, thickness and geometry can be dynamically adjusted based on position and size of the link. Here, blue links are made to point outward and show intrachromosomal connections. Red links emphasize connections from a short region on chr2.

RULES CAN CHANGE DATA GLYPH COLOR AND SIZE

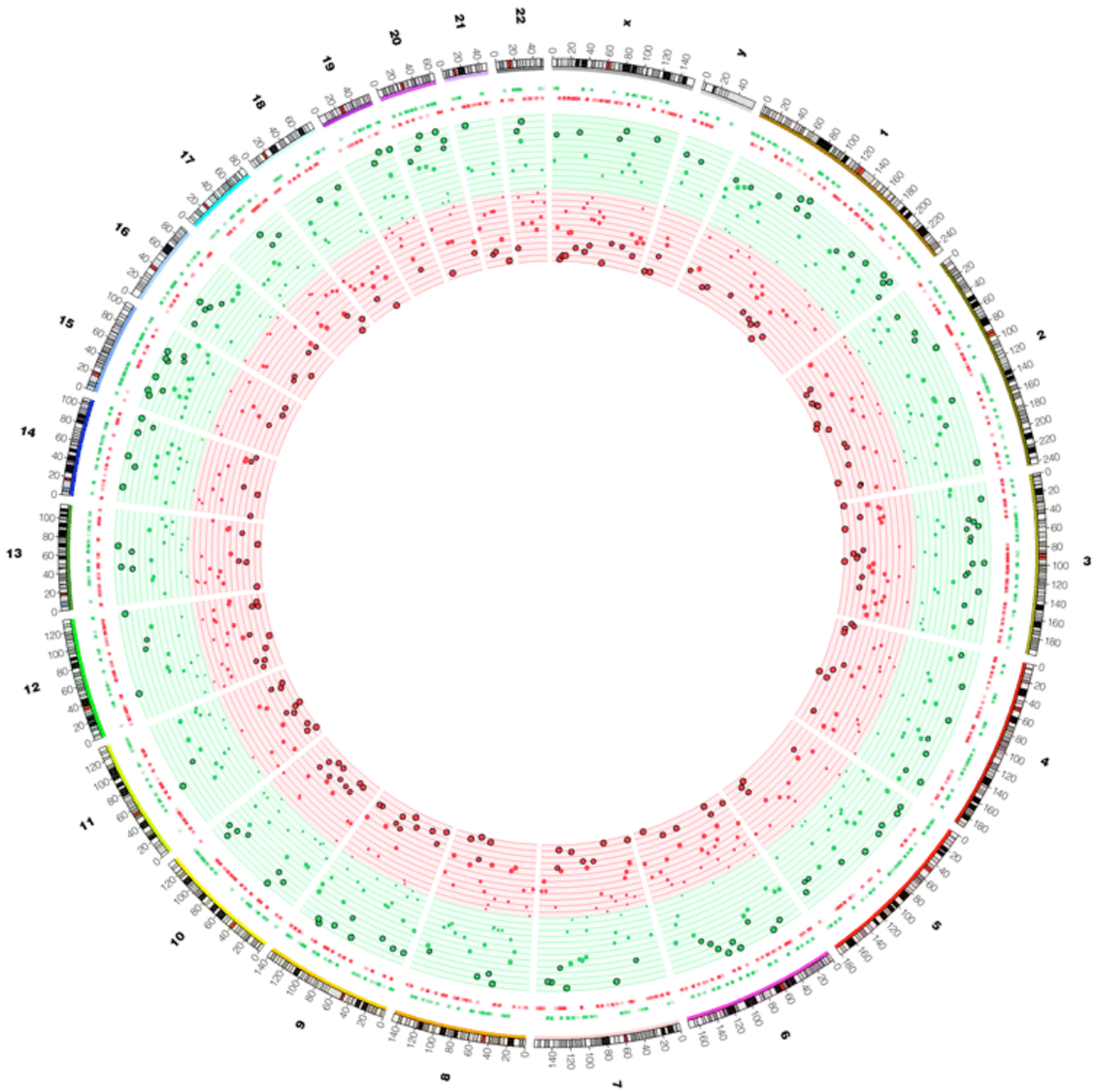

Resequencing with naïve and log pool designs. Prabhu, S. and I. Pe'er, Overlapping pools for high-throughput targeted resequencing. Genome Res, 2009. 19(7): p. 1254-61.

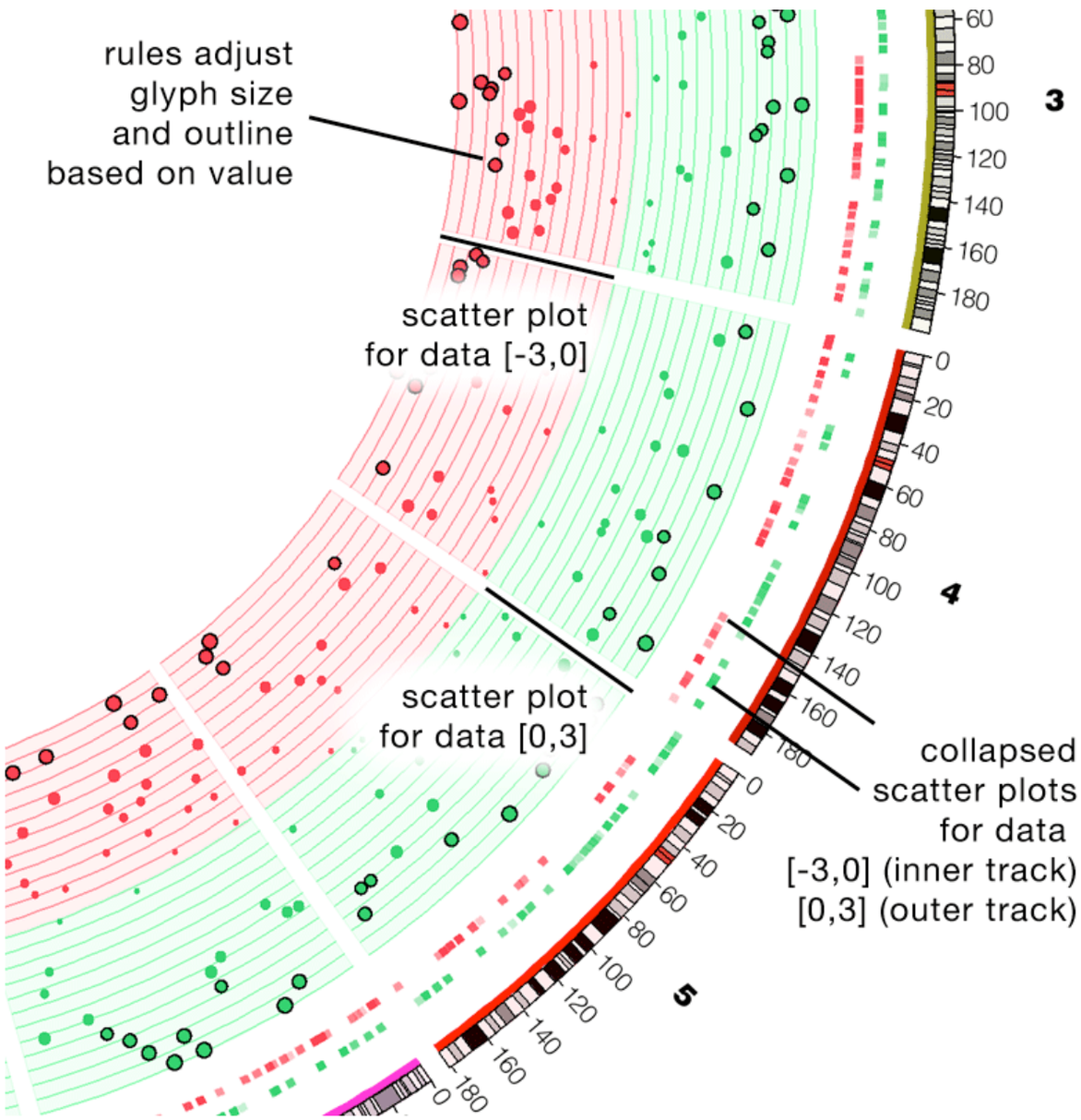

The size and outline of each scatter plot glyph is influenced by the data value. The data value itself can be altered, as see in the two outermost collapsed scatter plots, where the value for each point has been set to 0 to display the glyphs at the same radius.

RULES CAN CHANGE FORMAT OF ANY DATA POINT

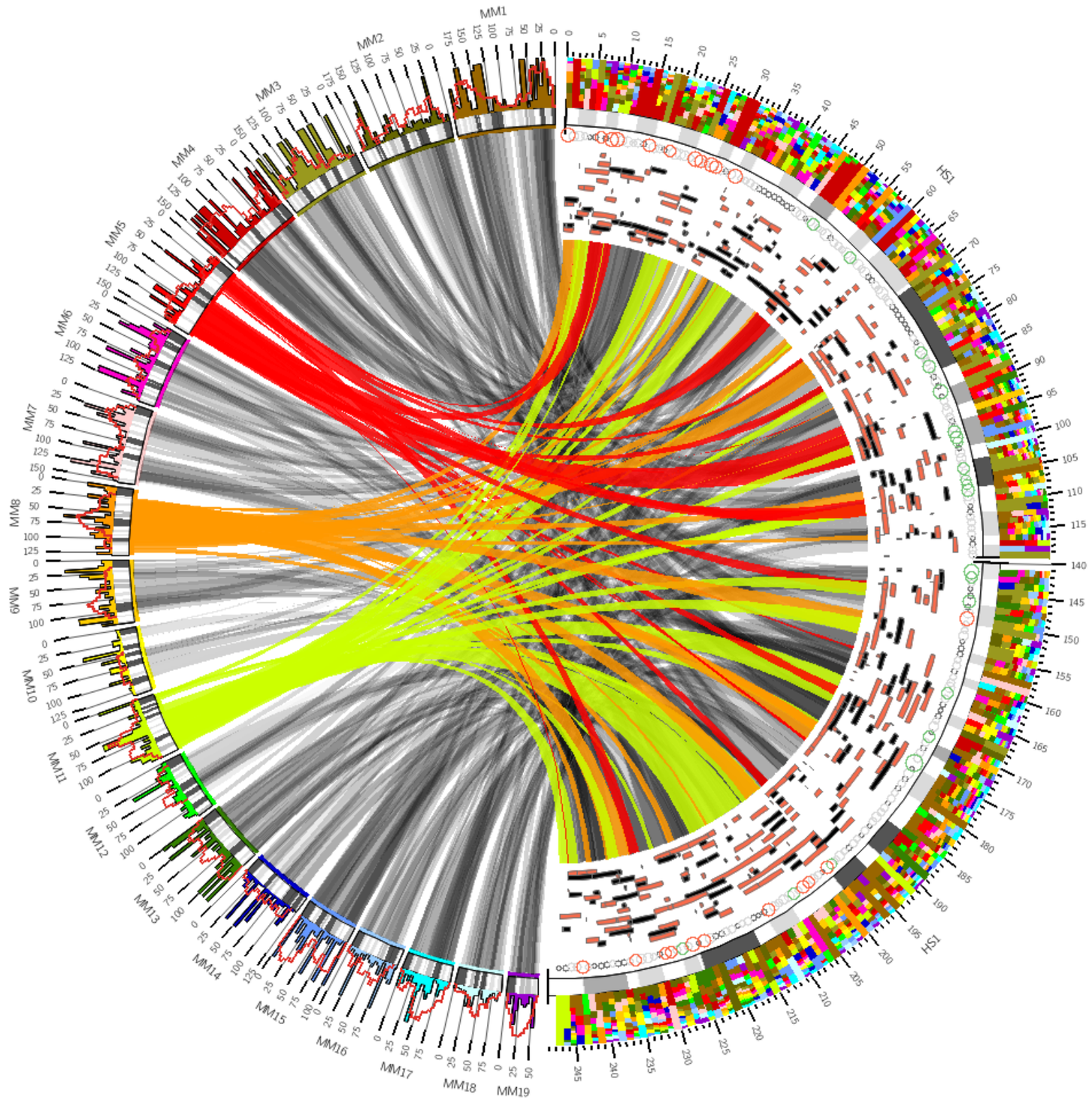

.

RULES APPLY FORMATTING FROM DATA

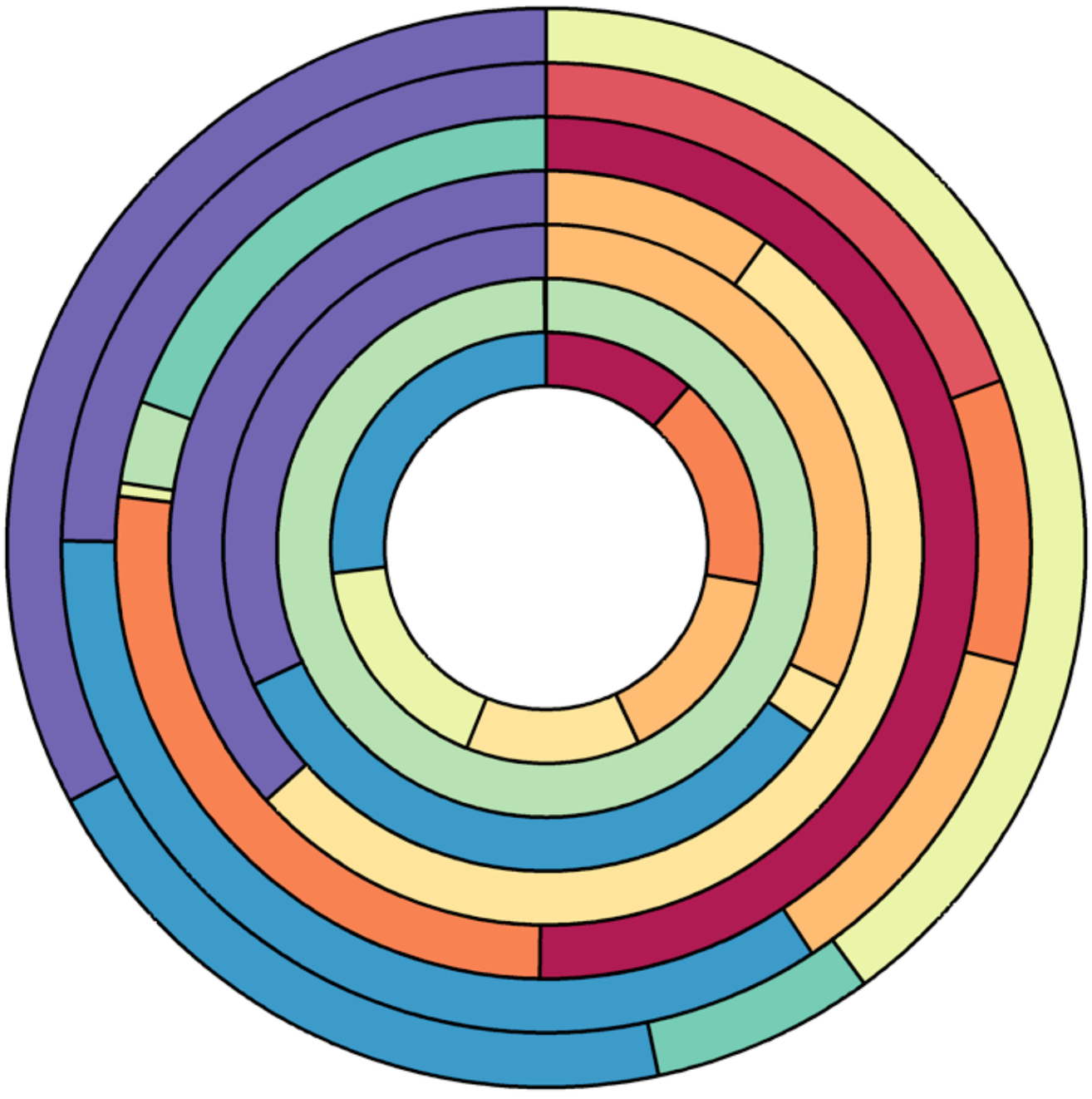

```
# species.0.txt
gh 0 401 id=gh6
gh 401 468 id=gh8
gh 468 674 id=gh9
...

# species.26.txt
gh 0 235 id=gh3
gh 235 454 id=gh4
gh 454 534 id=gh7
...


<rules>

<rule>
# data point must match the condition
# for the rule to apply
condition  = var(id) eq "gh1"
fill_color = spectral-10-div-1
</rule>

<rule>
condition  = var(id) eq "gh2"
fill_color = spectral-10-div-2
</rule>

...
```

.

TRACK DEFINITION WITH TEMPLATES

Each track is associated with several internal counters. The value of the counters are different for each track and can be used to drive track generation from a single template.

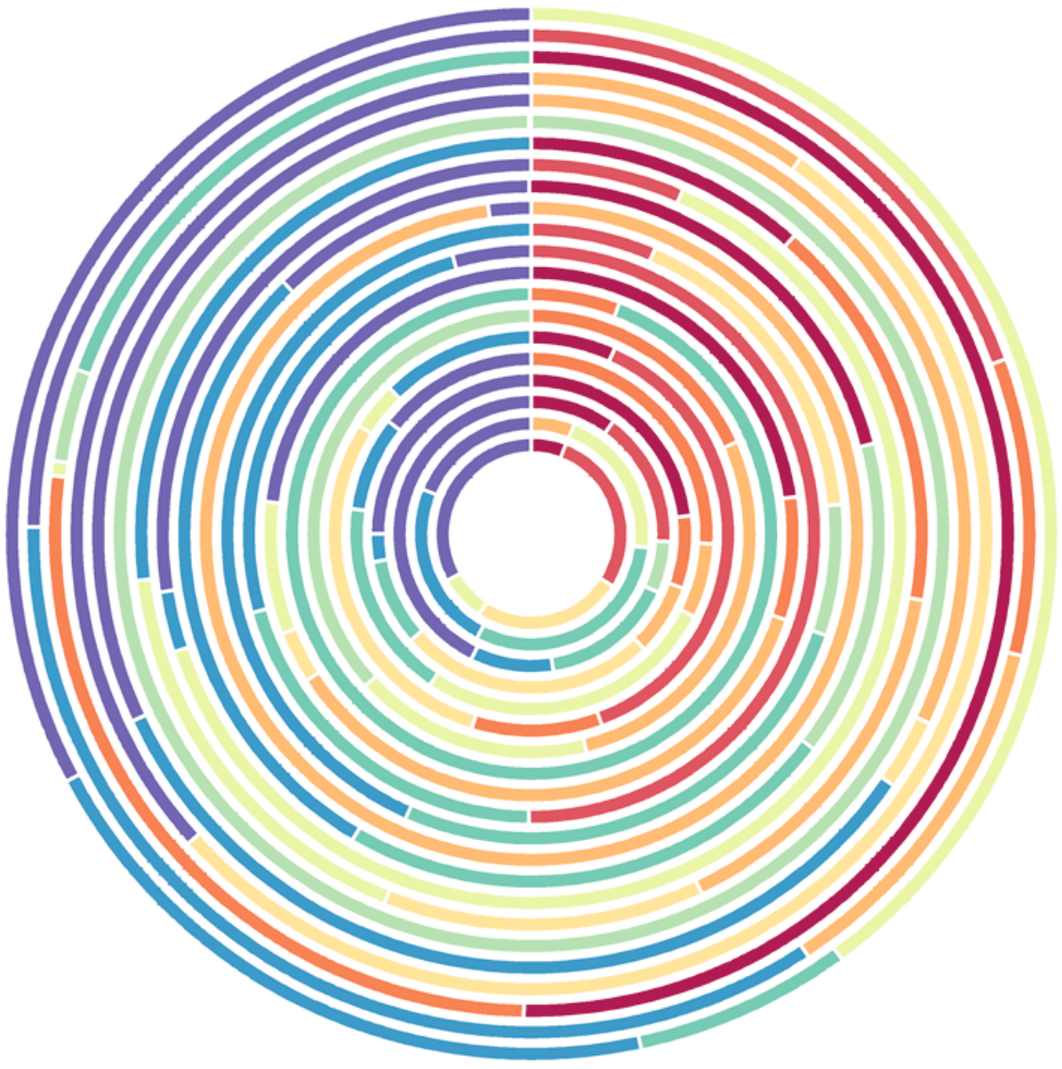

By referencing the template multiple times, new tracks can be created automatically, without having change the template.

implementation

CONTROL AND INTEGRATION

ALL INPUT IS PLAIN TEXT

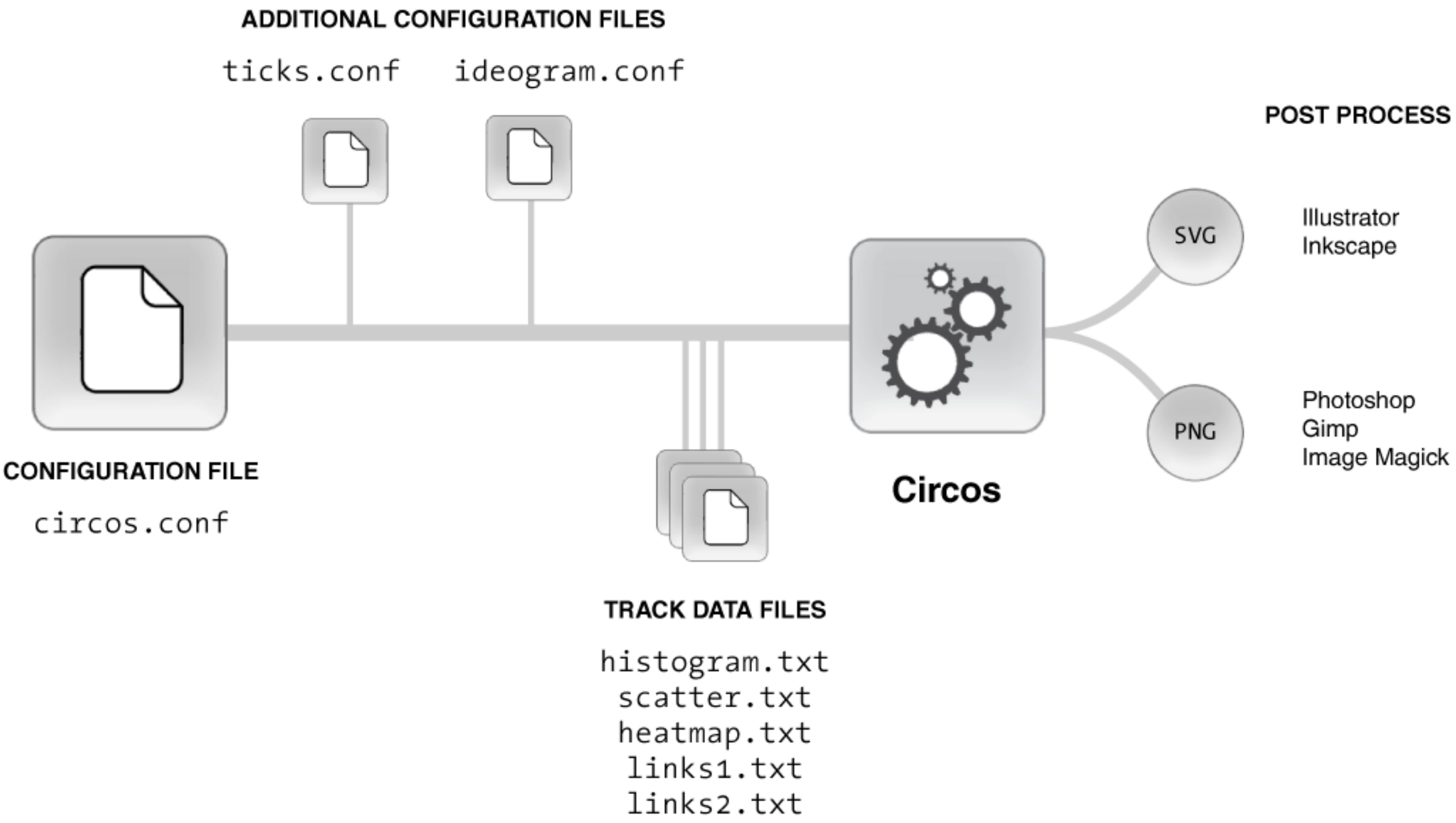

Central configuration file defines data track information and imports other configuration files that store parameters that change less frequently. Each data file can be used for multiple tracks. PNG image output is used for immediate viewing, web-based reporting or presentation. SVG output is ideal for high-res publication and post-processing individual elements.

CIRCOS IN A NUTSHELL

circos can adjust the visualization based on data values rules

rules are snippets of code associated with at track

circos is driven by plain text files and can be easily automated

circos does not have an interface

circos does not perform any analysis, several tools for this are included in tools/

beautiful visualizations—yes

ugly visualizations—yes

visualization guidelines

MAKING THINGS LEGIBLE, CLEAR + ATTRACTIVE

nature methods

POINTS OF VIEW

Wong · Krzywinski · Gehlenborg · Nielsen · Soresh · Kjaegaard · Savig · Cairo

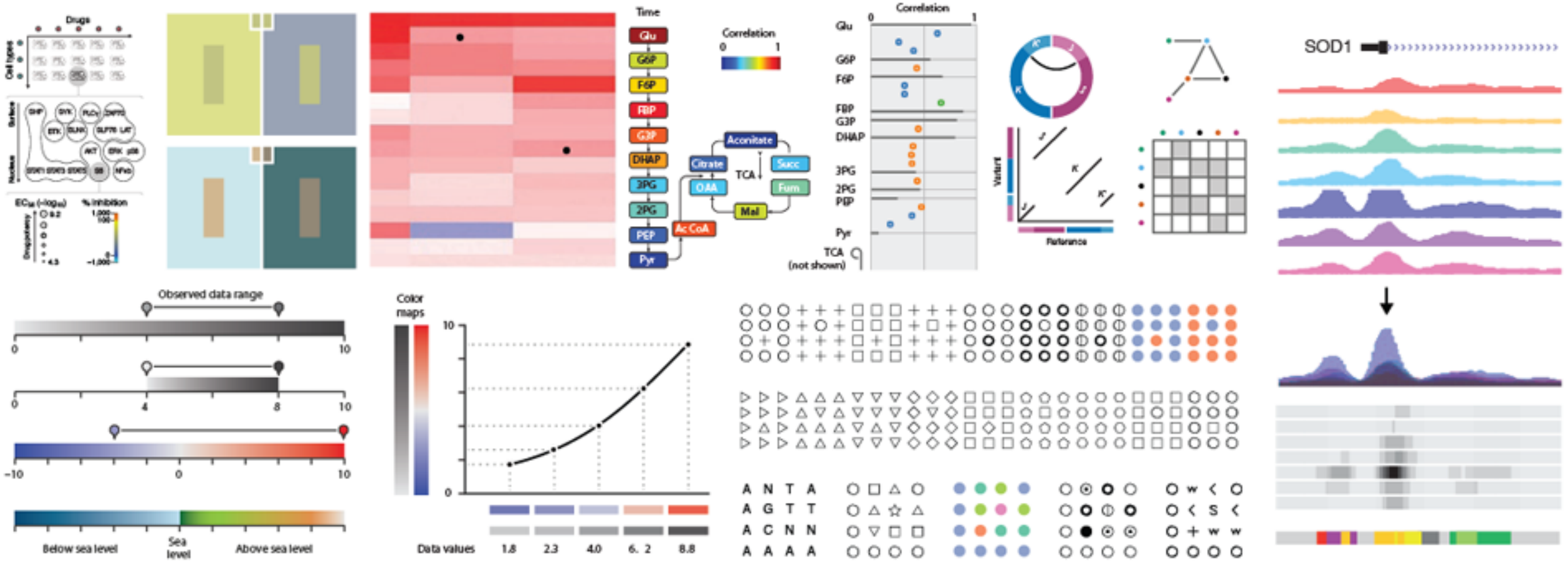

blogs.nature.com/methagora/2013/07/data-visualization-points-of-view.html

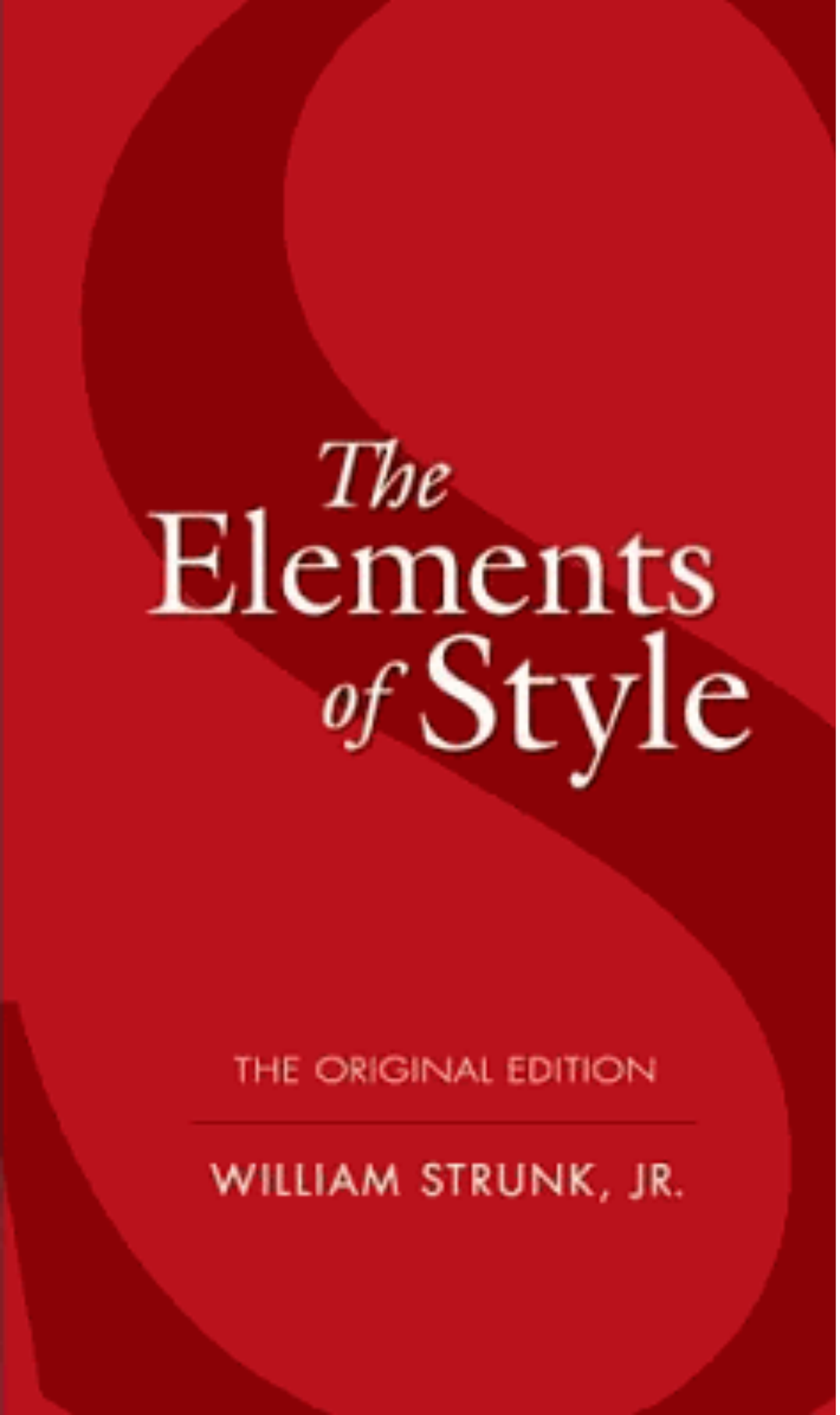

POINTS OF VIEW

Elements of visual style

Translate the principles of effective writing to the process of figure design.

We all use words to communicate information—our ability to do so is extremely sophisticated. We have large vocabularies, understand a variety of written styles and effortlessly parse errors in real time. But when we need to present complex information visually, we may find ourselves 'at a loss for words', graphically speaking.

We can rationalize figure creation by applying principles of effective written communication. By leveraging our training and experience with words, we can turn graphical improvisation into a structured and reproducible process in which we assess and optimize each part of a figure just as we would each paragraph, sentence and word in a manuscript. Let's look at how Strunk and White's classic but stern *The Elements of Style*[1] can be applied to figures. (I encourage you to revisit your own favorite writing resources in the context of visual representation.)

Figure 1 | A flood of identical symbols triggers semantic satiation, a phenomenon in which overwhelming repetition results in loss of meaning. As an accurate but visually unparsable representation of a breakpoint graph[5], the figure breaks Strunk and White's rule "Do not explain too much."[1]

A popular example of disregarding Strunk and White's dictum "Do not take shortcuts at the expense of clarity"[1] is the syntactically correct but incomprehensible sentence "Buffalo buffalo Buffalo buffalo buffalo buffalo Buffalo buffalo"[2]. Unfortunately, visual analogs of this construct appear all too frequently in the literature. If we cannot parse this eight-word sentence, how can we cope with the complexity of **Figure 1**?

Strunk and White also ask us to avoid overwriting because "rich, ornate prose is hard to digest, generally unwholesome, and sometimes nauseating"[1]. The visual equivalent is "chartjunk," a term coined by Tufte[3]. Examples are shimmering textures, gradients and a proliferation of shapes (**Fig. 2**), which all make interpreting the data more difficult, act as exclamation marks that make selective emphasis impossible, and "can never rescue a thin data set"[3]. If you cannot easily emphasize an element in your figure, chances are that it is overstated.

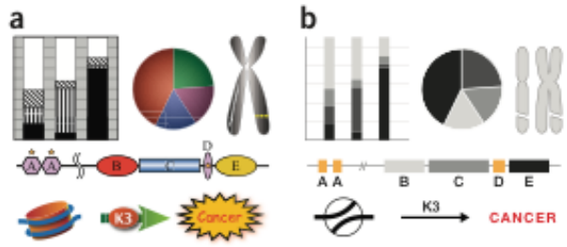

Figure 2 | Use the simplest visual representation[6] for objects and "omit needless words"[1]. (**a**) Visually garnished elements shout at the reader, who is at a loss to determine what is important. If you wouldn't write it this way, don't draw it either. (**b**) Simple shapes provide an elegant presentation. Complex shapes may carry unintended meaning (such as unduplicated versus duplicated chromosomes). In schematics, reserve the use of color for emphasis, where possible.

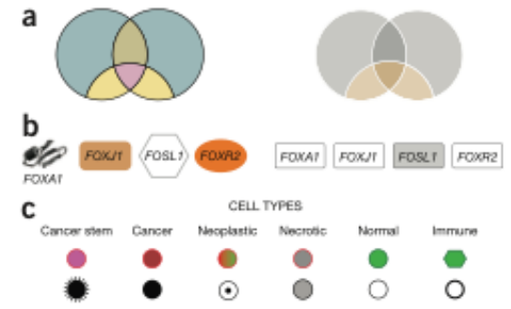

Figure 3 | Objects that interact or share common meaning should be formatted in a similar way that appeals to intuition. (**a**) Venn diagram colors should be selected to naturally communicate overlap. This can be automated by using blend modes in applications such as Illustrator or Inkscape. (**b**) Entity similarities in pathway diagrams are hard to identify when diverse icons are used. When only tone varies, *FOSL1* immediately stands out from the *FOX* gene family. (**c**) Symbols in a series should reflect the concept of progression as naturally as possible. For example, immune cells aren't actually a different shape, and it is not intuitive that pink cells should give rise to red cells.

To reinforce the content and function of related ideas, use the visual equivalent of parallel construction and "express coordinate ideas in similar form"[1]. Choose shapes and colors that intuitively embody overlap, category hierarchy and importance (**Fig. 3**).

Keep in mind the needs and experience of your audience and "place yourself in the background"[1]: do not rely solely on your personal aesthetic (for example, black text overlaid on your favorite color may lack sufficient contrast to be legible). Instead, strive for simplicity and clarity. "Use definite, specific, concrete language"[1]. Be legible without shouting. Concise, but not opaque.

In his play *Horace*, Corneille wrote, "Un premier mouvement ne fut jamais un crime" ("A first impulse was never a crime")[4]. But in the process of making figures, it can be. Avoid the temptation of going with your first idea. Instead, use it as the starting point and then refine and clarify your message. A good figure, like good writing, doesn't simply happen—it is crafted. "Revise and rewrite"[1] becomes "revise and redraw."

COMPETING FINANCIAL INTERESTS
The author declares no competing financial interests.

Martin Krzywinski

1. Strunk, W. Jr. & White, E.B. *The Elements of Style* 4th edn., Ch. 2, 21–26; Ch. 5, 70–75 (Longman, 1999.)
2. Pinker, S. *The Language Instinct* (W. Morrow, New York, 1994).
3. Tufte, E.R. *The Visual Display of Quantitative Information* 2nd edn., 107–121 (Graphic Press, Cheshire, Connecticut, USA, 2001).
4. Corneille, P. *Horace* (http://openlibrary.org/books/OL6939036M/Corneille's_Horace/) line 1648 (Heath, 1904).
5. Alekseyev, M.A. & Pevzner, P.A. *Genome Res.* **19**, 943–957 (2009).
6. Wong, B. *Nat. Methods* **8**, 611 (2011).

Martin Krzywinski is a staff scientist at Canada's Michael Smith Genome Sciences Centre.

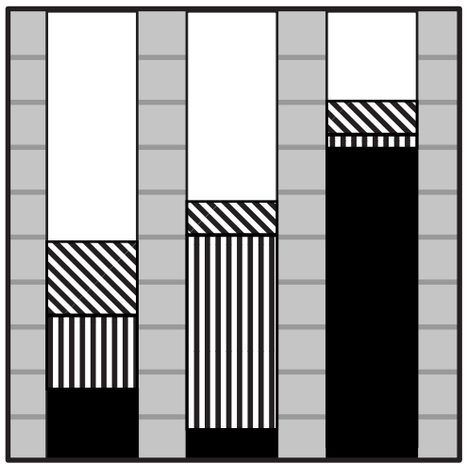

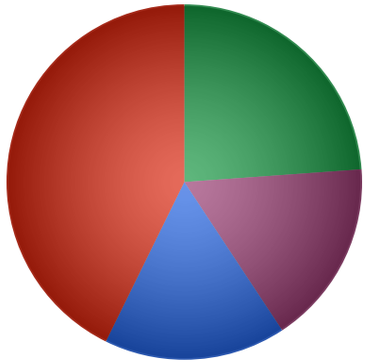

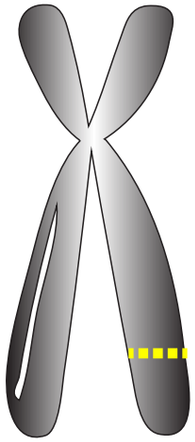

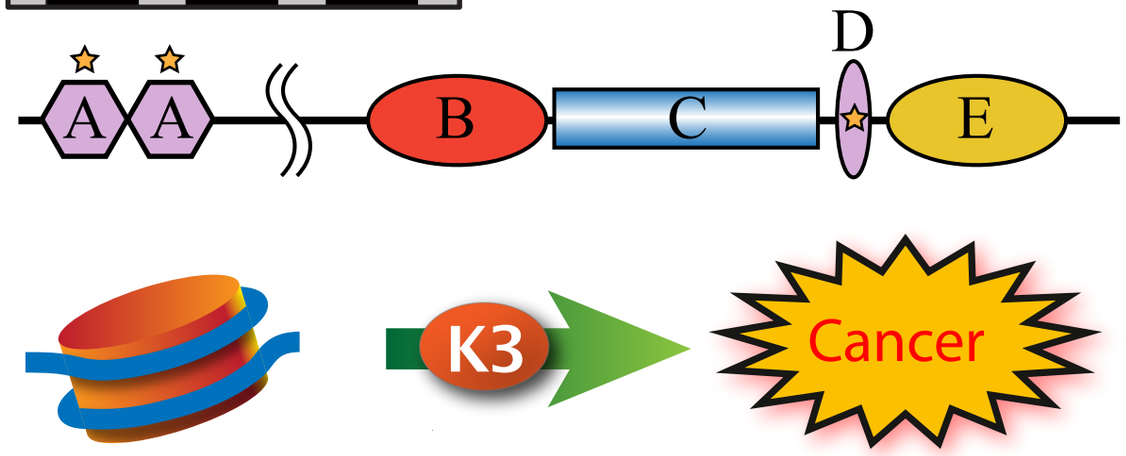

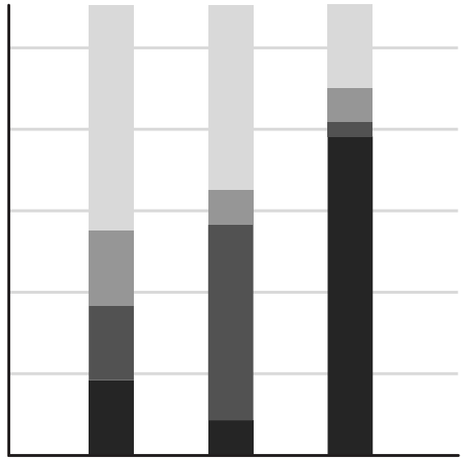

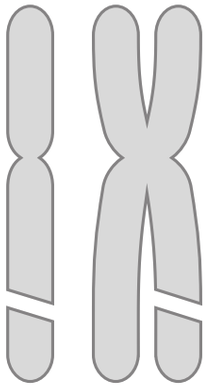

Krzywinski, M., Elements of visual style. Nat Methods, 2013. 10(5): p. 371.

top-down

bottom-up

redundancy

consistency

conciseness

clarity

focus & emphasis

salience & relevance

accuracy & detail

INFORMS

SATISFIES

data encoding

symbols

color

typeface

arrows

line weight

alignment

Prince Charles
Reference Chart
Natal Chart
November 14, 1948
9:14:00 PM GMT
London, England

Camilla Parker Bowles
2nd Chart
Natal Chart
July 17, 1947
7:00:00 AM BDST
London, England

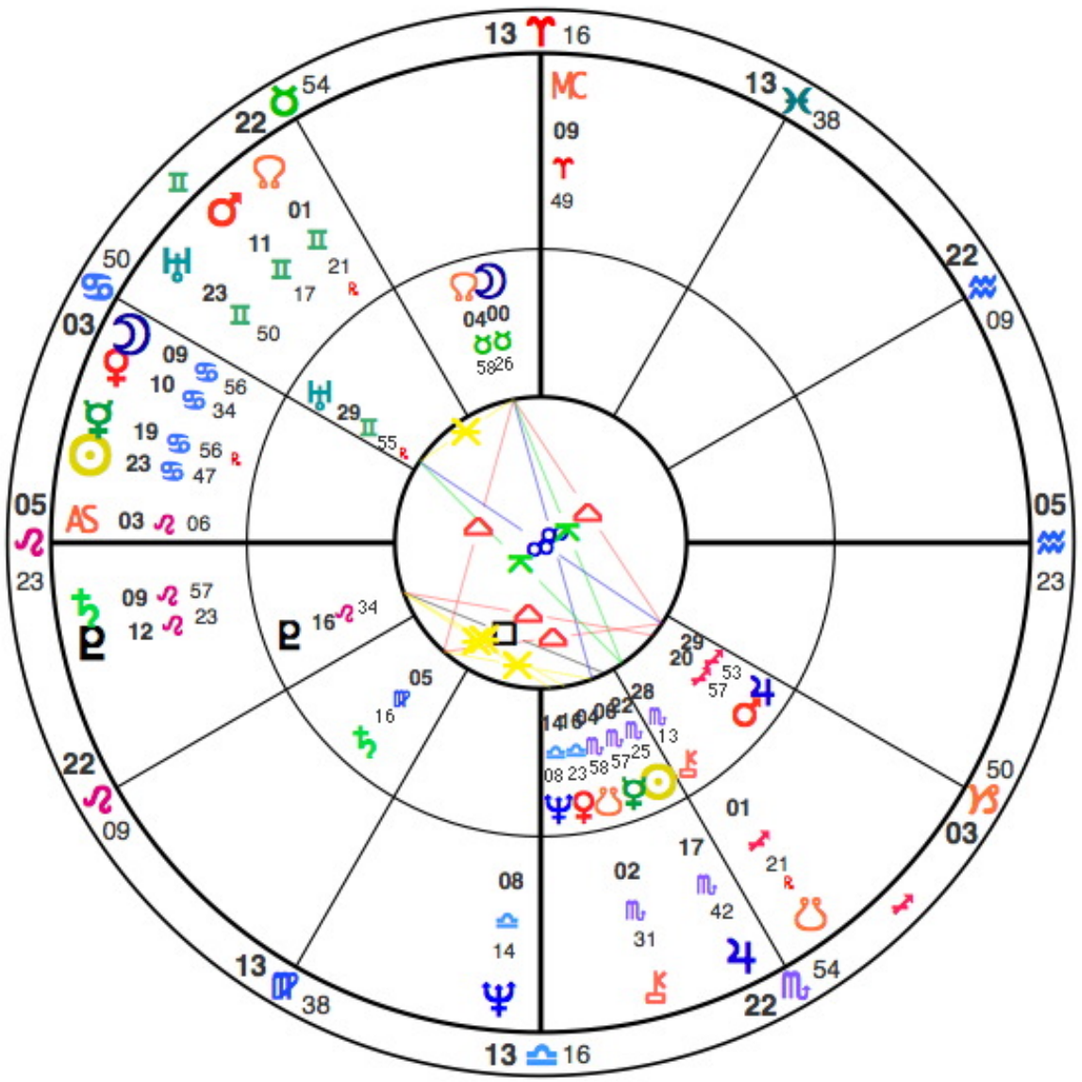

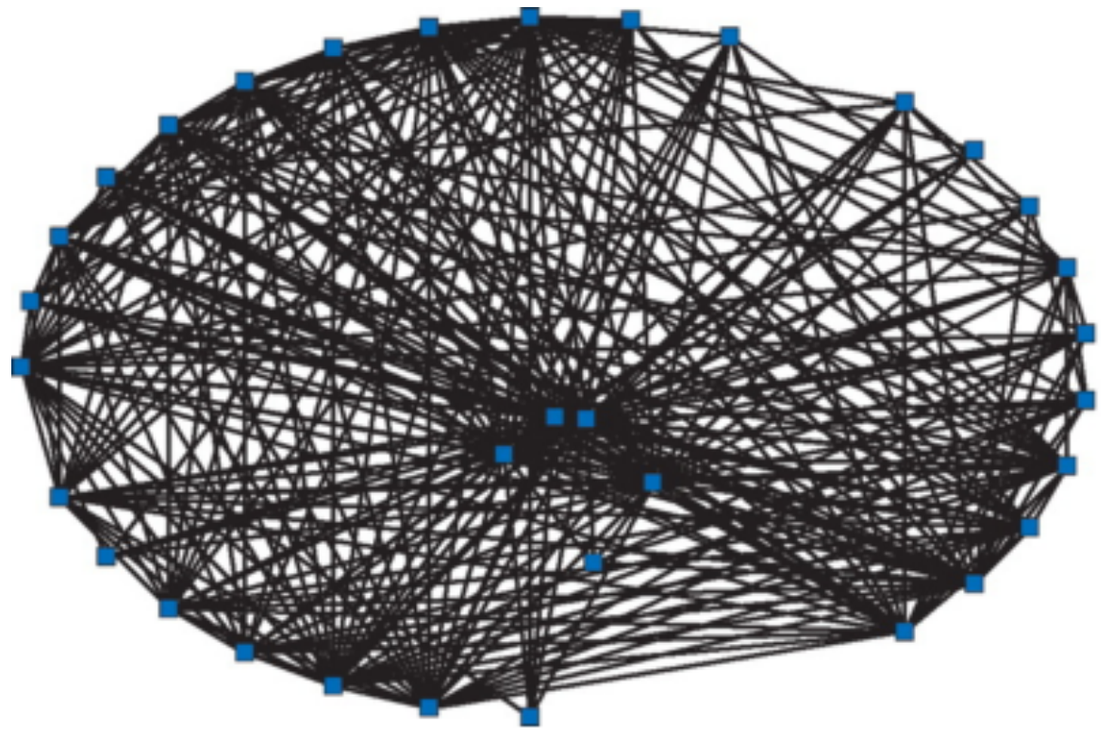

(left) Synastry chart. http://sasstrology.com/2011/03/the-astrology-of-marriage-in-the-royal-family-a-suitable-girl-and-the-bit-on-the-side.html
(right) Genome Res (2006) 16: 1529-36.

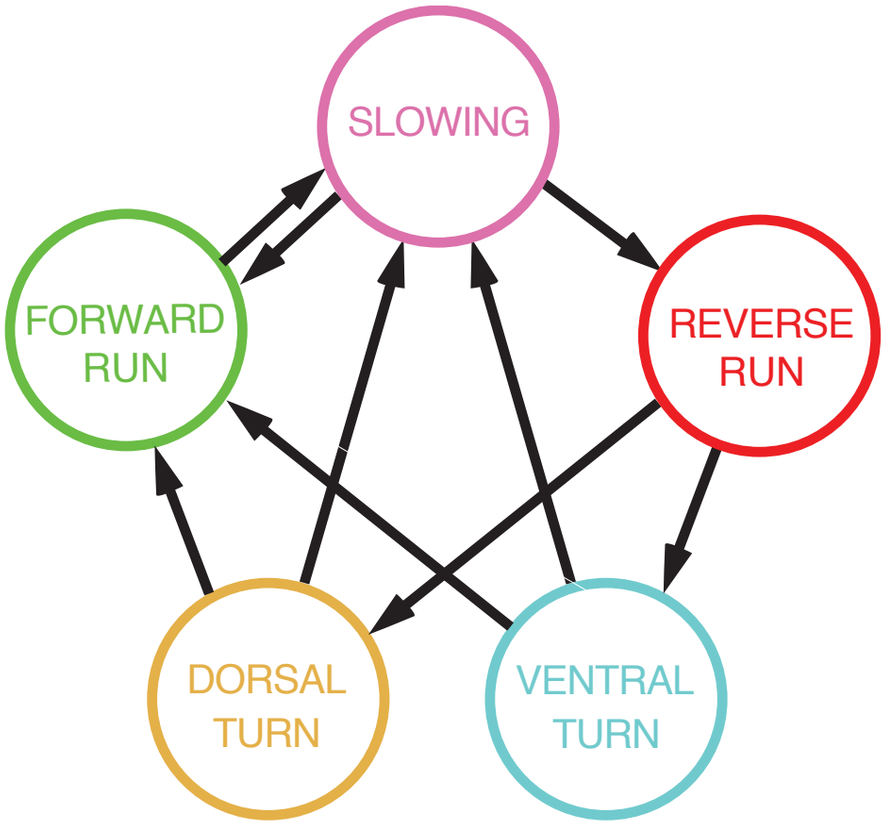
SLOWING
FORWARD RUN
REVERSE RUN
DORSAL TURN
VENTRAL TURN

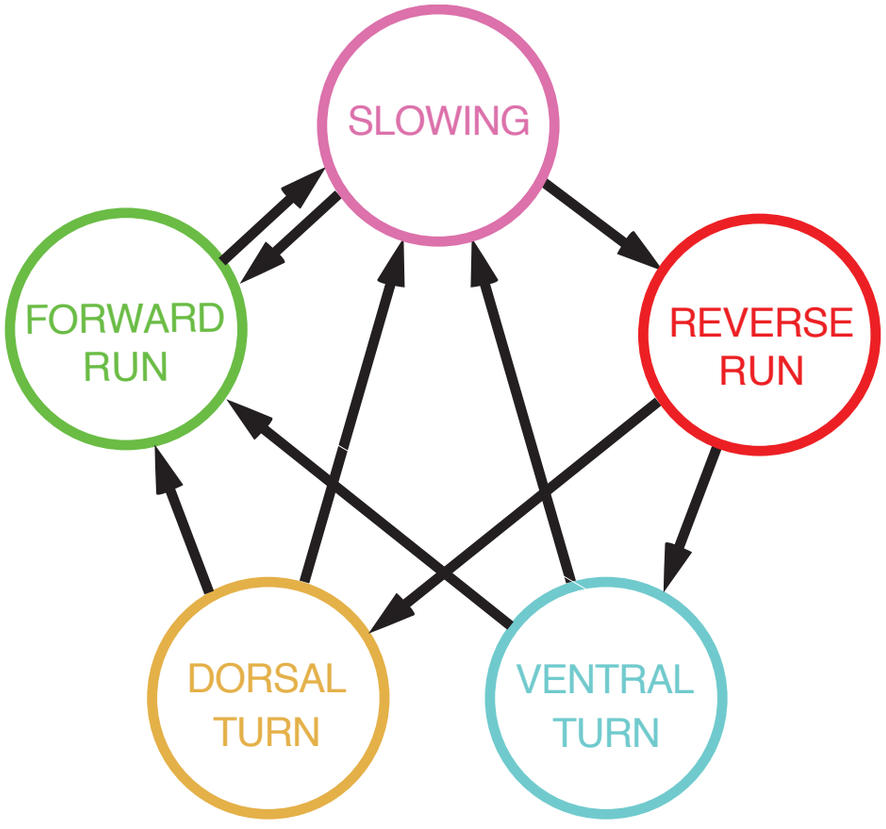
SLOWING
FORWARD RUN
REVERSE RUN
DORSAL TURN
VENTRAL TURN

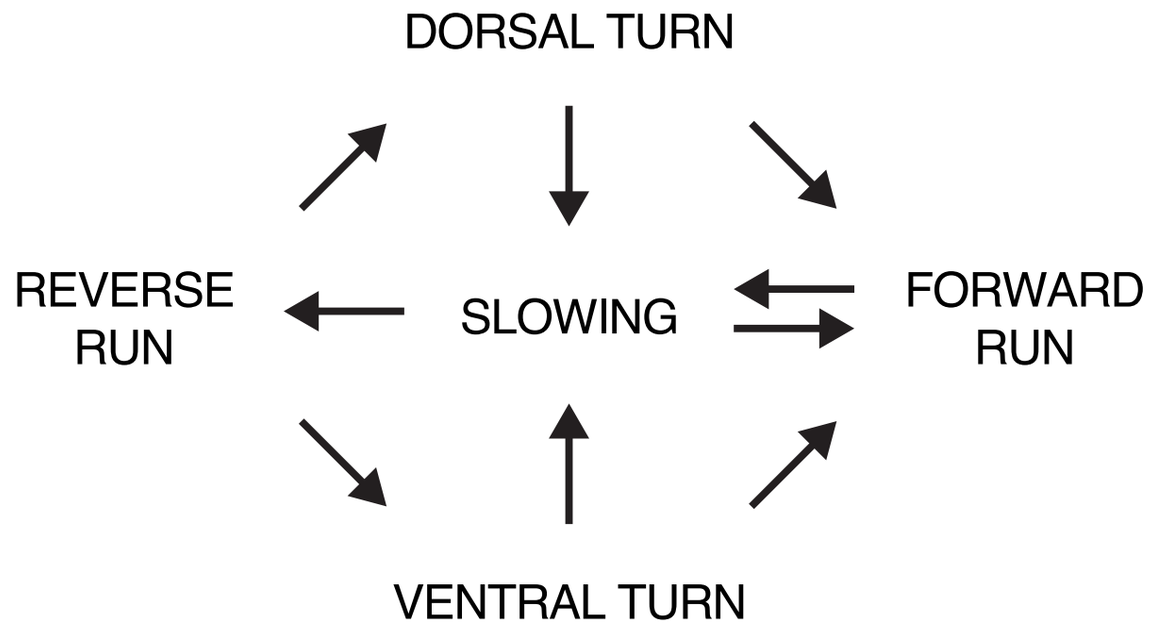
DORSAL TURN
REVERSE RUN
SLOWING
FORWARD RUN
VENTRAL TURN

Consider a spherical cow of radius R ... ∎

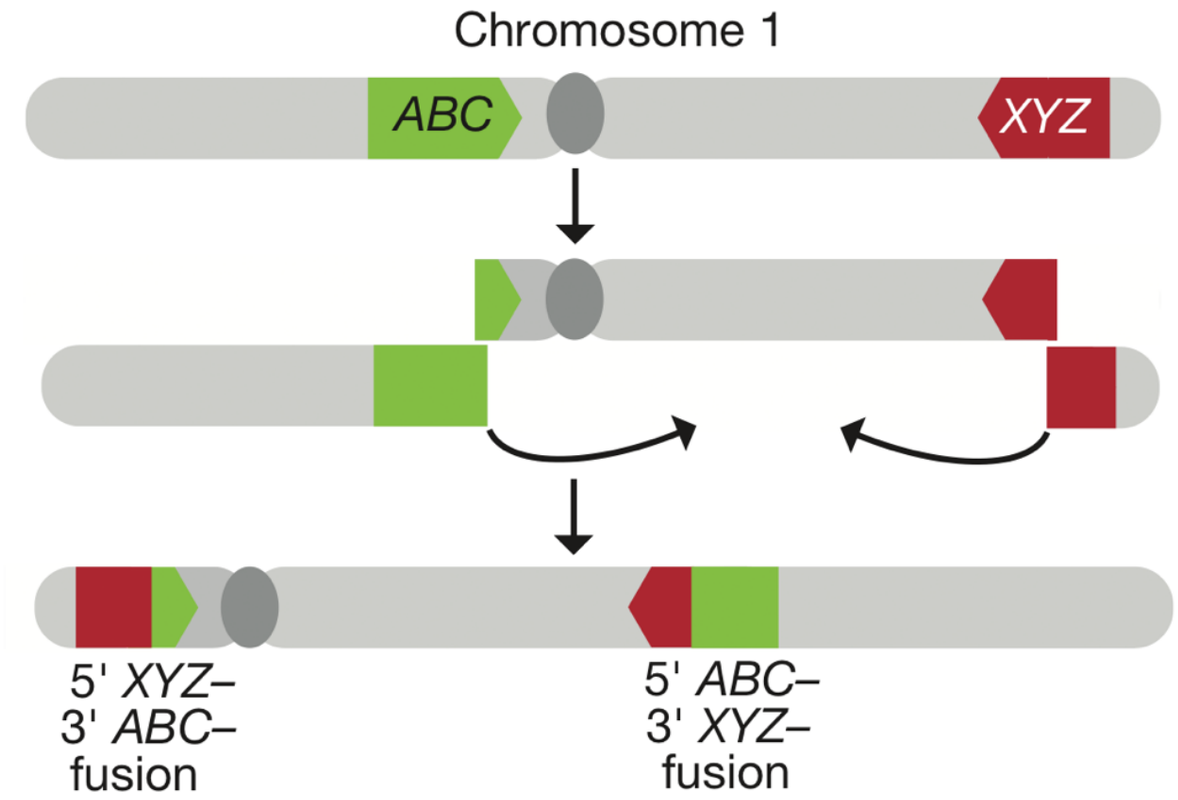

Wong, B. (2011) Points of View: Simplify to Clarify Nat Meth 8:611.

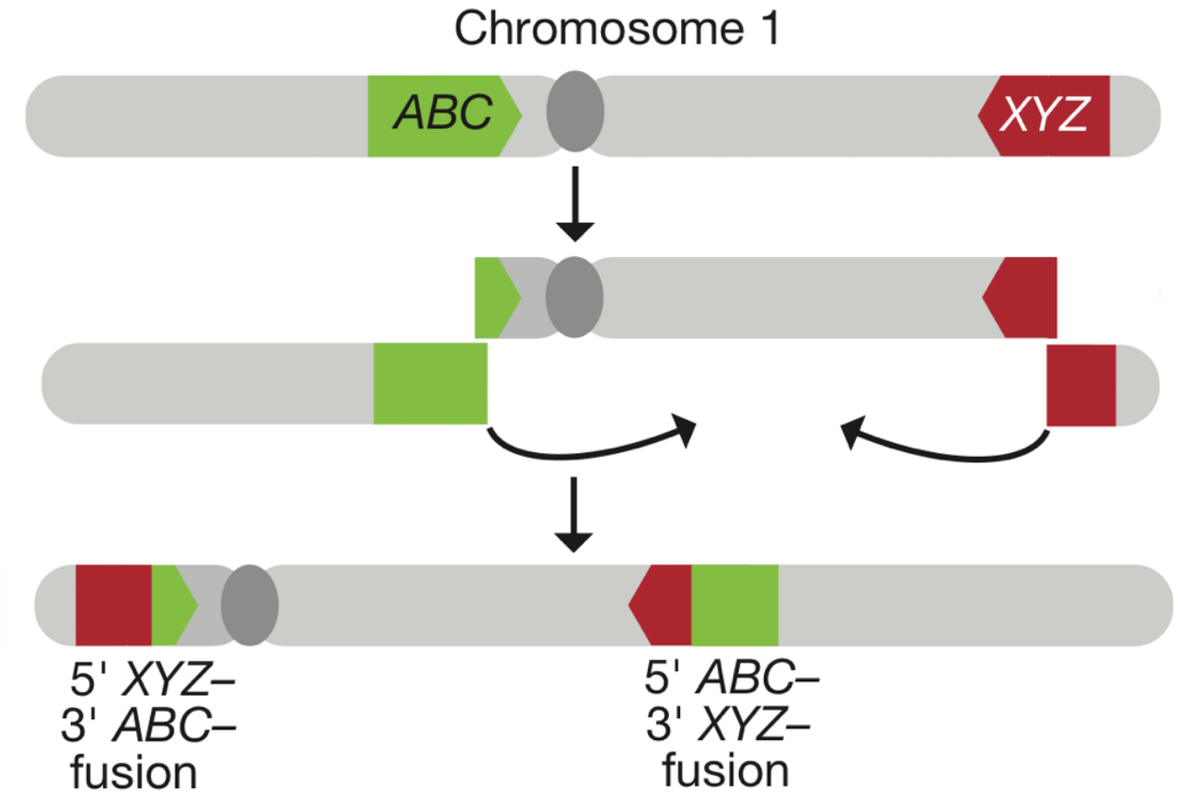

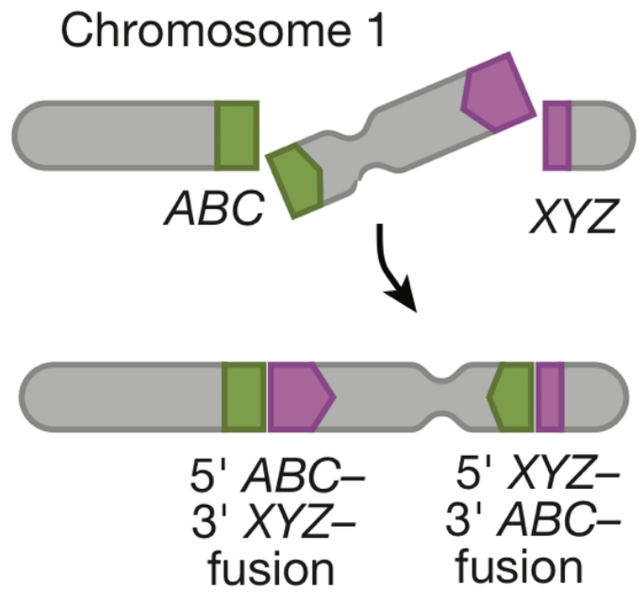

Wong, B. (2011) Points of View: Simplify to Clarify Nat Meth 8:611.

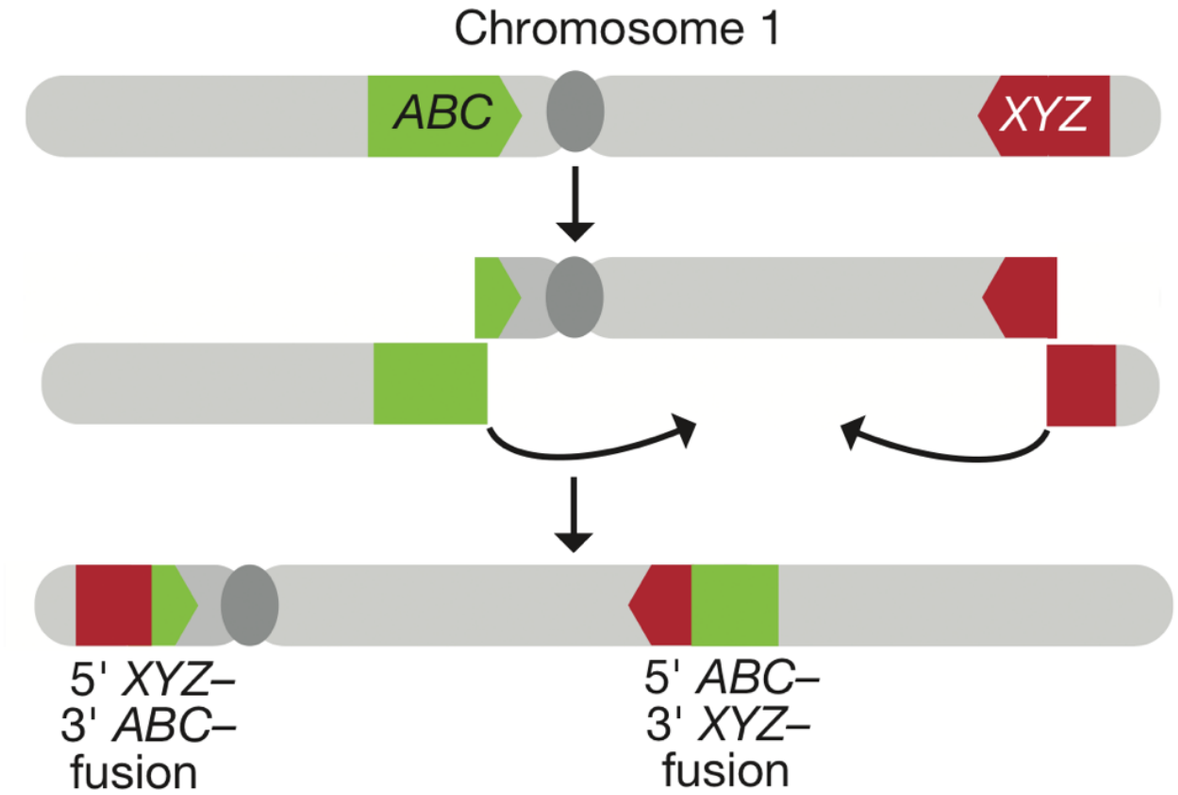

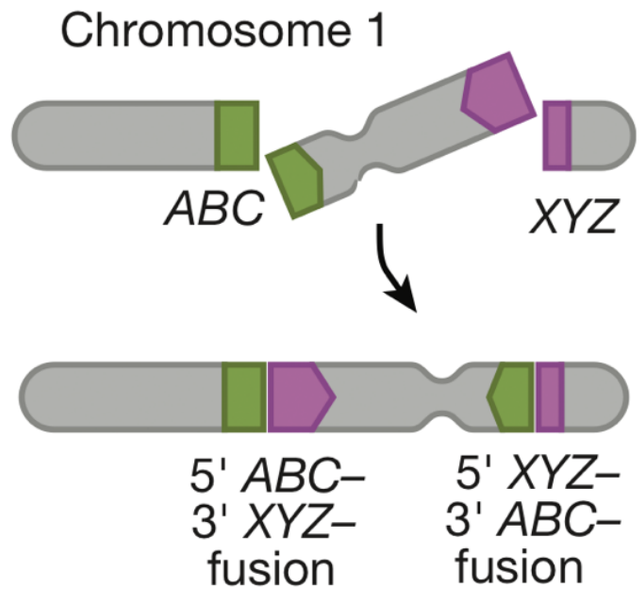

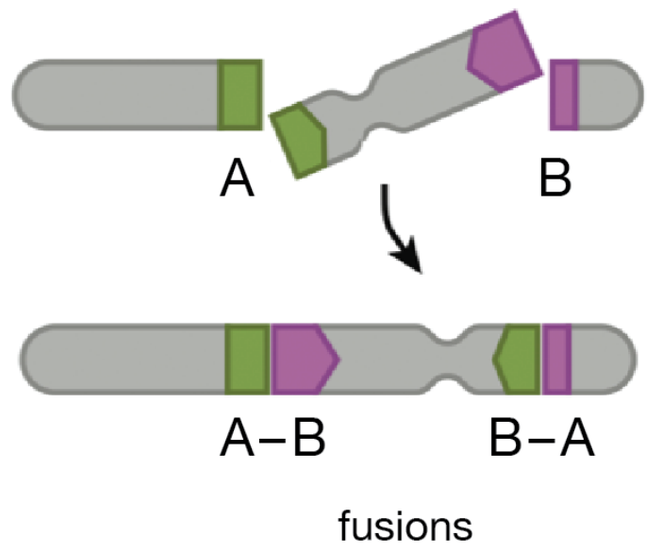

Wong, B. (2011) Points of View: Simplify to Clarify Nat Meth 8:611. Modification by M Krzywinski.

data data data data data data
data data data data data data
data data data data data data
data data data data data data
data data data data data data
data data data data data data
data data data data data data
data data data data data data
data data data data data data
data data data data data data
data data data data data data
data data data data data data
data data data data data data
data data data data data data
data data data data data data
data data data data data data
data data data data data data
data data data data data data

look here

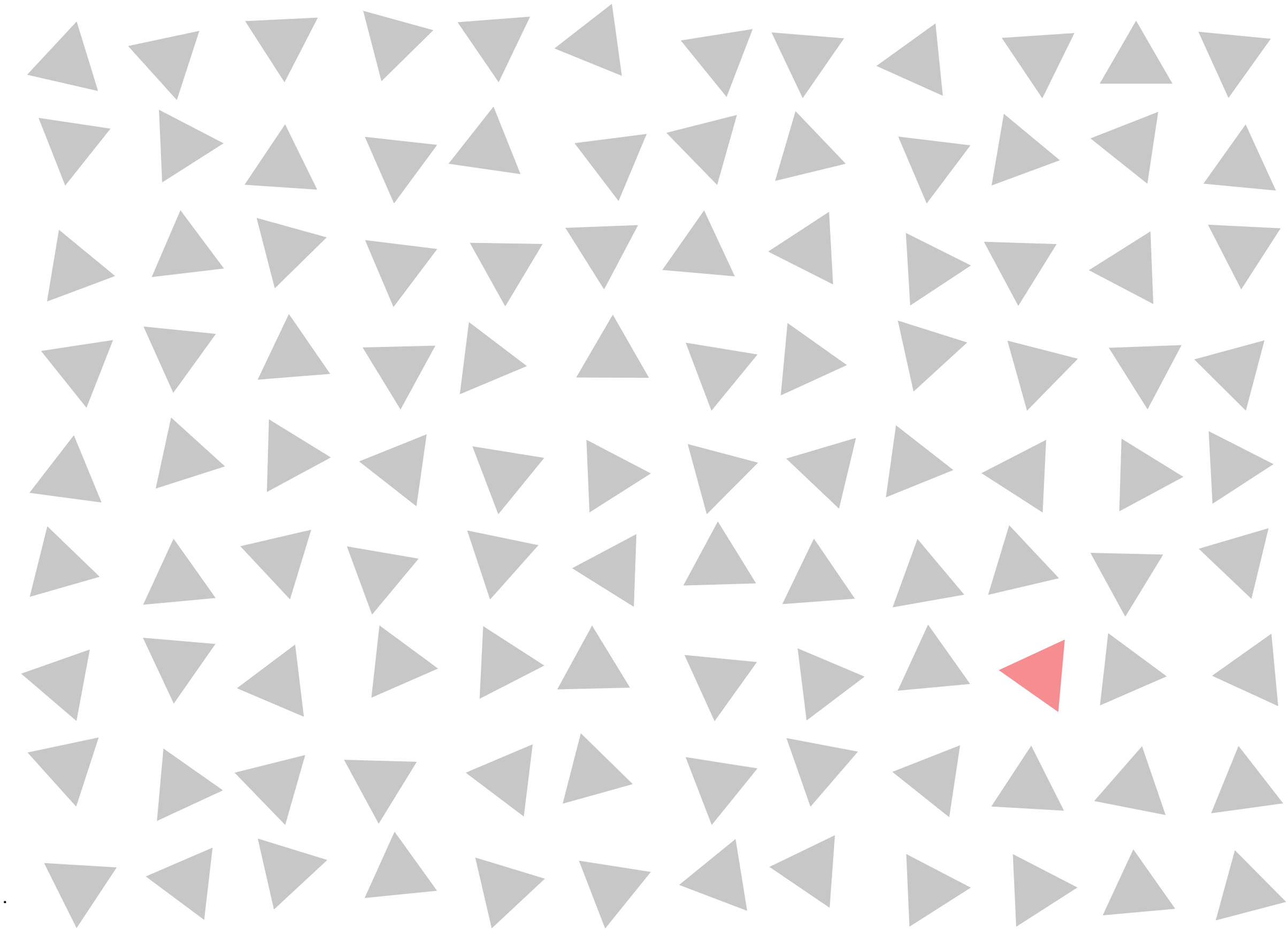

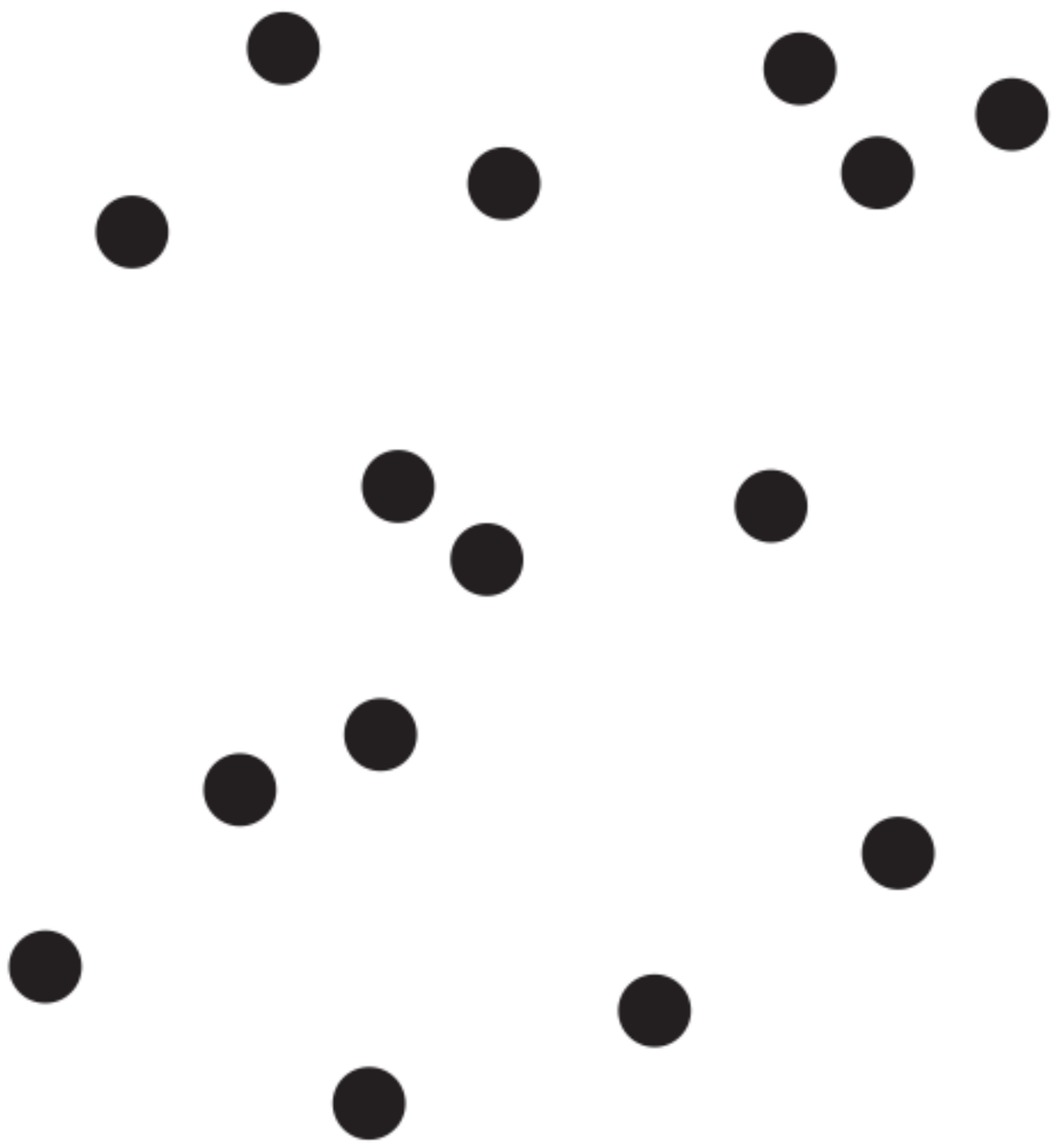

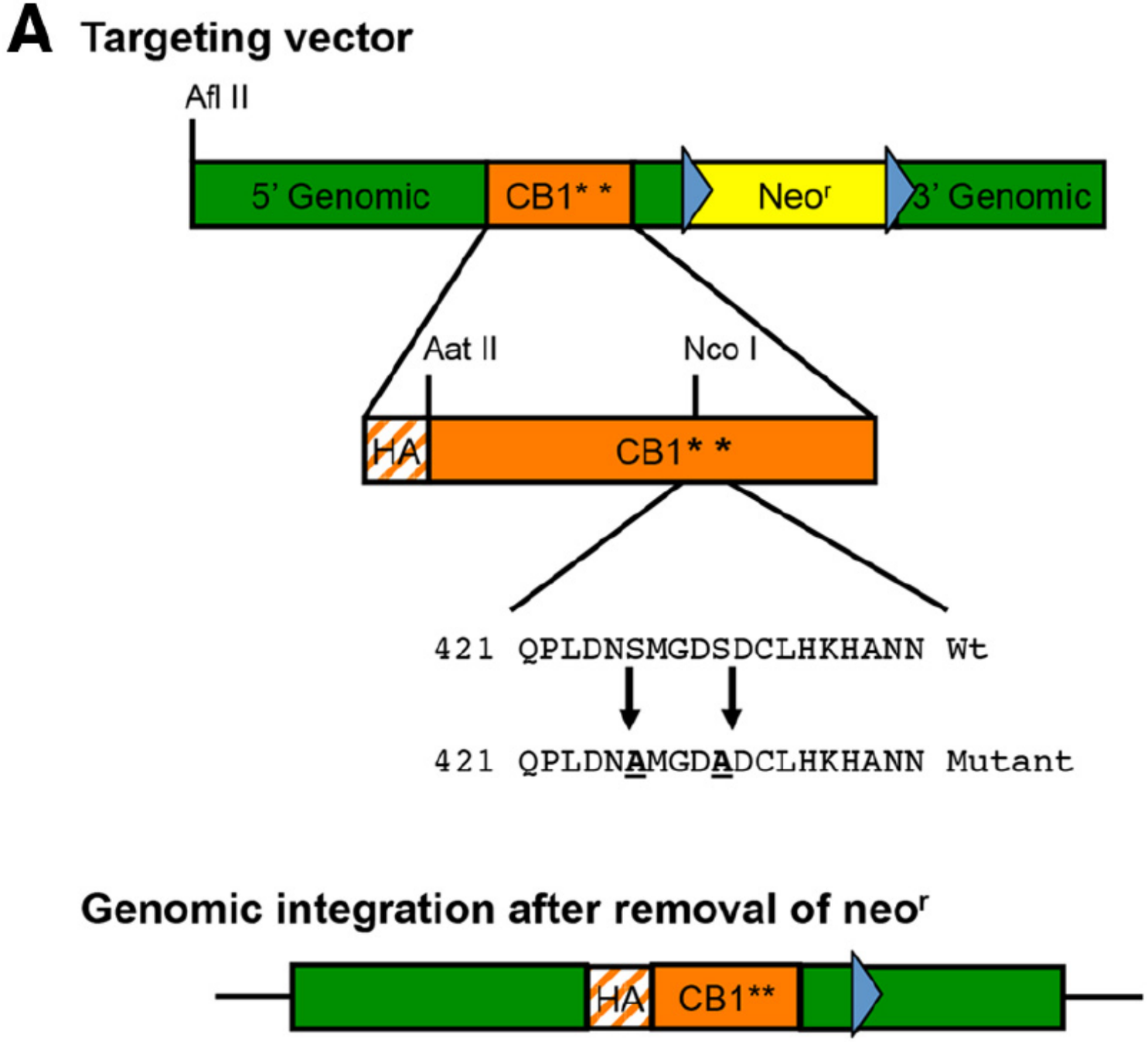
A Targeting vector
Afl II
5' Genomic
CB1* *
Neo^r
3' Genomic
Aat II
Nco I
HA
CB1* *
421 QPLDNSMGDSDCLHKHANN Wt
421 QPLDNAMGDADCLHKHANN Mutant
Genomic integration after removal of neo^r
HA
CB1**

421 QPLDNSMGDSDCLHKHANN Wt

QPLDNAMGDADCLHKHANN Mutant

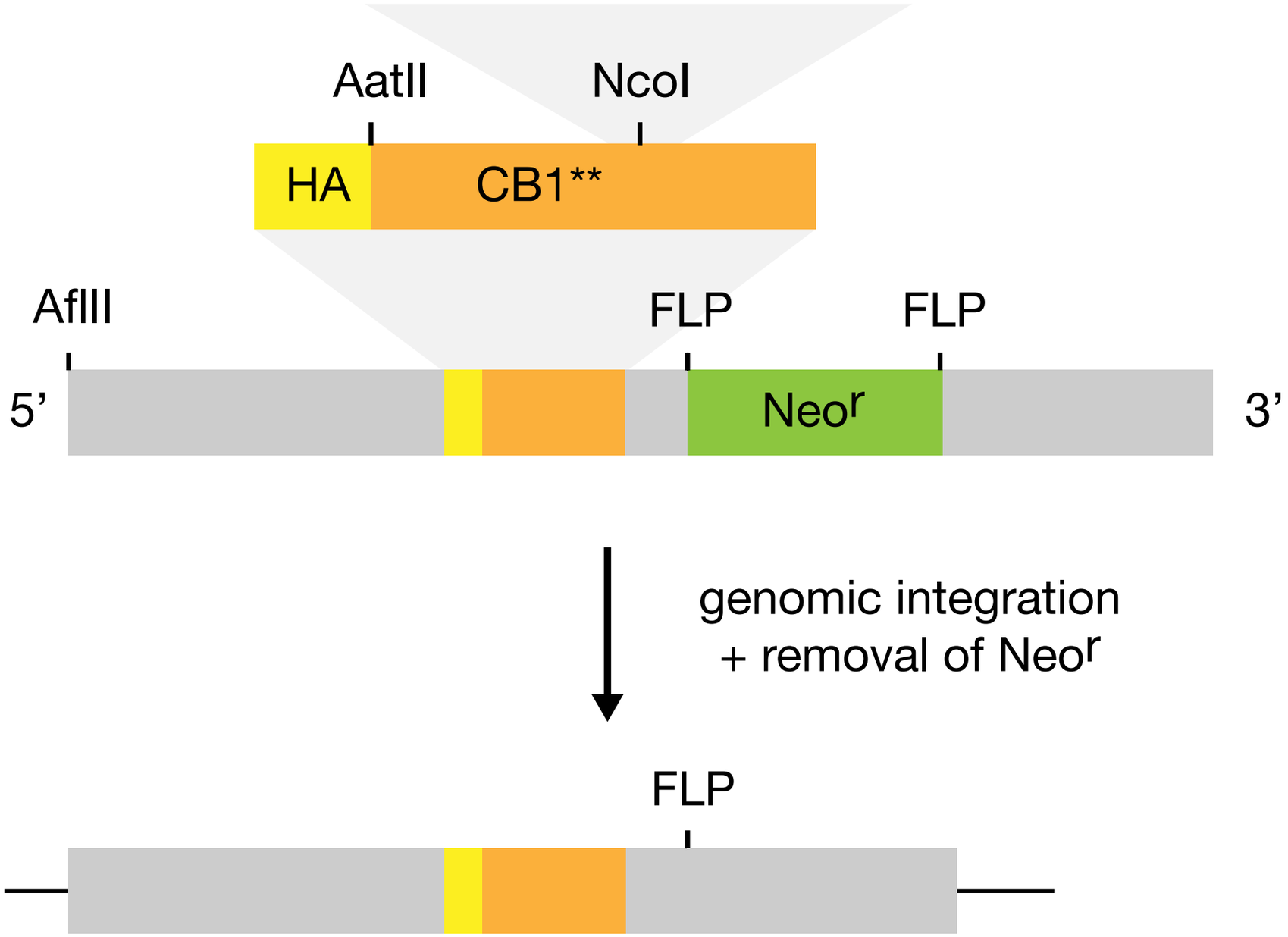

A **Targeting vector**

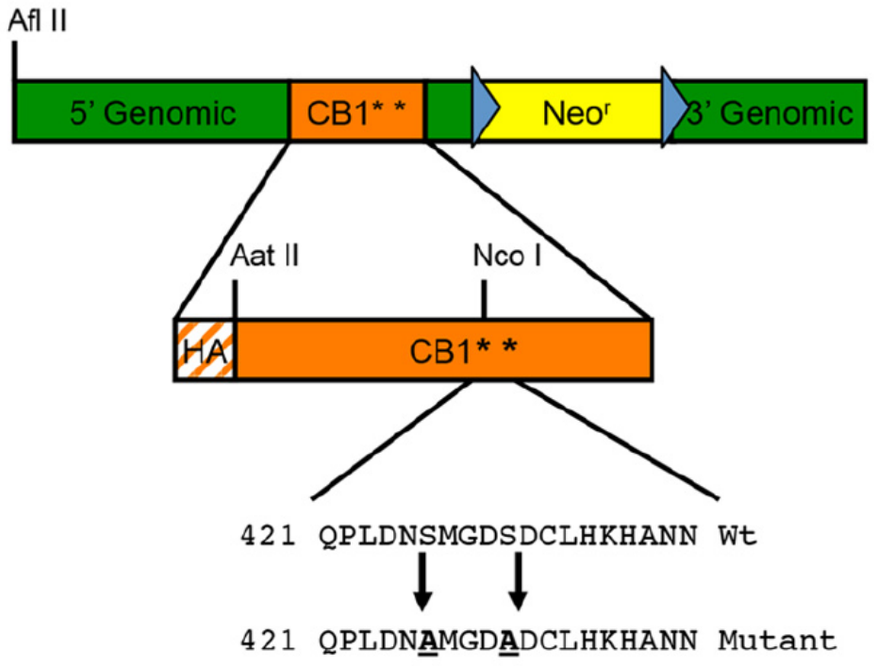

Genomic integration after removal of neo^r

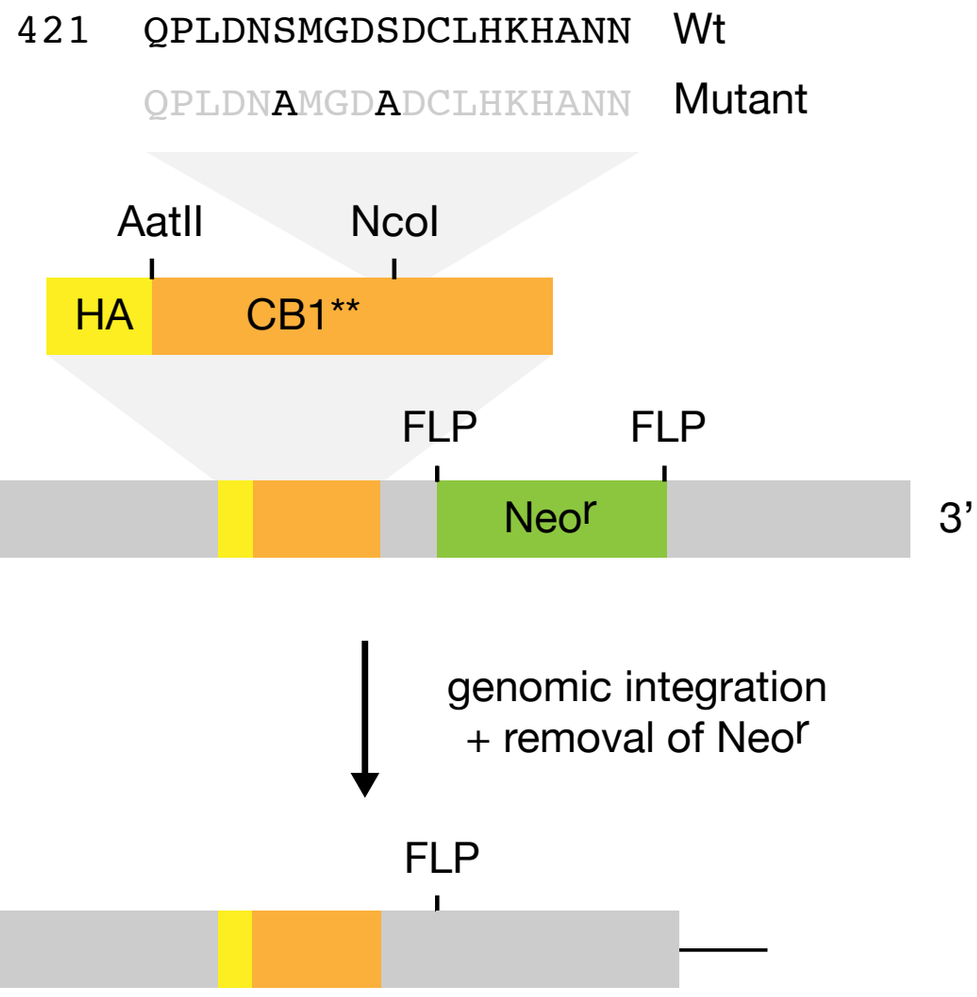

.

Species	ExF region		C-terminus
(human numbering)	420	430	500
GreenPuffer	avlg--rsgvrlecfrfstreep		pdclgeemav
Python	splgrsdclvklecfhflpsmg-		gdsledeval
Platypus	splgrrdssaklecfrflapgdr		gdslddeiav
Shark	splgmdncliklehfhflrdekr		gdclddeiav
Tasmanian Devil	splgrrdclvklecfrflppgdt		gdslddeiav
Molerat	splgrrdclvklecfrflpsedt		gdslddeiav
BushBaby	splgrrdclvklecfrflppedt		gdgldeiav
Human	**splgrrdclvklecfrflppedt**		**gdgldeiav**
Cow	splgrrdclvklecfrflppedt		gdslddeiav
Whale	splgrrdclvklecfrflppedt		gdslddeiav
Rat	splgrrdclvklecfrflpaedn		gdslddeiav
Hamster	splgrrdclvklecfrflppedt		gdslddeiav
Elephant	splgrrdclvklecfrflpsedt		gdslddeiav
Turtle	spigrsdclvkleyfrfppgaa-		gdslddeiav
Alligator	spigrsdclvklecyrflpnsm-		gdsledeiav
Finch	spigrkdclvklecyrflpd-sg		gdsledeiav
Hummingbird	spigrndclvklecyhflpdssg		gdslddeiav
Chicken	spigrndclvklecyhflps-sg		gdsledeiav
Trout	nhlgrdqcllklecfrflpgppt		pdclgdeiav
Rice Fish	splgrdqcllklerfrflpgppg		pdclgdeiav
Guppy	splgrdqcllklecfrflpgppg		pdclgdeiai
Moonfish	splgrdqcllklecfrflpgppg		pdclgdeiai
	:* . :** ::*		* * :*:*:

ExF region

C-terminus

		420												430																								500									
RESIDUE VARIATION		3	3	2	0	3	6	4	3	3	4	2	0	0	4	2	2	0	3	4	7	7	8	6		2	0	2	0	3	2	0	3	0	3
human		**s**	**p**	**l**	**g**	**r**	**r**	**d**	**c**	**l**	**v**	**k**	**l**	**e**	**c**	**f**	**r**	**f**	**l**	**p**	**p**	**e**	**d**	**t**		**g**	**d**	**g**	**l**	**d**	**d**	**e**	**i**	**a**	**v**
cow	0	·	·	·	·	·	·	·	·	·	·	·	·	·	·	·	·	·	·	·	·	·	·	·		·	·	·	·	·	·	·	·	·	·
whale	0	·	·	·	·	·	·	·	·	·	·	·	·	·	·	·	·	·	·	·	·	·	·	·		·	·	·	·	·	·	·	·	·	·
bushbaby	0	·	·	·	·	·	·	·	·	·	·	·	·	·	·	·	·	·	·	·	·	·	·	·		·	·	·	·	·	·	·	·	·	·
tasmanian devil	0	·	·	·	·	·	·	·	·	·	·	·	·	·	·	·	·	·	·	·	·	·	·	·		·	·	·	·	·	·	·	·	·	·
molerat	1	·	·	·	·	·	·	·	·	·	·	·	·	·	·	·	·	·	·	s	·	·	·			·	·	·	·	·	·	·	·	·	·
hamster	1	·	·	·	·	·	·	·	·	·	·	·	·	·	·	·	·	·	·	·	·	·	·	t		·	·	·	·	·	·	·	·	·	·
rat	2	·	·	·	·	·	·	·	·	·	·	·	·	·	·	·	·	·	·	a	·	·	n			·	·	·	·	·	·	·	·	·	·
elephant	2	·	·	·	·	·	·	·	·	·	·	·	·	·	·	·	·	·	·	s	·	·	t			·	·	·	·	·	·	·	·	·	·
platypus	6	·	·	·	·	·	·	s	s	a	·	·	·	·	·	·	·	·	·	a	·	g	·	r		·	·	·	·	·	·	·	·	·	·
alligator	7	·	·	i	·	·	s	·	·	·	·	·	·	·	·	y	·	·	·	n	s	m	–			·	·	·	·	·	·	·	·	·	·
finch	7	·	·	i	·	·	k	·	·	·	·	·	·	·	·	y	·	·	·	d	–	s	g			·	·	·	·	·	·	·	·	·	·
turtle	8	·	·	i	·	·	s	·	·	·	·	·	·	·	y	·	·	p	·	g	a	a	–			·	·	·	·	·	·	·	·	·	·
chicken	7	·	·	·	·	·	n	·	·	·	·	·	·	·	y	h	·	·	·	s	–	s	g			·	·	·	·	·	·	·	·	·	·
hummingbird	8	·	·	i	·	·	n	·	·	·	·	·	·	·	y	h	·	·	·	d	s	s	g			·	·	·	·	·	·	·	·	·	·
python	9	·	·	·	·	·	s	·	·	·	·	·	·	·	·	r	·	·	·	s	m	g	–			·	·	·	·	e	·	·	v	·	l
shark	10	·	·	·	·	m	d	n	·	·	i	·	·	h	·	h	·	·	r	d	·	k	r			·	·	·	·	·	·	·	·	·	·
guppy	11	·	·	·	·	·	d	q	c	·	l	·	·	·	·	·	·	·	·	g	p	p	g		p	·	c	·	g	·	·	·	·	·	·
moonfish	12	·	·	·	·	·	d	q	c	·	l	·	·	·	·	·	·	·	·	g	p	p	g		p	·	c	·	g	·	·	·	i		
rice fish	12	·	·	·	·	·	d	q	c	·	l	·	·	r	·	·	·	·	·	g	p	p	g		p	·	c	·	g	·	·	·	·	·	·
trout	12	n	h	·	·	d	q	c	·	l	·	·	·	·	·	·	·	·	·	g	p	p	t		p	·	c	·	g	·	·	·	·	·	·
green puffer	19	a	v	·	·	–	–	r	s	g	·	r	·	·	·	·	·	s	t	r	·	e	p		p	·	c	·	g	e	·	m	·	v	

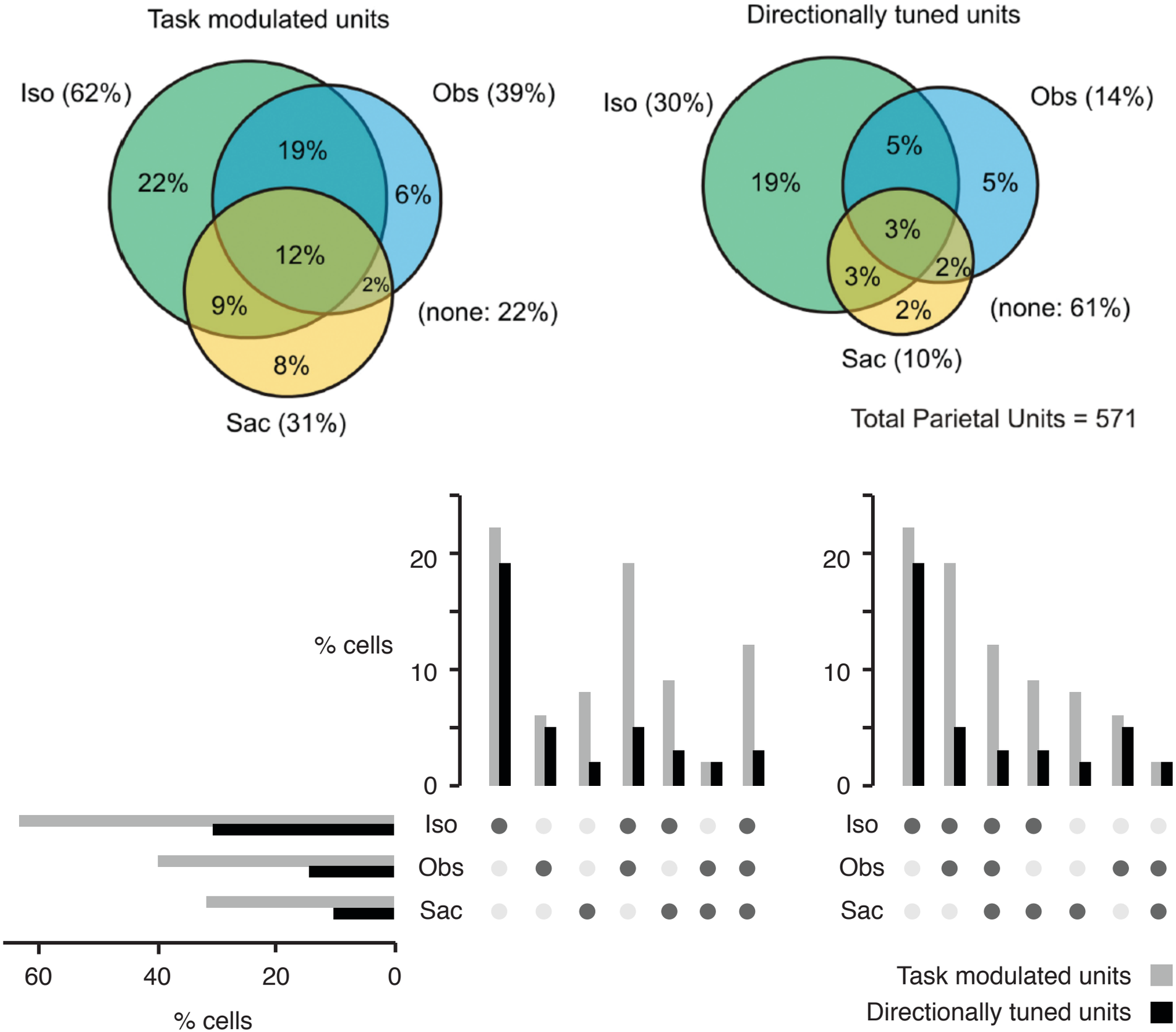

Ferrari-Toniolo, S., et al., *Posterior Parietal Cortex Encoding of Dynamic Hand Force Underlying Hand-Object Interaction.* Journal of Neuroscience, 2015. **35**(31): p. 10899-10910.

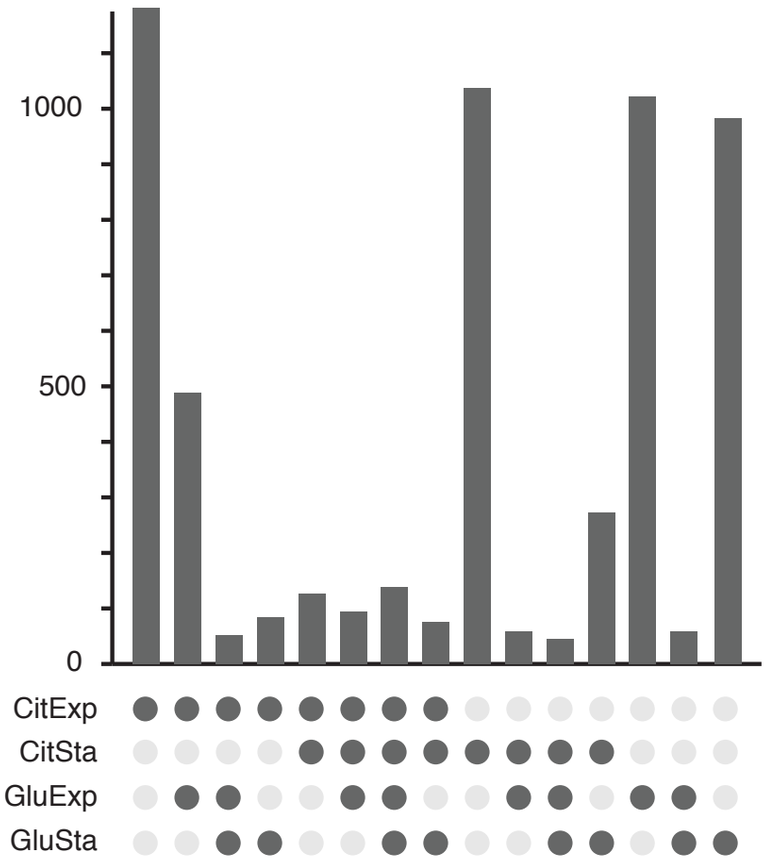

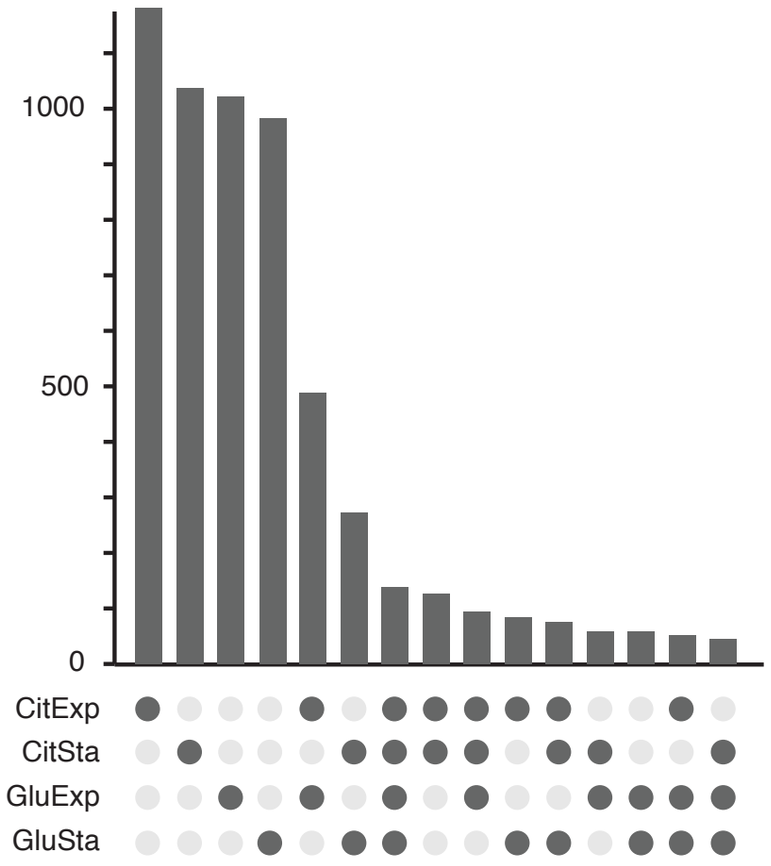

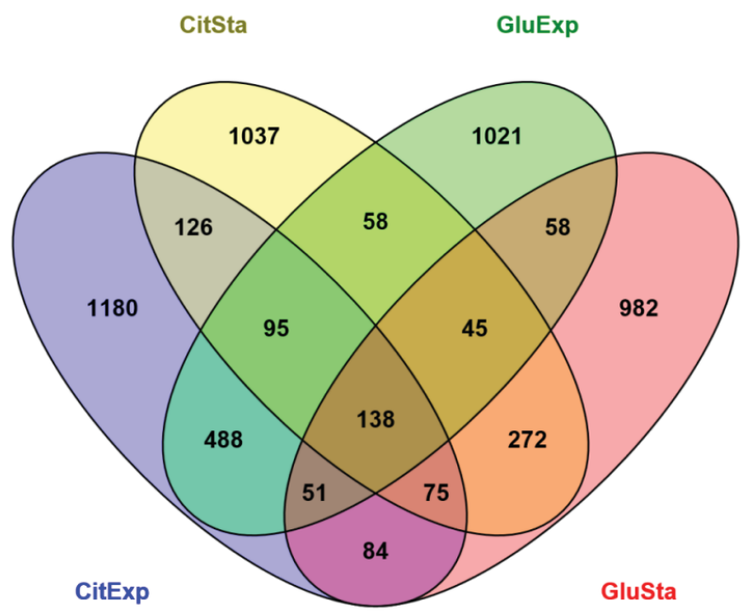

UpSet encoding

A

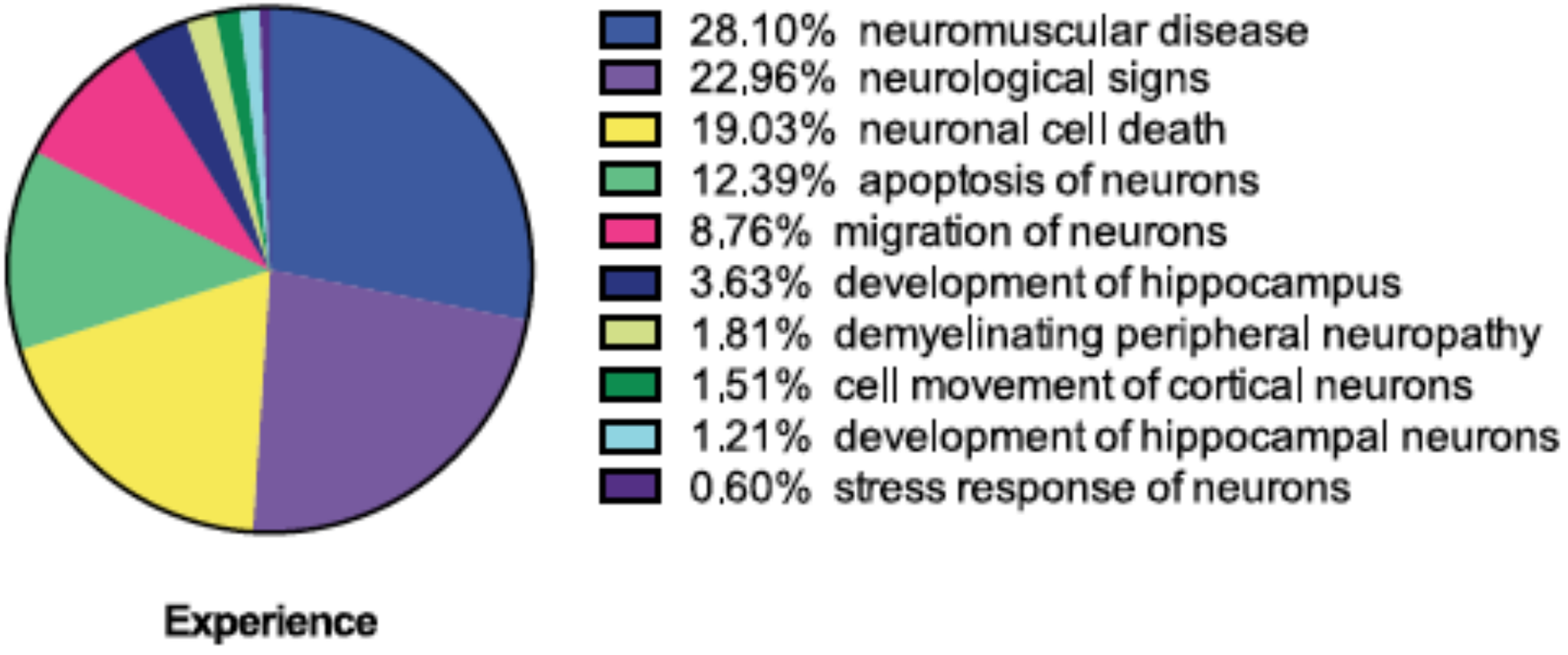

Experience

B

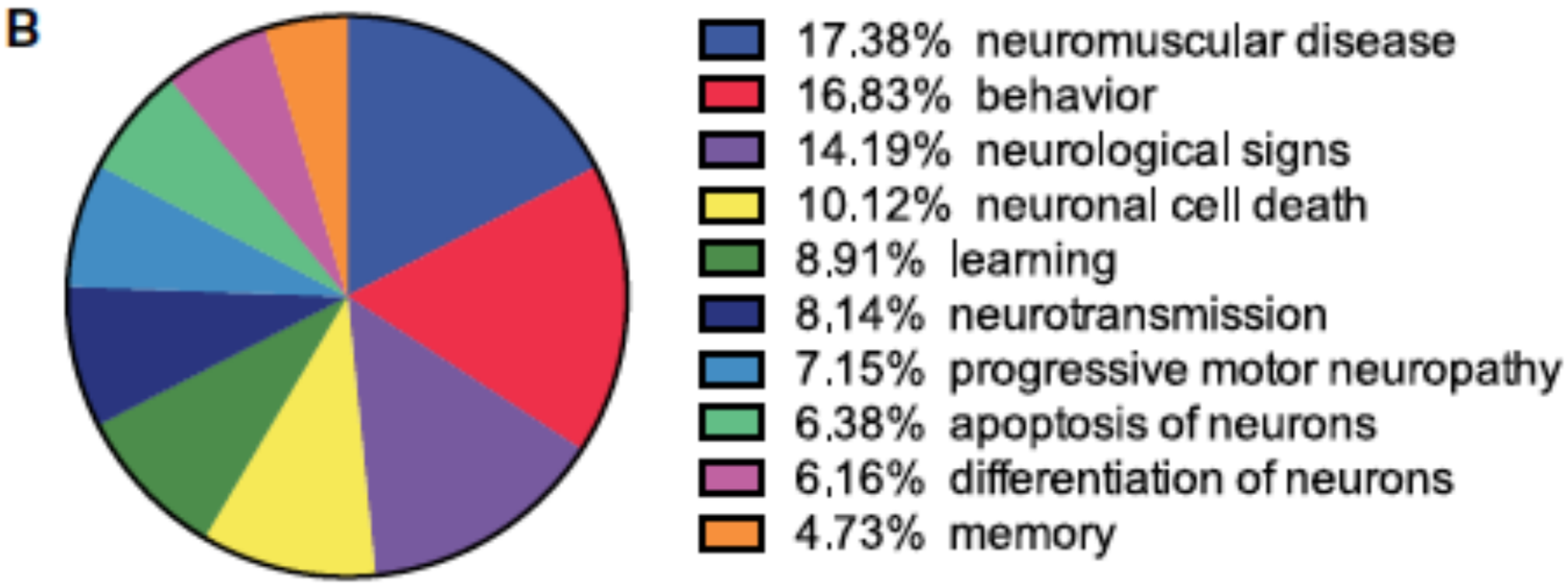

Experience + HDAC Inhibition

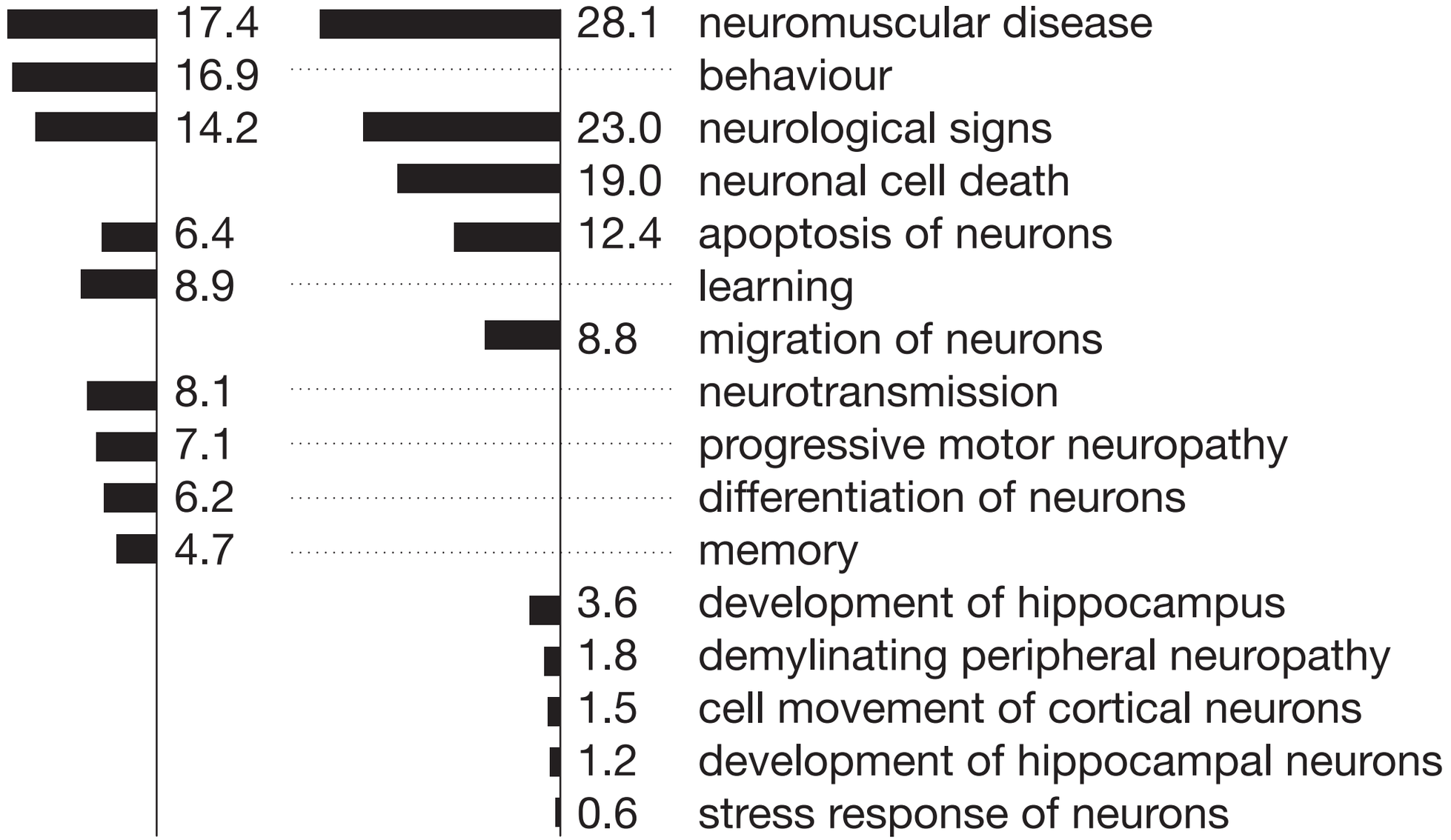
17.4
16.9
14.2
6.4
8.9
8.1
7.1
6.2
4.7
28.1 neuromuscular disease
behaviour
23.0 neurological signs
19.0 neuronal cell death
12.4 apoptosis of neurons
learning
8.8 migration of neurons
neurotransmission
progressive motor neuropathy
differentiation of neurons
memory
3.6 development of hippocampus
1.8 demylinating peripheral neuropathy
1.5 cell movement of cortical neurons
1.2 development of hippocampal neurons
0.6 stress response of neurons

A TYPICAL NETWORK ANALYSIS PIPELINE

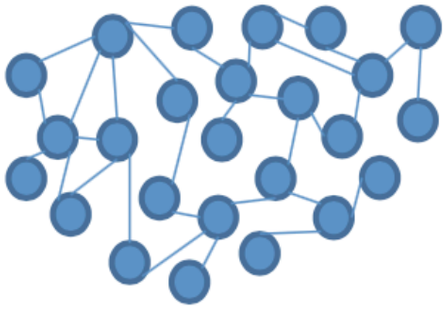

Biological network

Usually known gene co-expression networks, or Protein-Protein Interaction networks

Seed Gene List
FOXP2
CDH8
CDH5
…

Usually based on association with a particular phenotype, or determined to be of interest experimentally

Annotation with Seed list

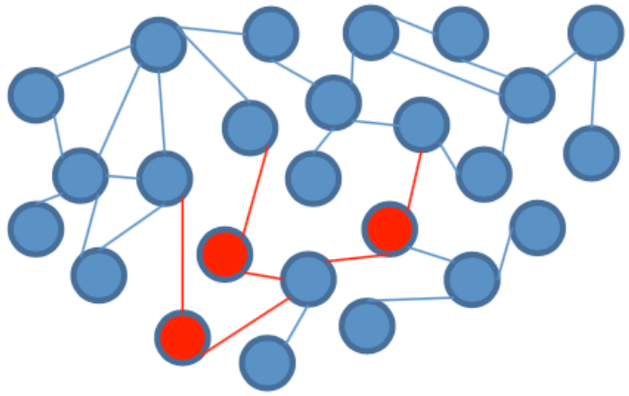

Clustering groups of genes

Can be based on specific pathways, functional annotation from KEGG, or other clustering methods

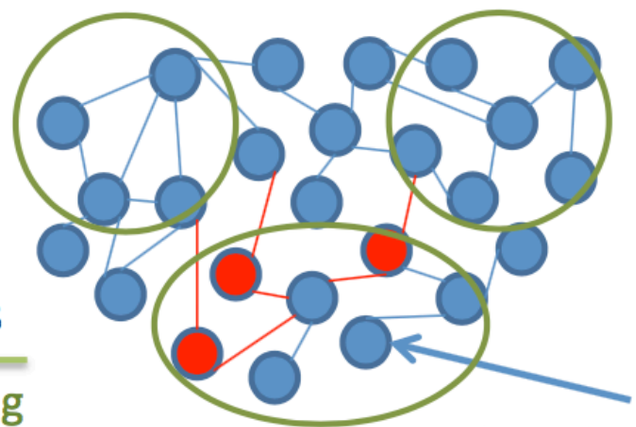

What does that do?

Get list of candidate genes

Derived from clusters containing genes from Seed list

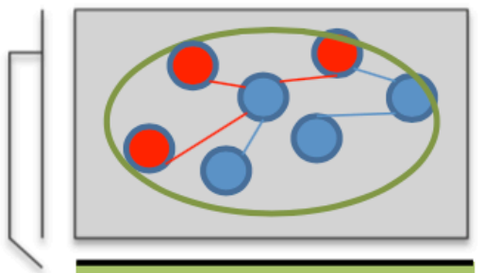

Candidate Gene List
FOXP2
BRCA1
TP53
…

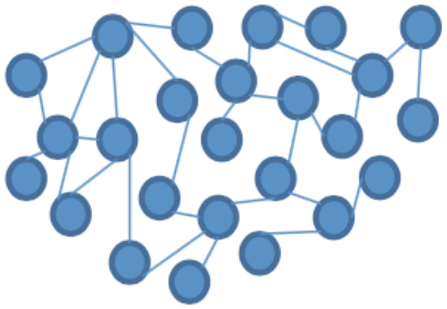

Seed Gene List
FOXP2
CDH8
CDH5
...

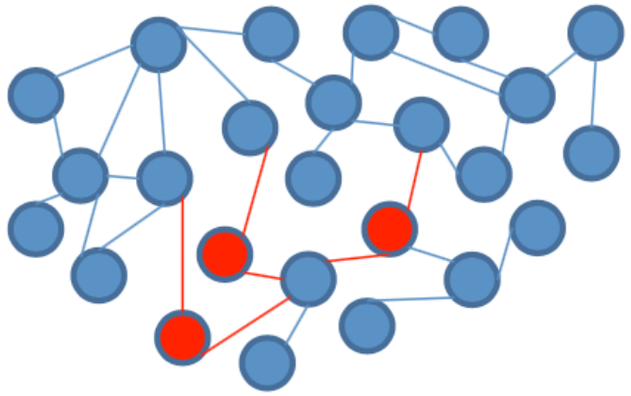

A TYPICAL NETWORK ANALYSIS PIPELINE

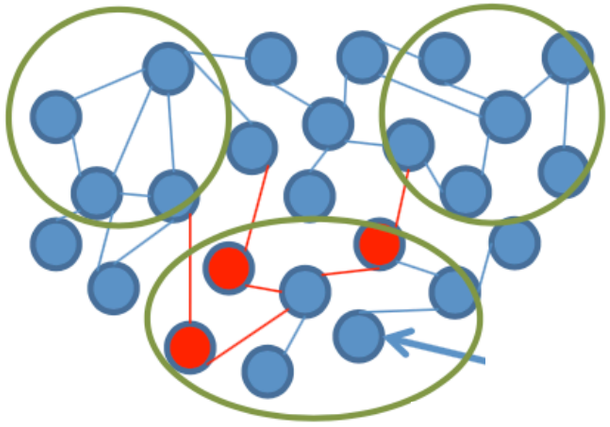

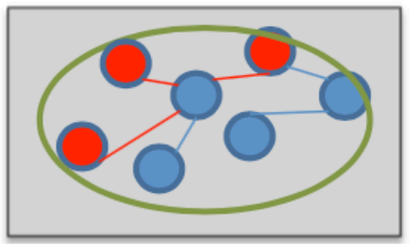

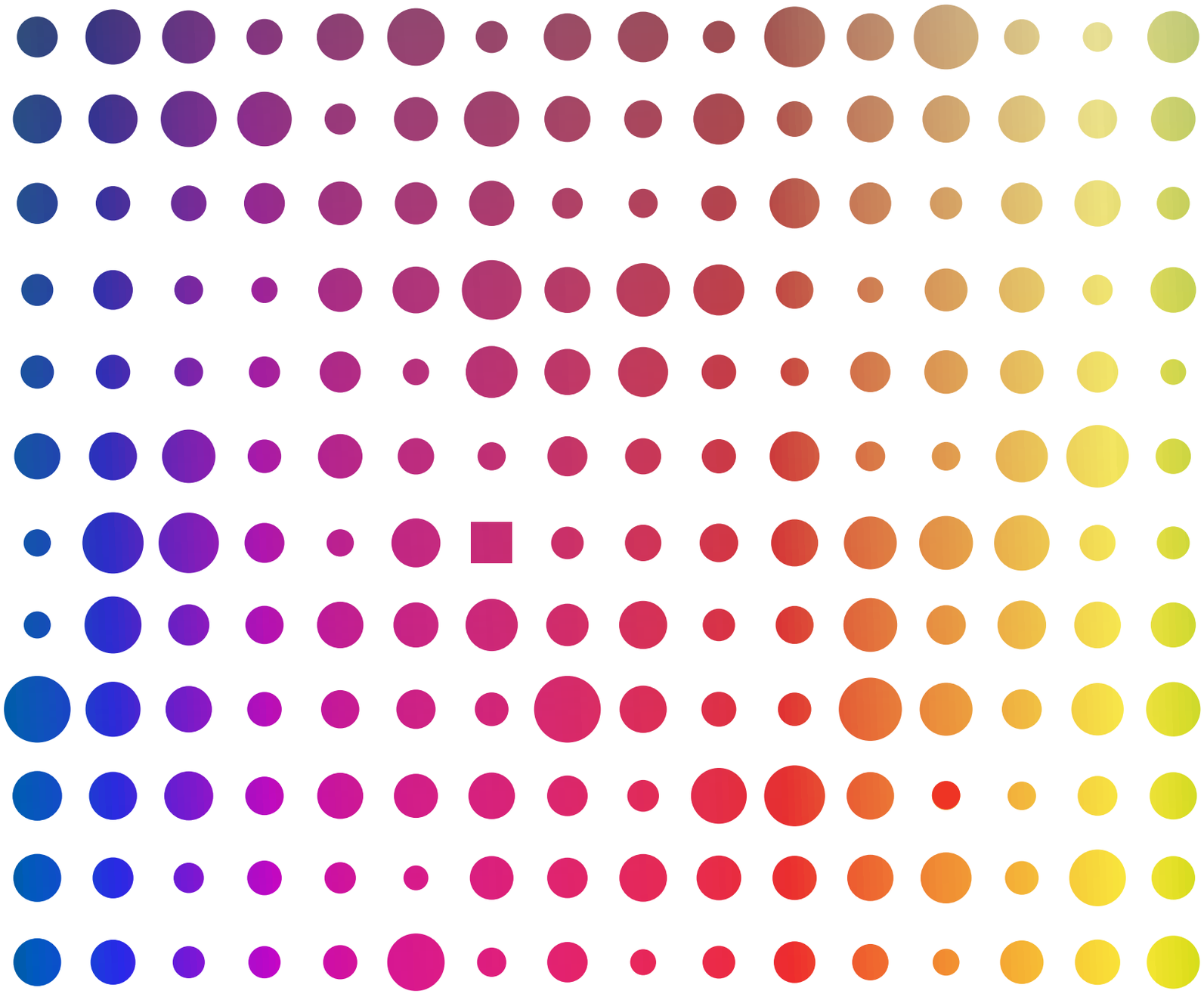

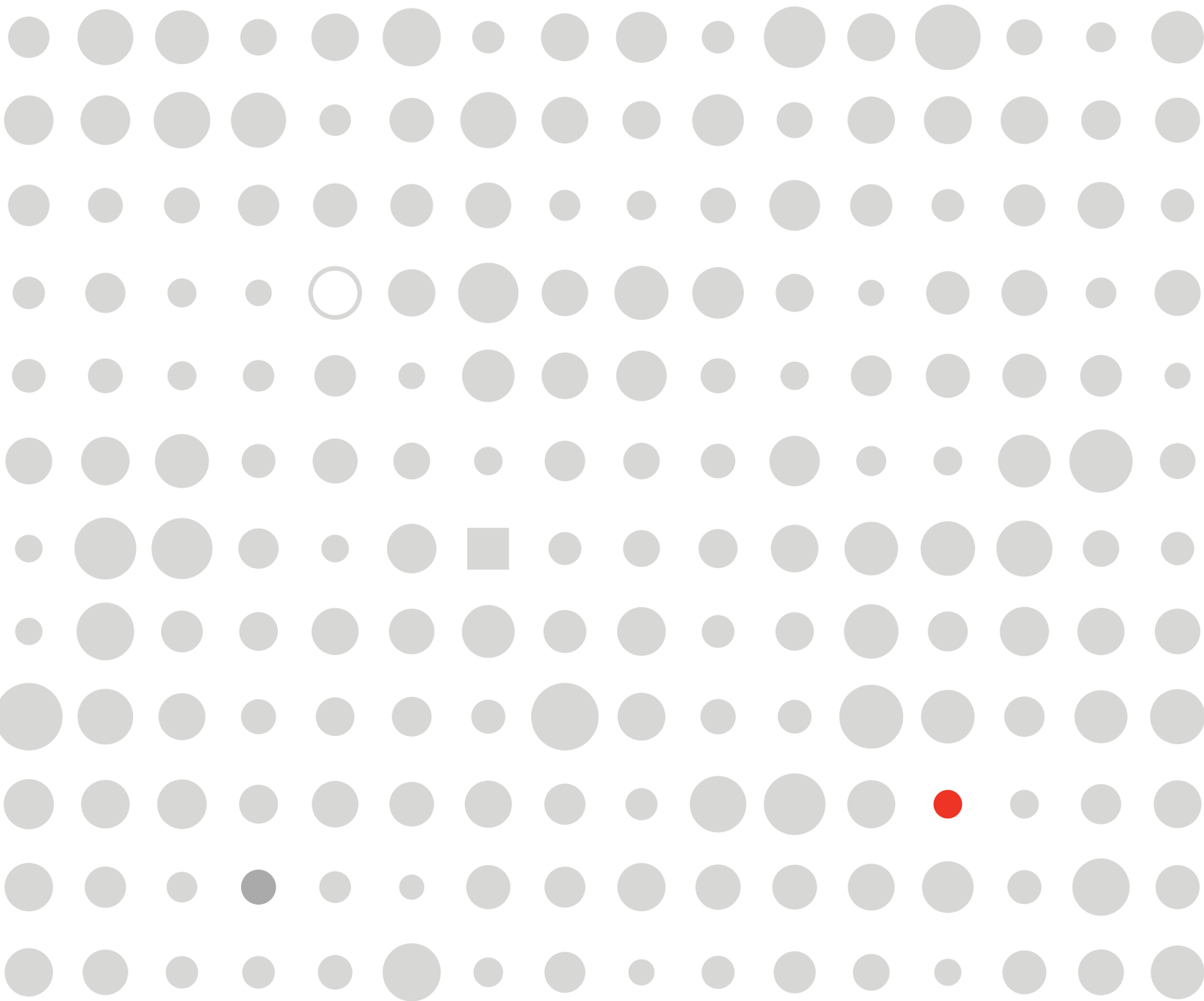

typical network analysis pipeline

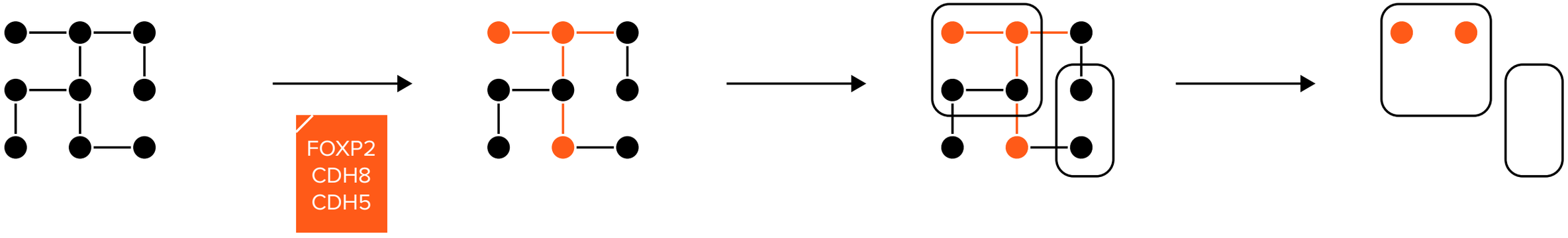

typical network analysis pipeline

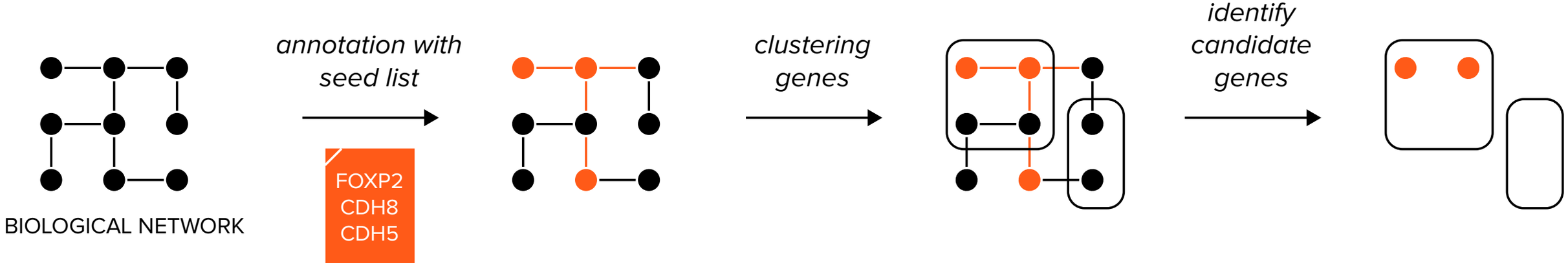

typical network analysis pipeline

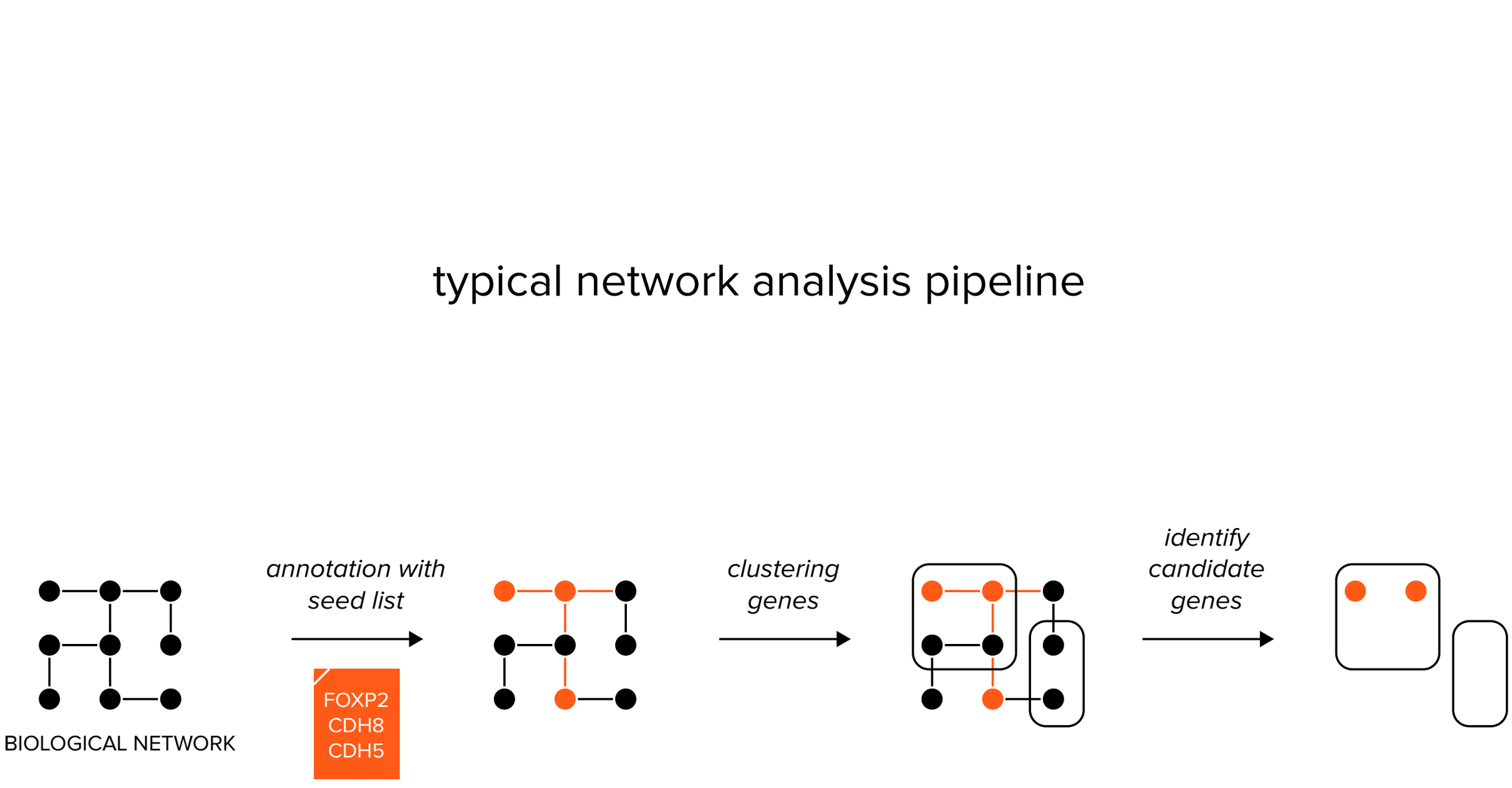

gene co-expression
protein-protein
interaction

association with
particular
phenotype or
otherwise
of interest

based on pathways,
functional
annotation (KEGG) or
other clustering methods

derived from clusters
containing genes from
seed list

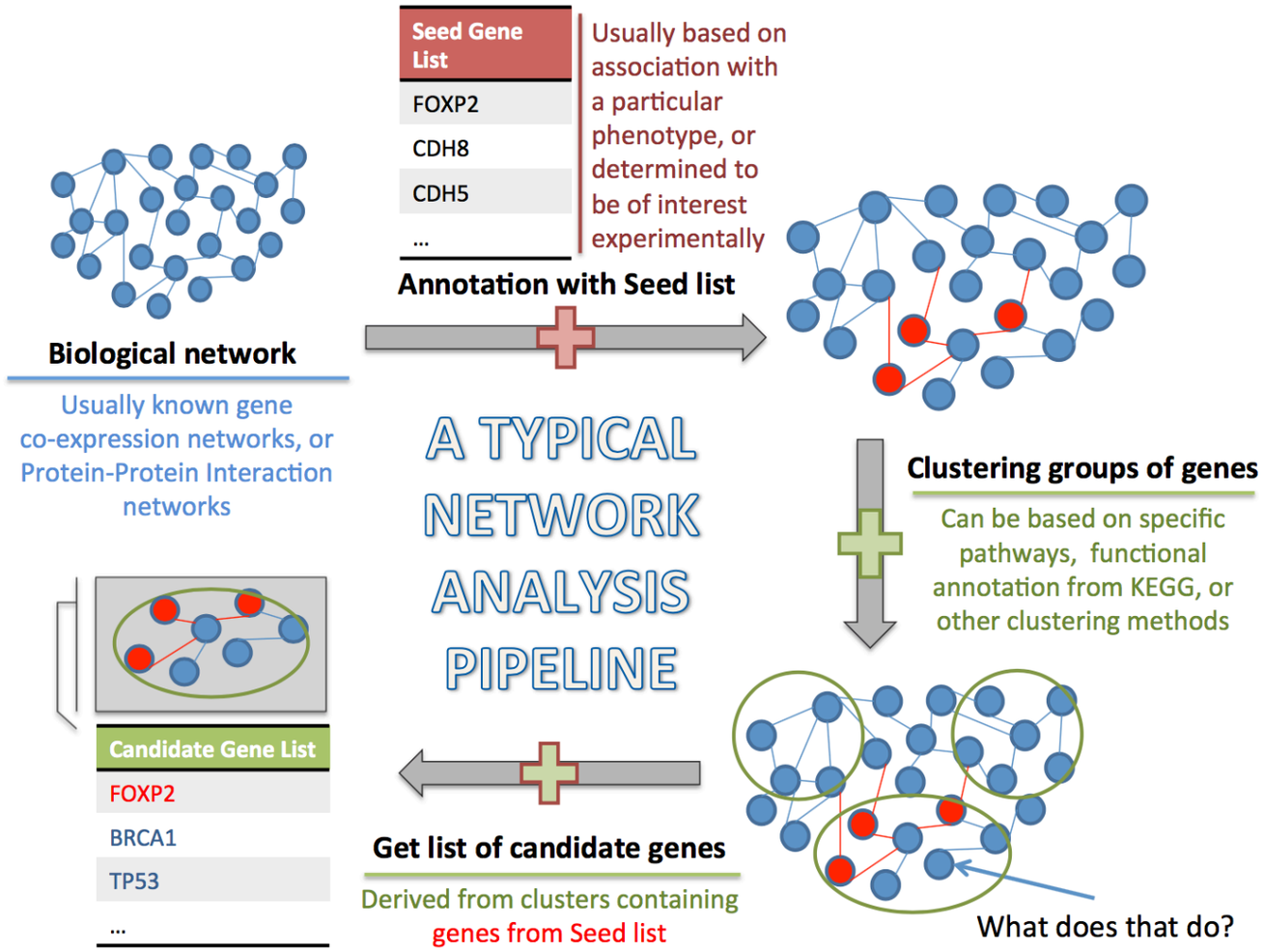
Seed Gene List
FOXP2
CDH8
CDH5
...
Usually based on association with a particular phenotype, or determined to be of interest experimentally
Annotation with Seed list
Biological network
Usually known gene co-expression networks, or Protein-Protein Interaction networks
A TYPICAL NETWORK ANALYSIS PIPELINE
Clustering groups of genes
Can be based on specific pathways, functional annotation from KEGG, or other clustering methods
Candidate Gene List
FOXP2
BRCA1
TP53
...
Get list of candidate genes
Derived from clusters containing genes from Seed list
What does that do?

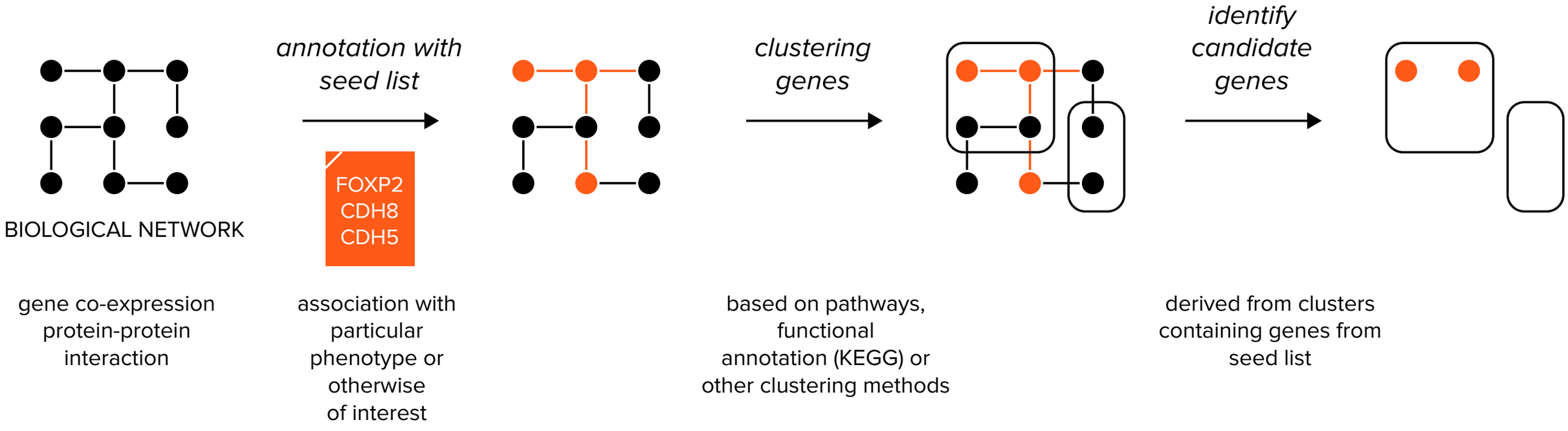
BIOLOGICAL NETWORK
gene co-expression
protein-protein
interaction
annotation with
seed list
FOXP2
CDH8
CDH5
association with
particular
phenotype or
otherwise
of interest
clustering
genes
based on pathways,
functional
annotation (KEGG) or
other clustering methods
identify
candidate
genes
derived from clusters
containing genes from
seed list

Real time imaging of live cell membrane using laser trapping, reflectance confocal microscopy, and multiphoton fluorescence microscopy

Yunxian Tian[a,b], Shangyuan Feng[a,b], Yimei Huang[a,b], Jianhua Zhao[a,b], Eddie Shen[a,b], Wenbo Wang[a,b,c], Caigan Du[d], and Haishan Zeng[a,b,*] (* hzeng@bccrc.ca)

[a]Imaging Unit-Integrative Oncology Department, British Columbia Cancer Research Centre [b]Photomedicine Institute – Department of Dermatology and Skin Science, University of British Columbia [c]Department of Biomedical Engineering, University of British Columbia [d]Department of Urologic Sciences, University of British Columbia

INTRODUCTION

Cell membrane would spontaneously reseal after injury. However this repair mechanism remains unknown. To study the repair process in detail, It is necessary to finely tune the wounding technology and acquire high speed real time imaging during the short repairing time. Traditional methods to induce plasma membrane damage such as mechanical tear and toxins fail to keep the cell alive. Current technology, neither micropipette nor electroporation/sonoporation can facilitate a precise control for studying single cell damage.

Two photon laser wounding technology combined with laser tweezer Raman spectroscopy (LTRS) has precise control of the membrane disruption size by tuning laser power and shutter time.

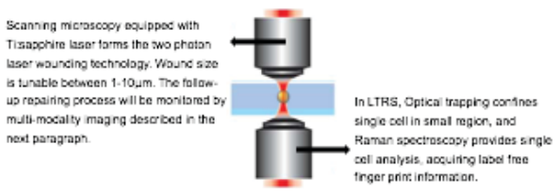

Laser scanning microscopy provides reflectance confocal (RCM) image and two photon fluorescence (TPF) image simultaneously at 15 frames per second.

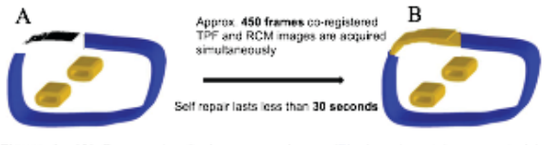

Figure 1 **(A)** Damaged cell plasma membrane (Blue) and protein generated in Endoplasmic reticulum (ER) (yellow) **(B)** repaired plasma membrane with patch (yellow), which is synthesized from these protein.

Technical challenges:

Imaging speed: high enough to monitor membrane repair process in 30 seconds.

Resolution: determines the image quality and how accurate the laser would induce the localized wounds.

Imaging cell stability: laser tweezer technique stabilize the cell avoiding any movement.

METHODS

We can acquire LTRS spectroscopy, RCM imaging and TPF imaging. Wide-field white light imaging is integrated in the system to facilitate large field of view imaging of the sample.

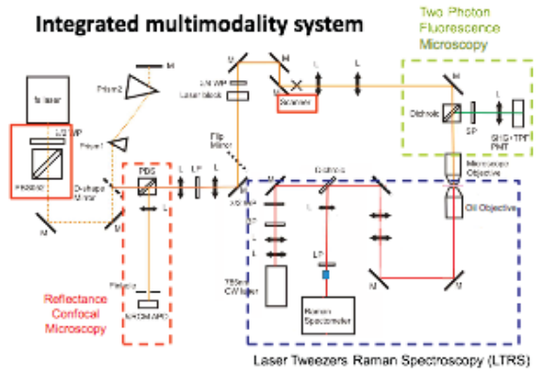

Figure 1 System diagram of LTRS, RCM and TPF imaging. WP: wave plate; PBS: polarization beam splitter; M: mirror; FM: flip mirror; APD: avalanche photodiode; L: lens; LP: long-pass filter; SP: short-pass filter; PMT: photon multiplier tube.

Example of single T lymphoma cell RCM image (A) and TPF image (B and C: membrane and nuclei). False colors were used for different imaging modalities to facilitate multimodality image overlay.

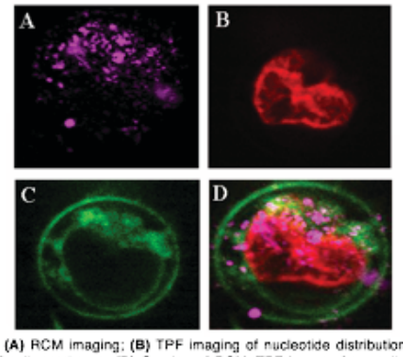

Figure 2 **(A)** RCM imaging; **(B)** TPF imaging of nucleotide distribution; **(C)** TPF imaging of cell membrane; **(D)** Overlay of RCM+TPF images from cell nucleotide and membrane.

Acknowledge Youngwood for figure demonstration

Experimental procedure:

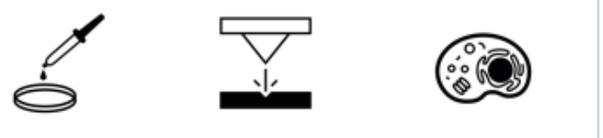

RESULTS

We have successfully demonstrate T lymphoma cell plasma membrane damage (Figure 3) and repair process (Figure 4) in real time. *In vivo* Raman spectra is shown in Figure 5.

Two photon laser wounding technique induce T cell membrane localized damage in short exposure time

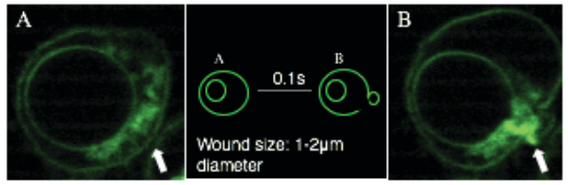

Figure 3 **(A)** TPF imaging of cell membrane before laser wounding. Endoplasmic reticulum (ER) is shown in between neuclei membrane and plasma membrane. **(B)** After laser wounding, cytoplasm leak through plasma membrane hole. At the edge of hole, blebs might be generated.

T cell plasma membrane reseals in 21 seconds

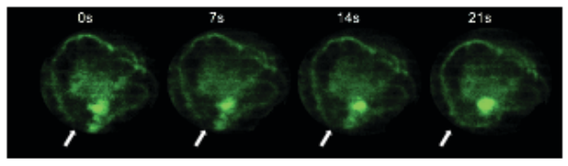

Figure 4 TPF imaging of plasma membrane resealing process. Extracted images from original video format shown as above at 0s, 7s, 14s, and 21s.

Raman spectra provide molecular composition *in vivo*

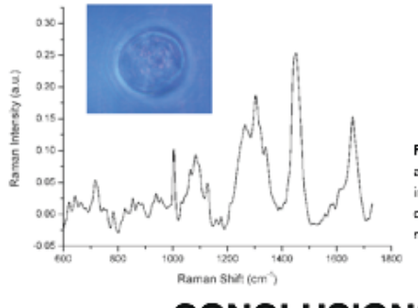

Figure 5 Raman spectra and (insert) white light image of T cell. Each peak correspond with unique molecular composition.

CONCLUSIONS

1. **Multi-modality system combined two photon laser wounding technology with LTRS, RCM imaging and TPF imaging for repairing monitoring has been demonstrated.**
2. **Combined multi-modality system has potential to analyze cellular dynamics.**

Declaration of conflict of interest: *The authors declare no conflict of interest*

Please contact Giselle (Yunxian Tian) ytian@bccrc.ca for further inquiry

Scanning microscopy equipped with Ti:sapphire laser forms the two photon laser wounding technology. Wound size is tunable between 1-10μm. The follow-up repairing process will be monitored by multi-modality imaging described in the next paragraph.

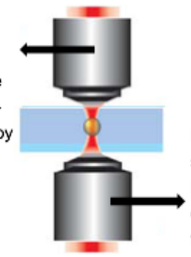

In LTRS, Optical trapping confines single cell in small region, and Raman spectroscopy provides single cell analysis, acquiring label free finger print information.

Laser scanning microscopy provides reflectance confocal (RCM) image and two photon fluorescence (TPF) image simultaneously at 15 frames per second.

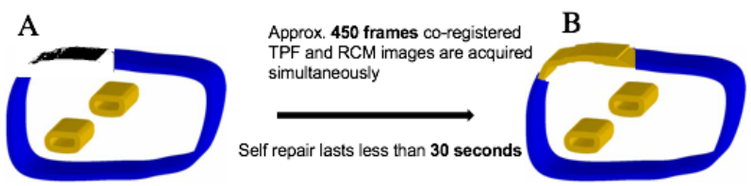

Figure 1 **(A)** Damaged cell plasma membrane (Blue) and protein generated in Endoplasmic reticulum (ER) (yellow) **(B)** repaired plasma membrane with patch (yellow), which is synthesized from these protein.

Technical challenges:

Imaging speed: high enough to monitor membrane repair process in 30 seconds.

Resolution: determines the image quality and how accurate the laser would induce the localized wounds.

Imaging cell stability: laser tweezer technique stabilize the cell avoiding any movement.

polarization beam splitter; M: mirror; FM: flip mirror; APD: avalanche photodiode; L: lens; LP: long-pass filter; SP: short-pass filter; PMT: photon multiplier tube.

Example of single T lymphoma cell RCM image (A) and TPF image (B and C: membrane and nuclei). False colors were used for different imaging modalities to facilitate multimodality image overlay.

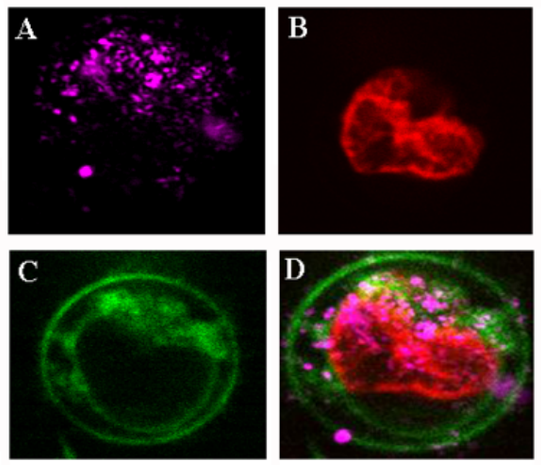

Figure 2 **(A)** RCM imaging; **(B)** TPF imaging of nucleotide distribution; **(C)** TPF imaging of cell membrane; **(D)** Overlay of RCM+TPF images from cell nucleotide and membrane.

Acknowledge Nounproject for figure demonstration

Experimental procedure:

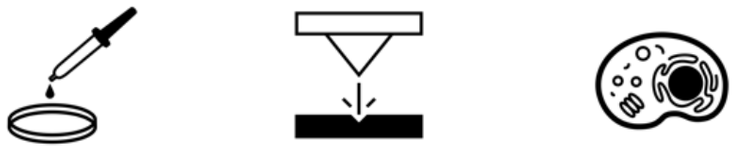

1) Culture T lymphoma cell line
2) Membrane staining

3) Trap single cell with LTRS
4) Induce membrane injury with two photon laser wounding technique

5) Observe membrane repair process

T cell plasma membrane reseals in 21 seconds

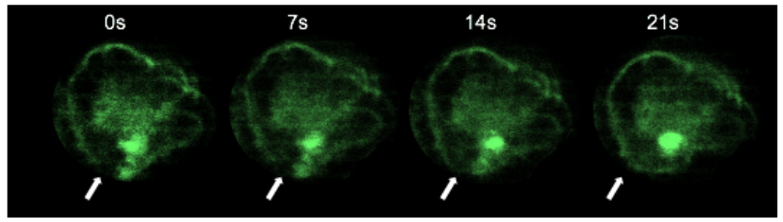

Figure 4 TPF imaging of plasma membrane resealing process. Extracted images from original video format shown as above at 0s, 7s, 14s, and 21s.

Raman spectra provide molecular composition *in vivo*

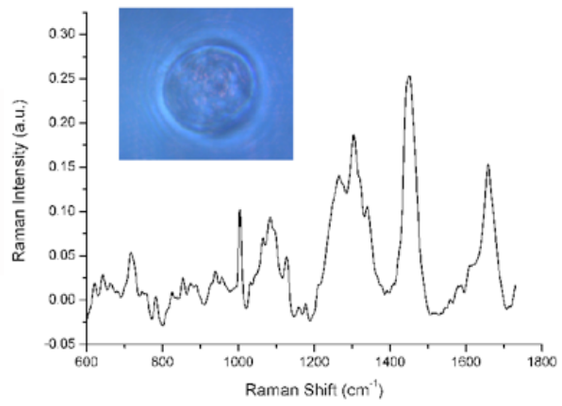

Figure 5 Raman spectra and (insert) white light image of T cell. Each peak correspond with unique molecular composition.

CONCLUSIONS

1. **Multi-modality system combined two photon laser wounding technology with LTRS, RCM imaging and TPF imaging for repairing monitoring has been demonstrated.**
2. **Combined multi-modality system has potential to analyze cellular dynamics.**

Real time imaging of live cell membrane using laser trapping, reflectance confocal microscopy, and multiphoton fluorescence microscopy

Yunxian Tian Shangyuan Feng Yimei Huang Jianhua Zhao Eddie Shen Wenbo Wang Caigan Dud Haishan Zenga

Imaging Unit-Integrative Oncology Department, British Columbia Cancer Research Centre
Photomedicine Institute – Department of Dermatology and Skin Science, University of British Columbia
Department of Biomedical Engineering, University of British Columbia dDepartment of Urologic Sciences, University of British Columbia

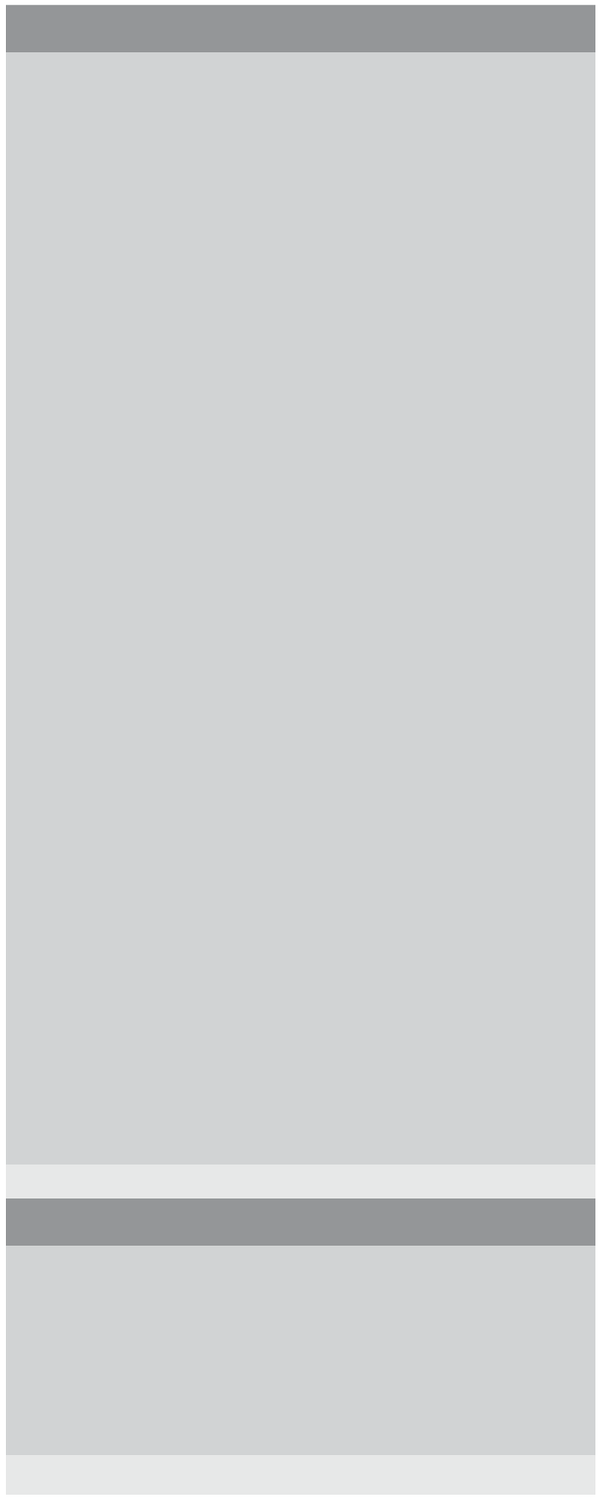

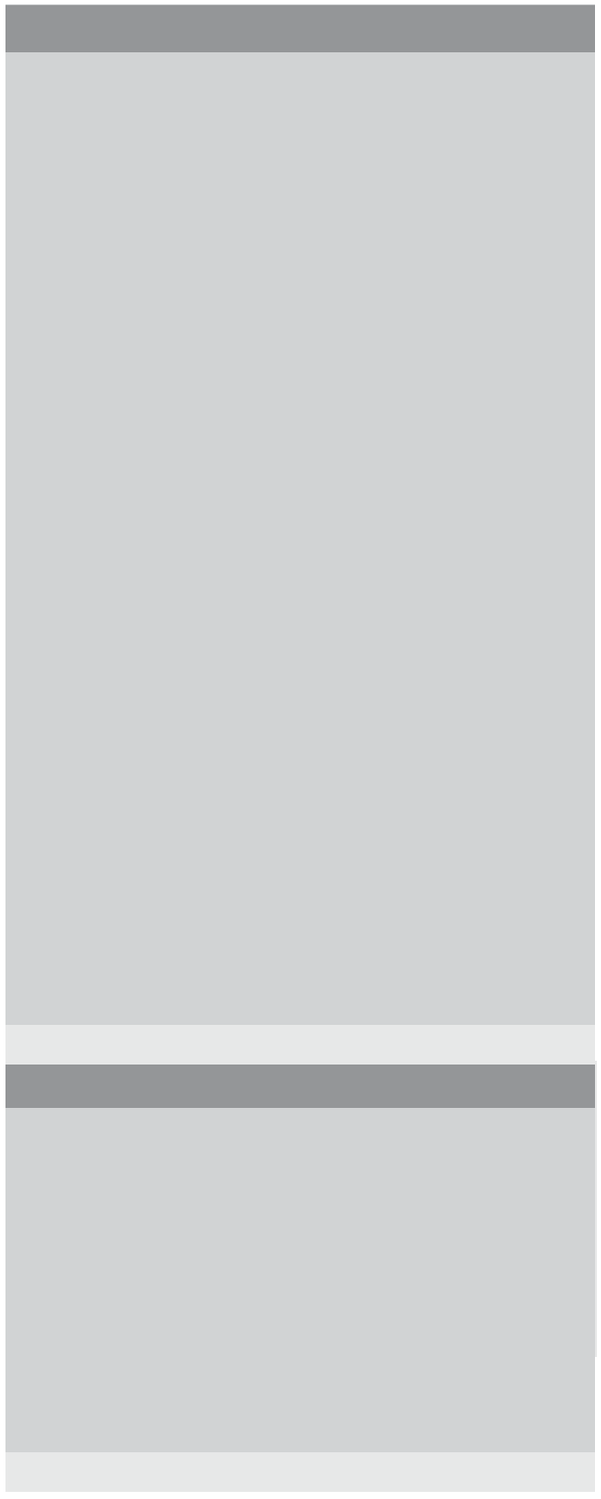

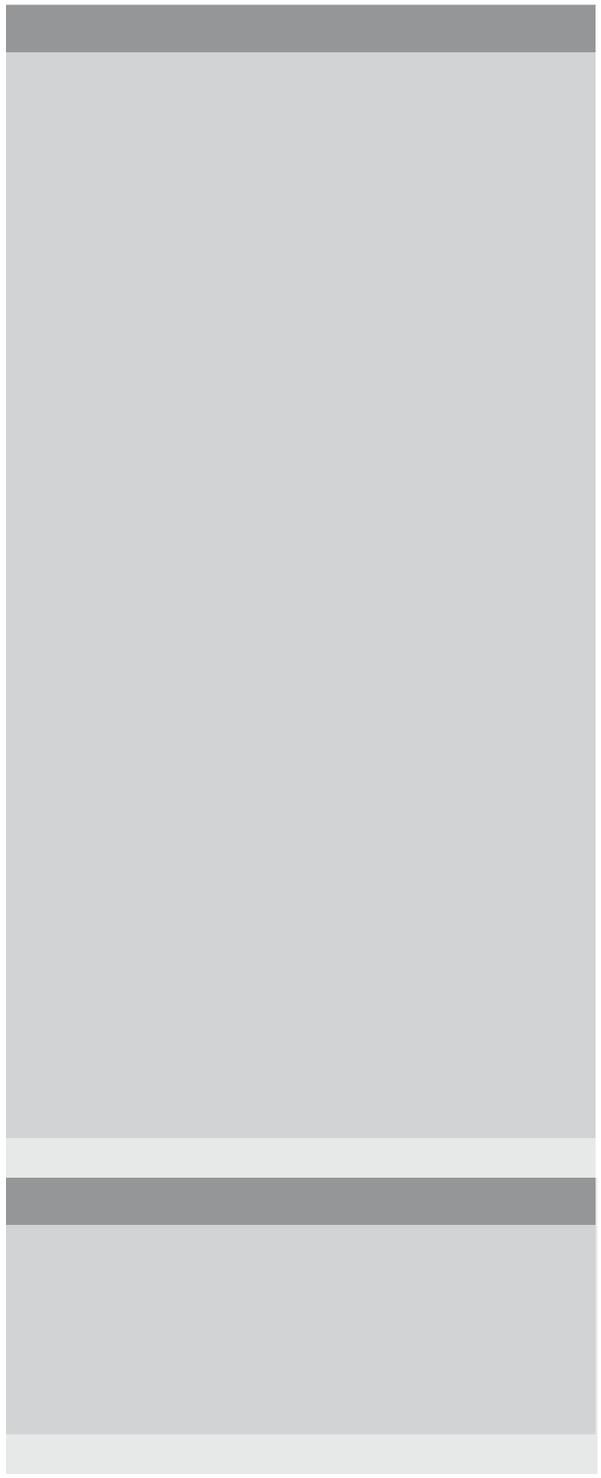

Real time imaging of live cell membrane using laser trapping, reflectance confocal microscopy, and multiphoton fluorescence microscopy

Yunxian Tian Shangyuan Feng Yimei Huang Jianhua Zhao Eddie Shen Wenbo Wang Caigan Dud Haishan Zenga

Imaging Unit-Integrative Oncology Department, British Columbia Cancer Research Centre
Photomedicine Institute – Department of Dermatology and Skin Science, University of British Columbia
Department of Biomedical Engineering, University of British Columbia dDepartment of Urologic Sciences, University of British Columbia

INTRODUCTION

Cell membrane would spontaneously reseal after injury. However this repair mechanism remains unknown. To study the repair process in detail, It is necessary to finely tune the wounding technology and acquire high speed real time imaging during the short repairing time. Traditional methods to induce plasma membrane damage such as mechanical tear and toxins fail to keep the cell alive. Current technology, neither micropipette nor electroporation/sonoporation can facilitate a precise control for studying single cell damage.

> Two photon laser wounding technology combined with laser tweezer Raman spectroscopy (LTRS) has precise control of the membrane disruption size by tuning laser power and shutter time.

Scanning microscopy equipped with Ti:sapphire laser forms the two photon laser wounding technology. Wound size is tunable between 1-10μm. The follow-up repairing process will be monitored by multi-modality imaging described in the next paragraph.

In LTRS, Optical trapping confines single cell in small region, and Raman spectroscopy provides single cell analysis, acquiring label free finger print information.

> Laser scanning microscopy provides reflectance confocal (RCM) image and two photon fluorescence (TPF) image simultaneously at 15 frames per second.

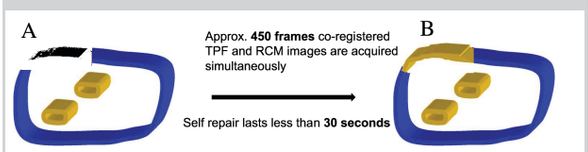

Figure 1 (A) Damaged cell plasma membrane (Blue) and protein generated in Endoplasmic reticulum (ER) (yellow) (B) repaired plasma membrane with patch (yellow), which is synthesized from these protein.

TECHNICAL CHALLENGES

Imaging speed — high enough to monitor membrane repair process in 30 seconds.
Resolution — determines the image quality and how accurate the laser would induce the localized wounds.
Imaging cell stability — laser tweezer technique stabilize the cell avoiding any movement.

METHODS

We can acquire LTRS spectroscopy, RCM imaging and TPF imaging. Wide-field white light imaging is integrated in the system to facilitate large field of view imaging of the sample.

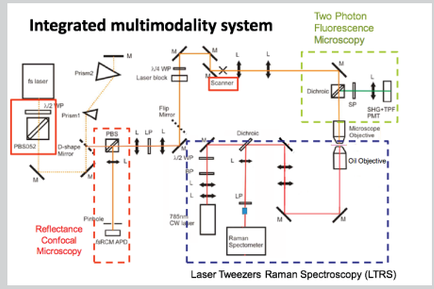

Figure 2 System diagram of LTRS, RCM and TPF imaging. WP: wave plate; PBS: polarization beam splitter; M: mirror; FM: flip mirror; APD: avalanche photodiode; L: lens; LP: long-pass filter; SP: short-pass filter; PMT: photon multiplier tube.

Example of single T lymphoma cell RCM image (A) and TPF image (B and C: membrane and nuclei). False colors were used for different imaging modalities to facilitate multimodality image overlay.

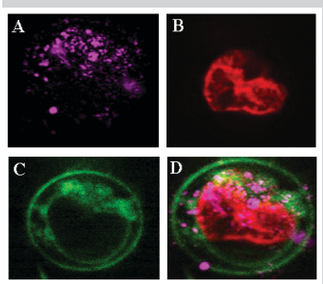

Figure 3 (A) RCM imaging; (B) TPF imaging of nucleotide distribution; (C) TPF imaging of cell membrane; (D) Overlay of RCM+TPF images from cell nucleotide and membrane.

EXPERIMENTAL PROCEDURE

1 Culture T lymphoma cell line

2 Membrane staining

3 Trap single cell with LTRS

4 Induce membrane injury with two photon laser wounding technique

5 Observe membrane repair process

RESULTS

We have successfully demonstrate T lymphoma cell plasma membrane damage (Figure 3) and repair process (Figure 4) in real time. In vivo Raman spectra is shown in Figure 5.

> Two photon laser wounding technique induce T cell membrane localized damage in short exposure time

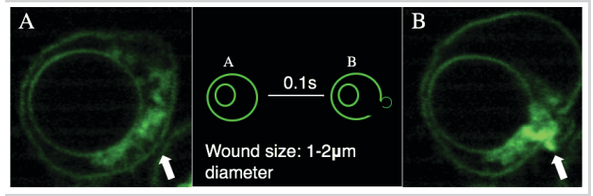

Figure 3 (A) TPF imaging of cell membrane before laser wounding. Endoplasmic reticulum (ER) is shown in between neuclei membrane and plasma membrane. (B) After laser wounding, cytoplasm leak through plasma membrane hole. At the edge of hole, bleb might be generated.

> T cell plasma membrane reseals in 21 seconds

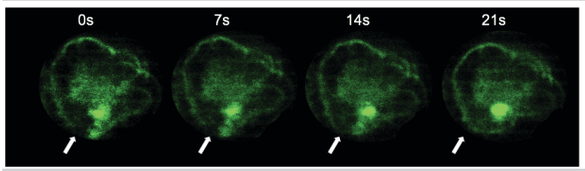

Figure 4 TPF imaging of plasma membrane resealing process. Extracted images from original video format shown as above at 0s, 7s, 14s, and 21s.

> Raman spectra provide molecular composition in vivo

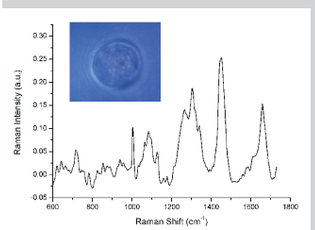

Figure 5 Raman spectra and (insert) white light image of T cell. Each peak correspond with unique molecular composition.

CONCLUSION

Multi-modality system combined two photon laser wounding technology with LTRS, RCM imaging and TPF imaging for repairing monitoring has been demonstrated.

Combined multi-modality system has potential to analyze cellular dynamics.

Declaration of conflict of interest: The authors declare no conflict of interest

Contact Giselle (Yunxian Tian) ytian@bccrc.ca for further inquiry

Real time imaging of live cell membrane using laser trapping, reflectance confocal microscopy, and multiphoton fluorescence microscopy

Yunxian Tian Shangyuan Feng Yimei Huang Jianhua Zhao Eddie Shen Wenbo Wang Caigan Dud Haishan Zenga

Imaging Unit-Integrative Oncology Department, British Columbia Cancer Research Centre
Photomedicine Institute – Department of Dermatology and Skin Science, University of British Columbia
Department of Biomedical Engineering, University of British Columbia dDepartment of Urologic Sciences, University of British Columbia

INTRODUCTION

Cell membrane would spontaneously reseal after injury. However this repair mechanism remains unknown. To study the repair process in detail, It is necessary to finely tune the wounding technology and acquire high speed real time imaging during the short repairing time. Traditional methods to induce plasma membrane damage such as mechanical tear and toxins fail to keep the cell alive. Current technology, neither micropipette nor electroporation/sonoporation can facilitate a precise control for studying single cell damage.

> Two photon laser wounding technology combined with laser tweezer Raman spectroscopy (LTRS) has precise control of the membrane disruption size by tuning laser power and shutter time.

Scanning microscopy equipped with Ti:sapphire laser forms the two photon laser wounding technology. Wound size is tunable between 1-10μm. The follow-up repairing process will be monitored by multi-modality imaging described in the next paragraph.

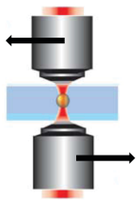

In LTRS, Optical trapping confines single cell in small region, and Raman spectroscopy provides single cell analysis, acquiring label free finger print information.

> Laser scanning microscopy provides reflectance confocal (RCM) image and two photon fluorescence (TPF) image simultaneously at 15 frames per second.

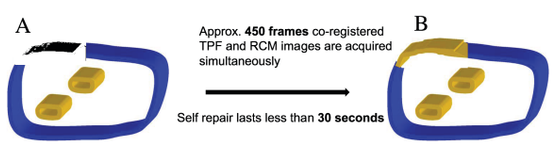

Figure 1 (A) Damaged cell plasma membrane (Blue) and protein generated in Endoplasmic reticulum (ER) (yellow) (B) repaired plasma membrane with patch (yellow), which is synthesized from these protein.

TECHNICAL CHALLENGES

Imaging speed — high enough to monitor membrane repair process in 30 seconds.
Resolution — determines the image quality and how accurate the laser would induce the localized wounds.
Imaging cell stability — laser tweezer technique stabilize the cell avoiding any movement.

METHODS

We can acquire LTRS spectroscopy, RCM imaging and TPF imaging. Wide-field white light imaging is integrated in the system to facilitate large field of view imaging of the sample.

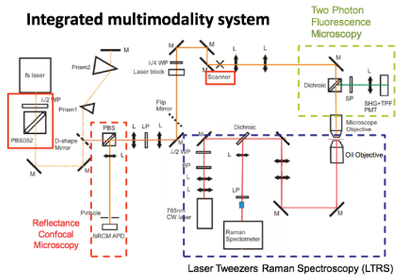

Figure 2 System diagram of LTRS, RCM and TPF imaging. WP: wave plate; PBS: polarization beam splitter; M: mirror; FM: flip mirror; APD: avalanche photodiode; L: lens; LP: long-pass filter; SP: short-pass filter; PMT: photon multiplier tube.

Example of single T lymphoma cell RCM image (A) and TPF image (B and C: membrane and nuclei). False colors were used for different imaging modalities to facilitate multimodality image overlay.

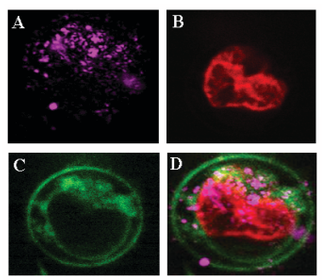

Figure 3 (A) RCM imaging; (B) TPF imaging of nucleotide distribution; (C) TPF imaging of cell membrane; (D) Overlay of RCM+TPF images from cell nucleotide and membrane.

EXPERIMENTAL PROCEDURE

1 Culture T lymphoma cell line

2 Membrane staining

3 Trap single cell with LTRS

4 Induce membrane injury with two photon laser wounding technique

5 Observe membrane repair process

RESULTS

We have successfully demonstrate T lymphoma cell plasma membrane damage (Figure 3) and repair process (Figure 4) in real time. In vivo Raman spectra is shown in Figure 5.

> Two photon laser wounding technique induce T cell membrane localized damage in short exposure time

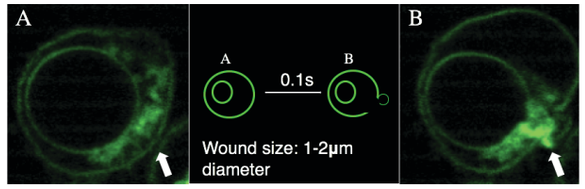

Figure 3 (A) TPF imaging of cell membrane before laser wounding. Endoplasmic reticulum (ER) is shown in between neuclei membrane and plasma membrane. (B) After laser wounding, cytoplasm leak through plasma membrane hole. At the edge of hole, bleb might be generated.

> T cell plasma membrane reseals in 21 seconds

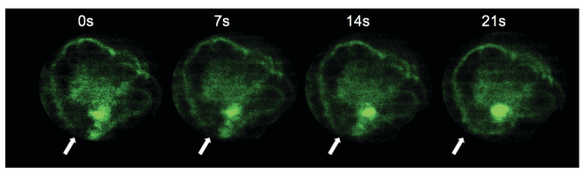

Figure 4 TPF imaging of plasma membrane resealing process. Extracted images from original video format shown as above at 0s, 7s, 14s, and 21s.

> Raman spectra provide molecular composition in vivo

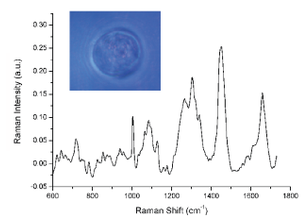

Figure 5 Raman spectra and (insert) white light image of T cell. Each peak correspond with unique molecular composition.

CONCLUSION

Multi-modality system combined two photon laser wounding technology with LTRS, RCM imaging and TPF imaging for repairing monitoring has been demonstrated.

Combined multi-modality system has potential to analyze cellular dynamics.

Declaration of conflict of interest: The authors declare no conflict of interest

Contact Giselle (Yunxian Tian) ytian@bccrc.ca for further inquiry

Real time imaging of live cell membrane using laser trapping, reflectance confocal microscopy, and multiphoton fluorescence microscopy

Yunxian Tian Shangyuan Feng Yimei Huang Jianhua Zhao Eddie Shen Wenbo Wang Caigan Dud Haishan Zenga

Imaging Unit-Integrative Oncology Department, British Columbia Cancer Research Centre
Photomedicine Institute – Department of Dermatology and Skin Science, University of British Columbia
Department of Biomedical Engineering, University of British Columbia dDepartment of Urologic Sciences, University of British Columbia

INTRODUCTION

Cell membrane would spontaneously reseal after injury. However this repair mechanism remains unknown. To study the repair process in detail, It is necessary to finely tune the wounding technology and acquire high speed real time imaging during the short repairing time. Traditional methods to induce plasma membrane damage such as mechanical tear and toxins fail to keep the cell alive. Current technology, neither micropipette nor electroporation/sonoporation can facilitate a precise control for studying single cell damage.

▼ *Two photon laser wounding technology combined with laser tweezer Raman spectroscopy (LTRS) has precise control of the membrane disruption size by tuning laser power and shutter time.*

Scanning microscopy equipped with Ti:sapphire laser forms the two photon laser wounding technology. Wound size is tunable between 1-10μm. The follow-up repairing process will be monitored by multi-modality imaging described in the next paragraph.

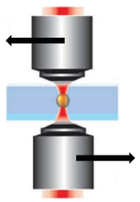

In LTRS, Optical trapping confines single cell in small region, and Raman spectroscopy provides single cell analysis, acquiring label free finger print information.

▼ *Laser scanning microscopy provides reflectance confocal (RCM) image and two photon fluorescence (TPF) image simultaneously at 15 frames per second.*

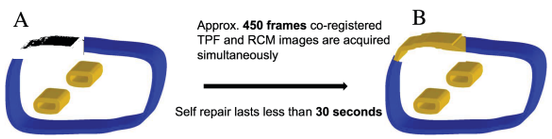

Figure 1 (A) Damaged cell plasma membrane (Blue) and protein generated in Endoplasmic reticulum (ER) (yellow) (B) repaired plasma membrane with patch (yellow), which is synthesized from these protein.

TECHNICAL CHALLENGES

Imaging speed — high enough to monitor membrane repair process in 30 seconds.
Resolution — determines the image quality and how accurate the laser would induce the localized wounds.
Imaging cell stability — laser tweezer technique stabilize the cell avoiding any movement.

METHODS

We can acquire LTRS spectroscopy, RCM imaging and TPF imaging. Wide-field white light imaging is integrated in the system to facilitate large field of view imaging of the sample.

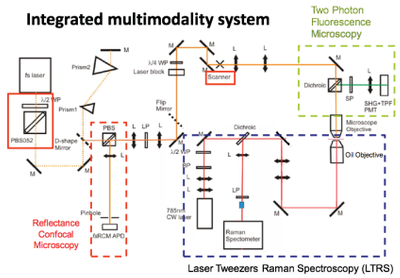

Figure 2 System diagram of LTRS, RCM and TPF imaging. WP: wave plate; PBS: polarization beam splitter; M: mirror; FM: flip mirror; APD: avalanche photodiode; L: lens; LP: long-pass filter; SP: short-pass filter; PMT: photon multiplier tube.

Example of single T lymphoma cell RCM image (A) and TPF image (B and C: membrane and nuclei). False colors were used for different imaging modalities to facilitate multimodality image overlay.

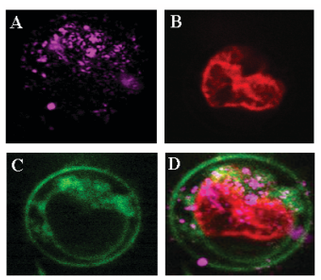

Figure 3 (A) RCM imaging; (B) TPF imaging of nucleotide distribution; (C) TPF imaging of cell membrane; (D) Overlay of RCM+TPF images from cell nucleotide and membrane.

EXPERIMENTAL PROCEDURE

1 Culture T lymphoma cell line

2 Membrane staining

3 Trap single cell with LTRS

4 Induce membrane injury with two photon laser wounding technique

5 Observe membrane repair process

RESULTS

We have successfully demonstrate T lymphoma cell plasma membrane damage (Figure 3) and repair process (Figure 4) in real time. In vivo Raman spectra is shown in Figure 5.

▼ *Two photon laser wounding technique induce T cell membrane localized damage in short exposure time*

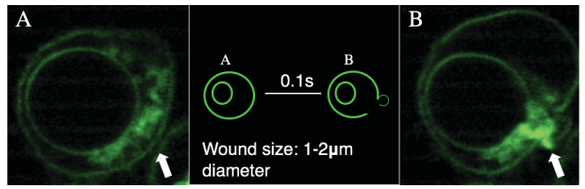

Figure 3 (A) TPF imaging of cell membrane before laser wounding. Endoplasmic reticulum (ER) is shown in between neuclei membrane and plasma membrane. (B) After laser wounding, cytoplasm leak through plasma membrane hole. At the edge of hole, bleb might be generated.

▼ *T cell plasma membrane reseals in 21 seconds*

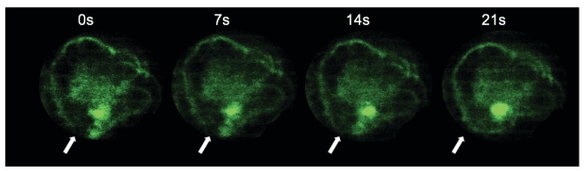

Figure 4 TPF imaging of plasma membrane resealing process. Extracted images from original video format shown as above at 0s, 7s, 14s, and 21s.

▼ *Raman spectra provide molecular composition in vivo*

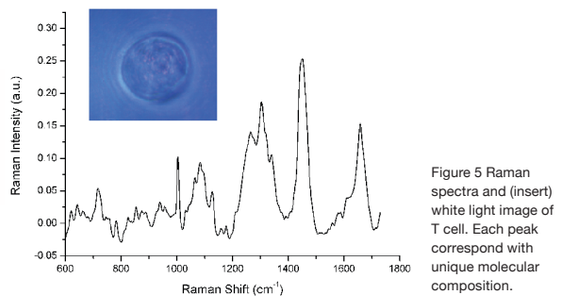

Figure 5 Raman spectra and (insert) white light image of T cell. Each peak correspond with unique molecular composition.

CONCLUSION

Multi-modality system combined two photon laser wounding technology with LTRS, RCM imaging and TPF imaging for repairing monitoring has been demonstrated.

Combined multi-modality system has potential to analyze cellular dynamics.

Declaration of conflict of interest: The authors declare no conflict of interest

Contact Giselle (Yunxian Tian) ytian@bccrc.ca for further inquiry

Real time imaging of live cell membrane using laser trapping, reflectance confocal microscopy, and multiphoton fluorescence microscopy

Yunxian Tian Shangyuan Feng Yimei Huang Jianhua Zhao Eddie Shen Wenbo Wang Caigan Dud Haishan Zenga

Imaging Unit-Integrative Oncology Department, British Columbia Cancer Research Centre
Photomedicine Institute – Department of Dermatology and Skin Science, University of British Columbia
Department of Biomedical Engineering, University of British Columbia dDepartment of Urologic Sciences, University of British Columbia

INTRODUCTION

Cell membrane would spontaneously reseal after injury. However this repair mechanism remains unknown. To study the repair process in detail, It is necessary to finely tune the wounding technology and acquire high speed real time imaging during the short repairing time. Traditional methods to induce plasma membrane damage such as mechanical tear and toxins fail to keep the cell alive. Current technology, neither micropipette nor electroporation/sonoporation can facilitate a precise control for studying single cell damage.

▼ Two photon laser wounding technology combined with laser tweezer Raman spectroscopy (LTRS) has precise control of the membrane disruption size by tuning laser power and shutter time.

Scanning microscopy equipped with Ti:sapphire laser forms the two photon laser wounding technology. Wound size is tunable between 1-10μm. The follow-up repairing process will be monitored by multi-modality imaging described in the next paragraph.

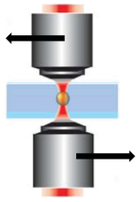

In LTRS, Optical trapping confines single cell in small region, and Raman spectroscopy provides single cell analysis, acquiring label free finger print information.

▼ Laser scanning microscopy provides reflectance confocal (RCM) image and two photon fluorescence (TPF) image simultaneously at 15 frames per second.

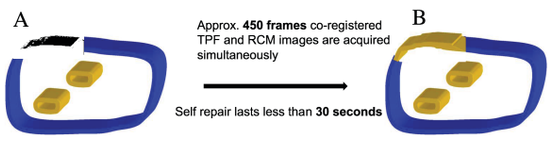

Figure 1 (A) Damaged cell plasma membrane (Blue) and protein generated in Endoplasmic reticulum (ER) (yellow) (B) repaired plasma membrane with patch (yellow), which is synthesized from these protein.

TECHNICAL CHALLENGES

Imaging speed — high enough to monitor membrane repair process in 30 seconds.
Resolution — determines the image quality and how accurate the laser would induce the localized wounds.
Imaging cell stability — laser tweezer technique stabilize the cell avoiding any movement.

METHODS

We can acquire LTRS spectroscopy, RCM imaging and TPF imaging. Wide-field white light imaging is integrated in the system to facilitate large field of view imaging of the sample.

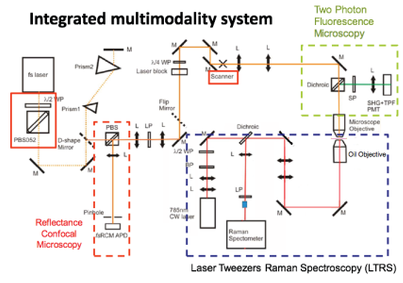

Figure 2 System diagram of LTRS, RCM and TPF imaging. WP: wave plate; PBS: polarization beam splitter; M: mirror; FM: flip mirror; APD: avalanche photodiode; L: lens; LP: long-pass filter; SP: short-pass filter; PMT: photon multiplier tube.

Example of single T lymphoma cell RCM image (A) and TPF image (B and C: membrane and nuclei). False colors were used for different imaging modalities to facilitate multimodality image overlay.

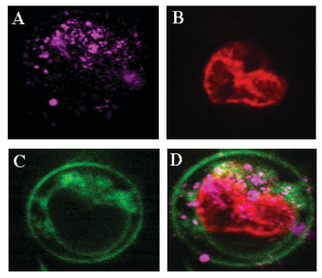

Figure 3 (A) RCM imaging; (B) TPF imaging of nucleotide distribution; (C) TPF imaging of cell membrane; (D) Overlay of RCM+TPF images from cell nucleotide and membrane.

EXPERIMENTAL PROCEDURE

1 Culture T lymphoma cell line

2 Membrane staining

3 Trap single cell with LTRS

4 Induce membrane injury with two photon laser wounding technique

5 Observe membrane repair process

RESULTS

We have successfully demonstrate T lymphoma cell plasma membrane damage (Figure 3) and repair process (Figure 4) in real time. In vivo Raman spectra is shown in Figure 5.

▼ Two photon laser wounding technique induce T cell membrane localized damage in short exposure time

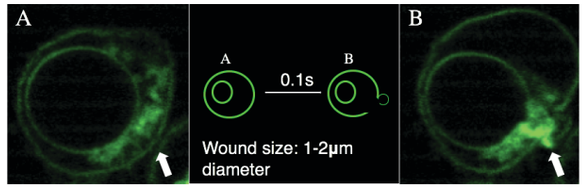

Figure 3 (A) TPF imaging of cell membrane before laser wounding. Endoplasmic reticulum (ER) is shown in between neuclei membrane and plasma membrane. (B) After laser wounding, cytoplasm leak through plasma membrane hole. At the edge of hole, bleb might be generated.

▼ T cell plasma membrane reseals in 21 seconds

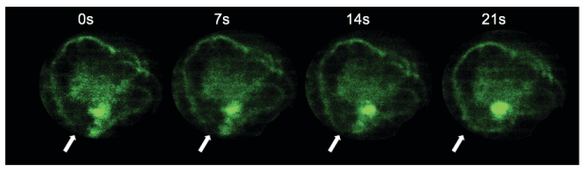

Figure 4 TPF imaging of plasma membrane resealing process. Extracted images from original video format shown as above at 0s, 7s, 14s, and 21s.

▼ Raman spectra provide molecular composition in vivo

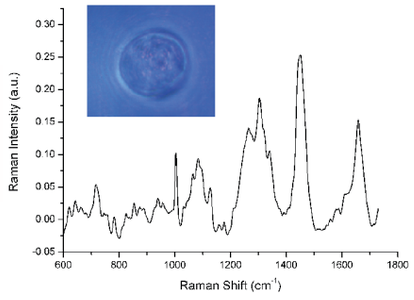

Figure 5 Raman spectra and (insert) white light image of T cell. Each peak correspond with unique molecular composition.

CONCLUSION

Multi-modality system combined two photon laser wounding technology with LTRS, RCM imaging and TPF imaging for repairing monitoring has been demonstrated.

Combined multi-modality system has potential to analyze cellular dynamics.

Declaration of conflict of interest: The authors declare no conflict of interest

Contact Giselle (Yunxian Tian) ytian@bccrc.ca for further inquiry

Bernd Merkel, Royal Melb. Hospital, Department of Radiology:

AIBL Active - Physical Activity and Alzheimer‘s Disease

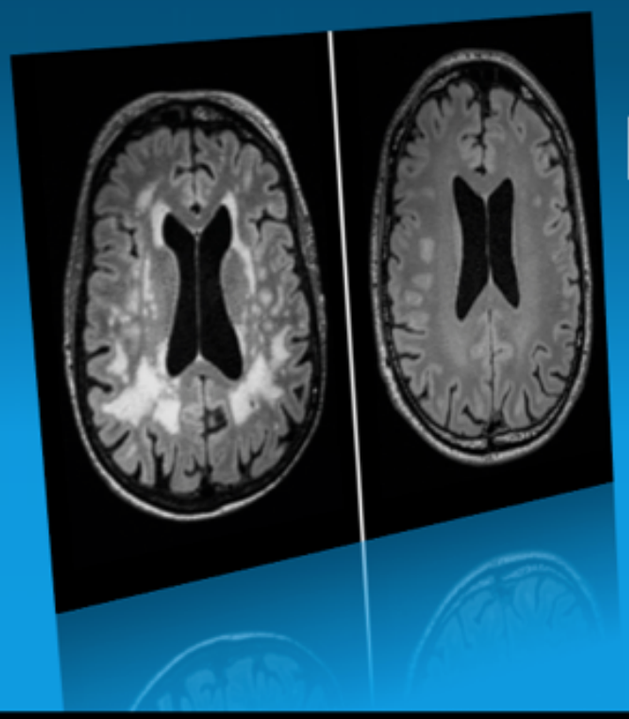

Postgraduate Masterclass

VLSCI
Fri, 10-Oct-2014

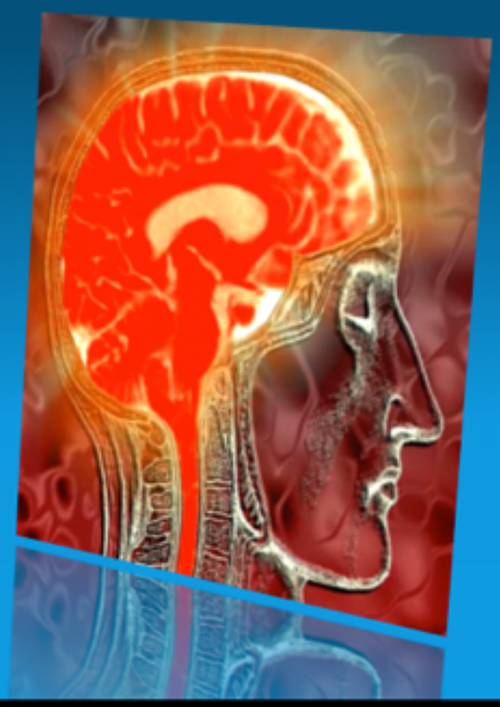

AIBL Active-Physical Activity & Alzheimer's Disease

Bernd Merkel
Department of Radiology
Royal Melbourne Hospital

postgraduate masterclass
VLSCI 10.10.2014

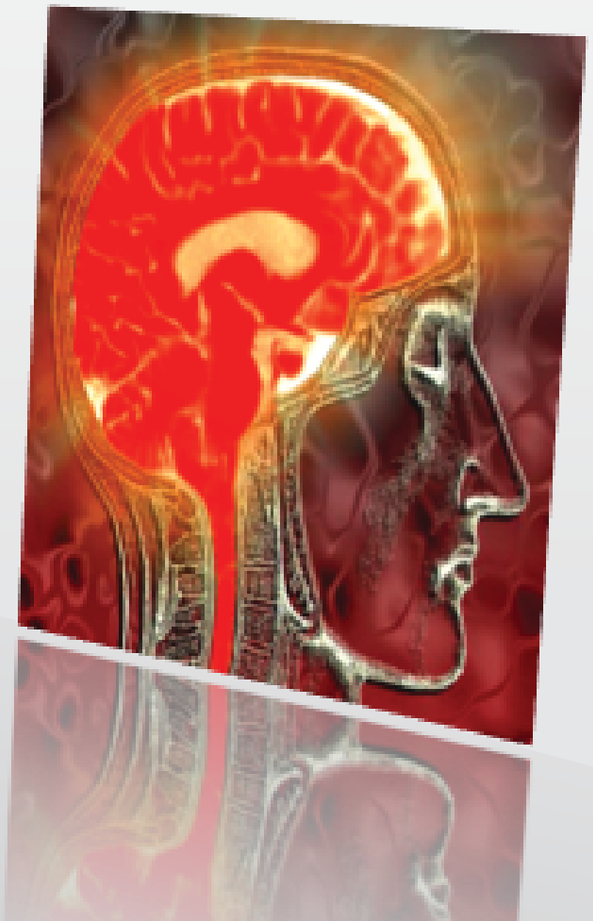

Click to add title

Population growth & urbanization

Challenge 1: water pollution

Challenge 2: water sanitation

Phylogenomics of Land snails

Luisa Teasdale

Museum Victoria and

The University of Melbourne

phylogenomics of land snails

VISUALIZATION GUIDELINES

What are the major questions that the figure should help the reader answer?

What are you trying to communicate? Does the figure communicate it clearly?

Is it clear to the reader where they should look?

Have you selected the simplest visual representation sufficient for your purpose?

Are there extraneous or ornamental elements? What can you safely remove?

practical sessions

SESSION 6—LEISHMANIA GENE EXPRESSION

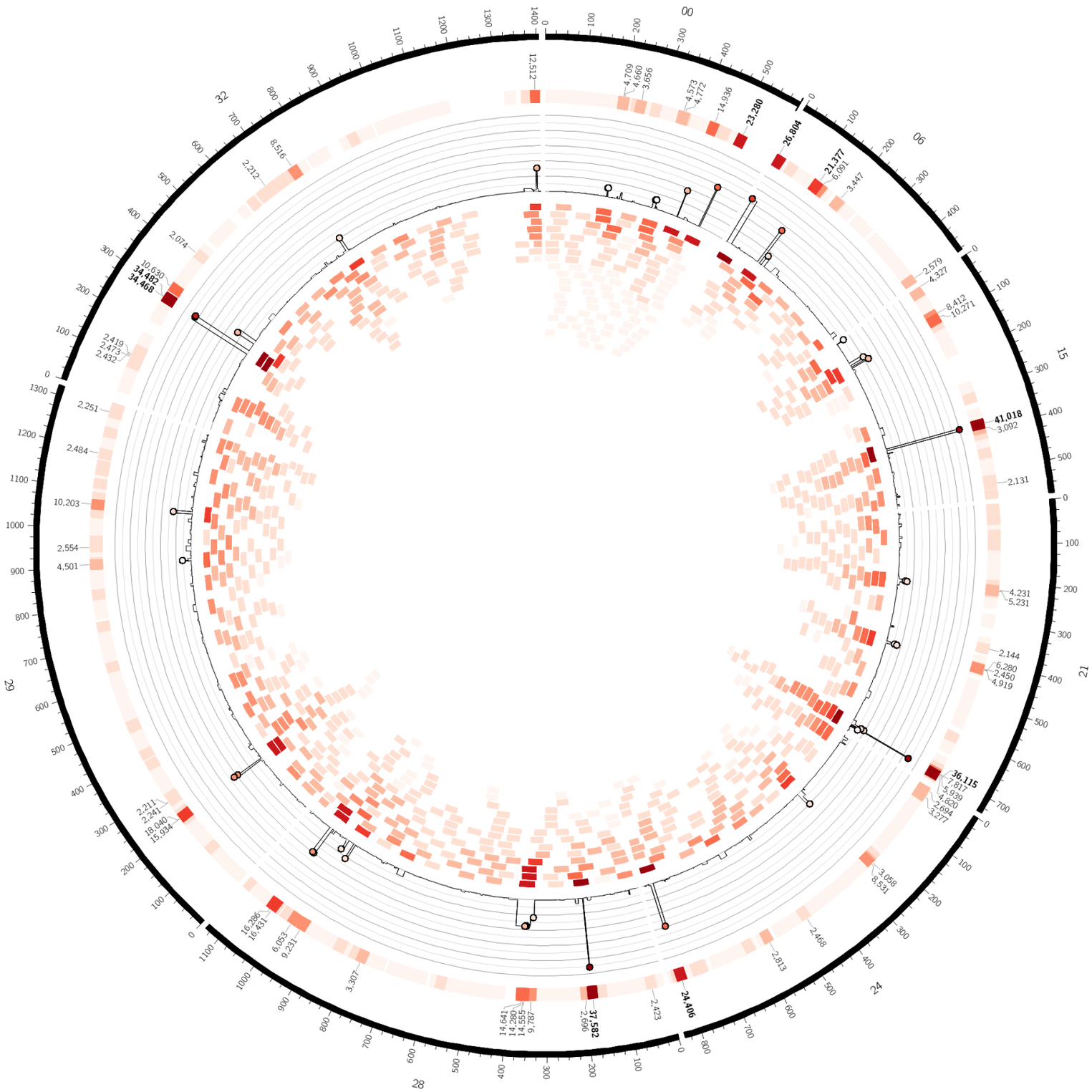

.

SESSION 7 — LEISHMANIA ORTHOLOGUES

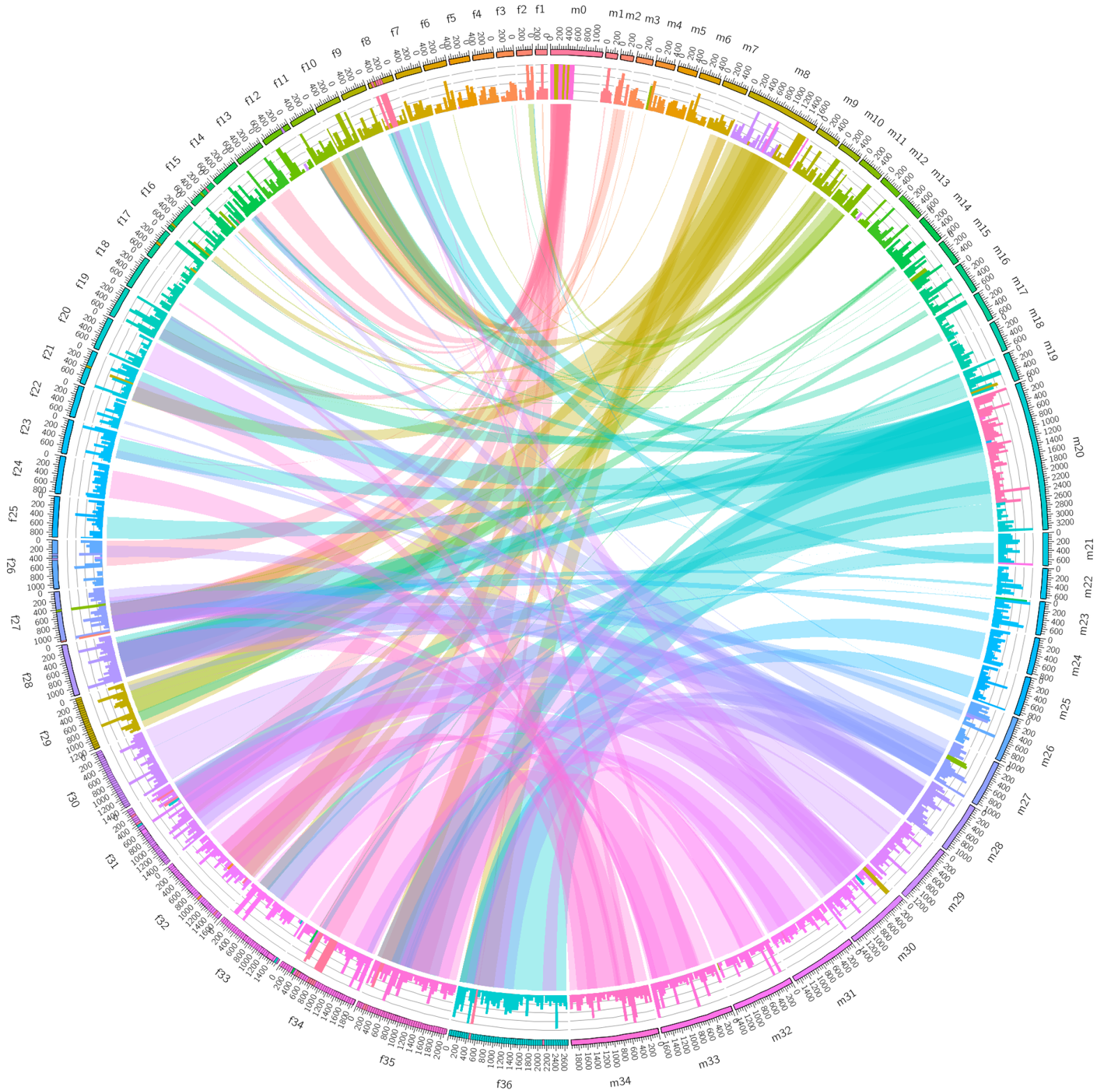

.

SESSION 4—YEAST GENOME COMPARISON

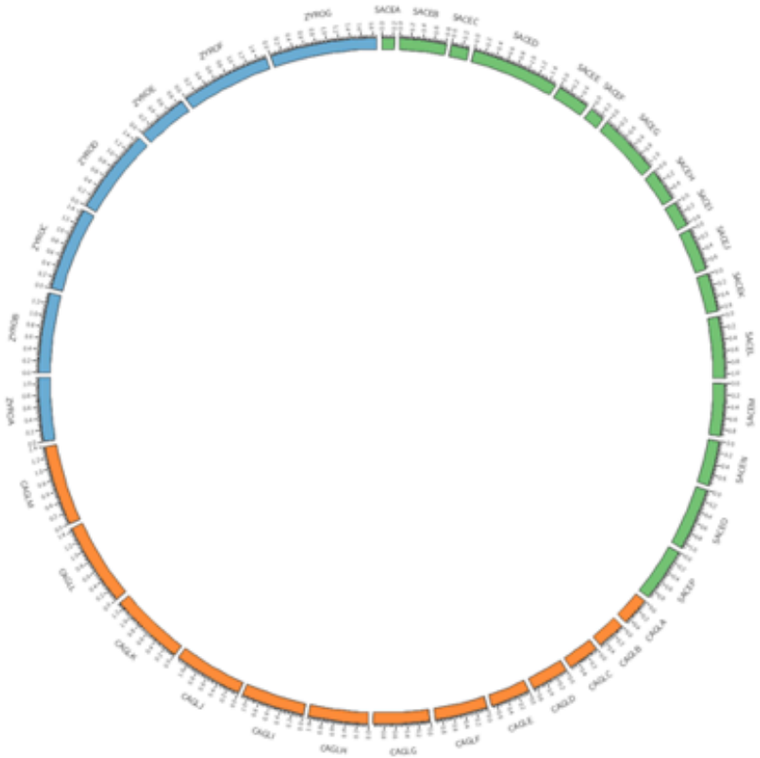

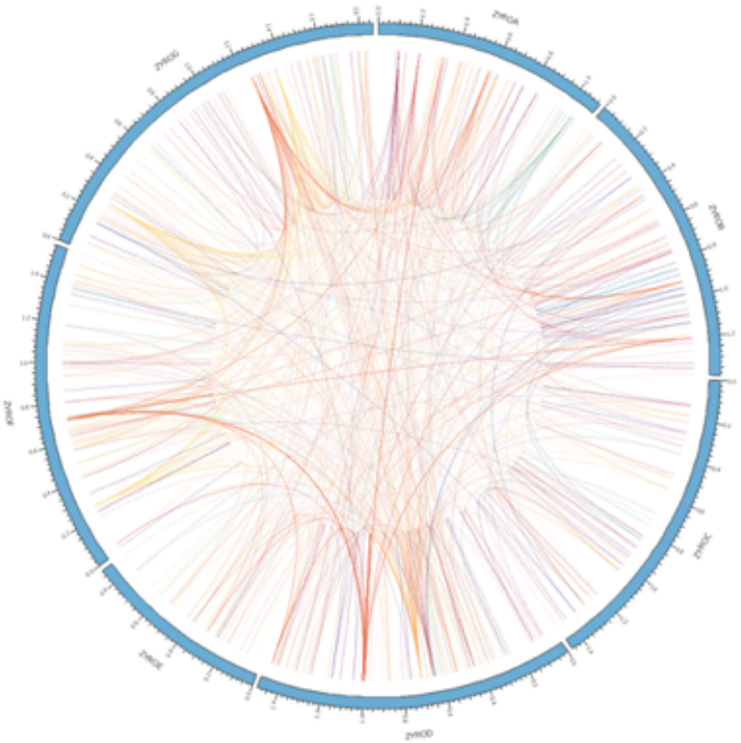

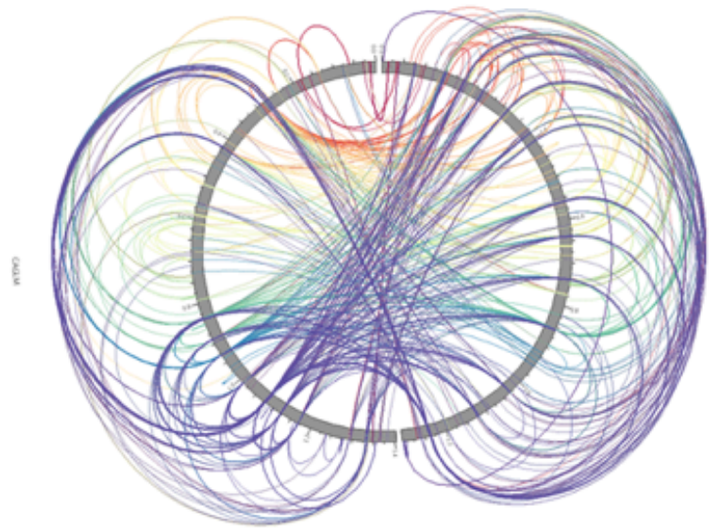

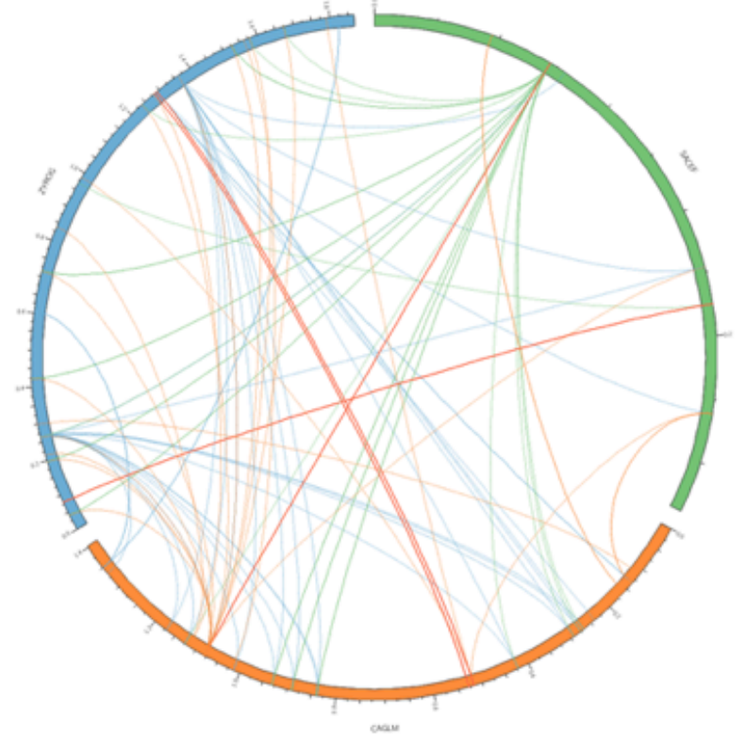

.

SESSION 1—IDEOGRAM LAYOUT AND FORMATTING

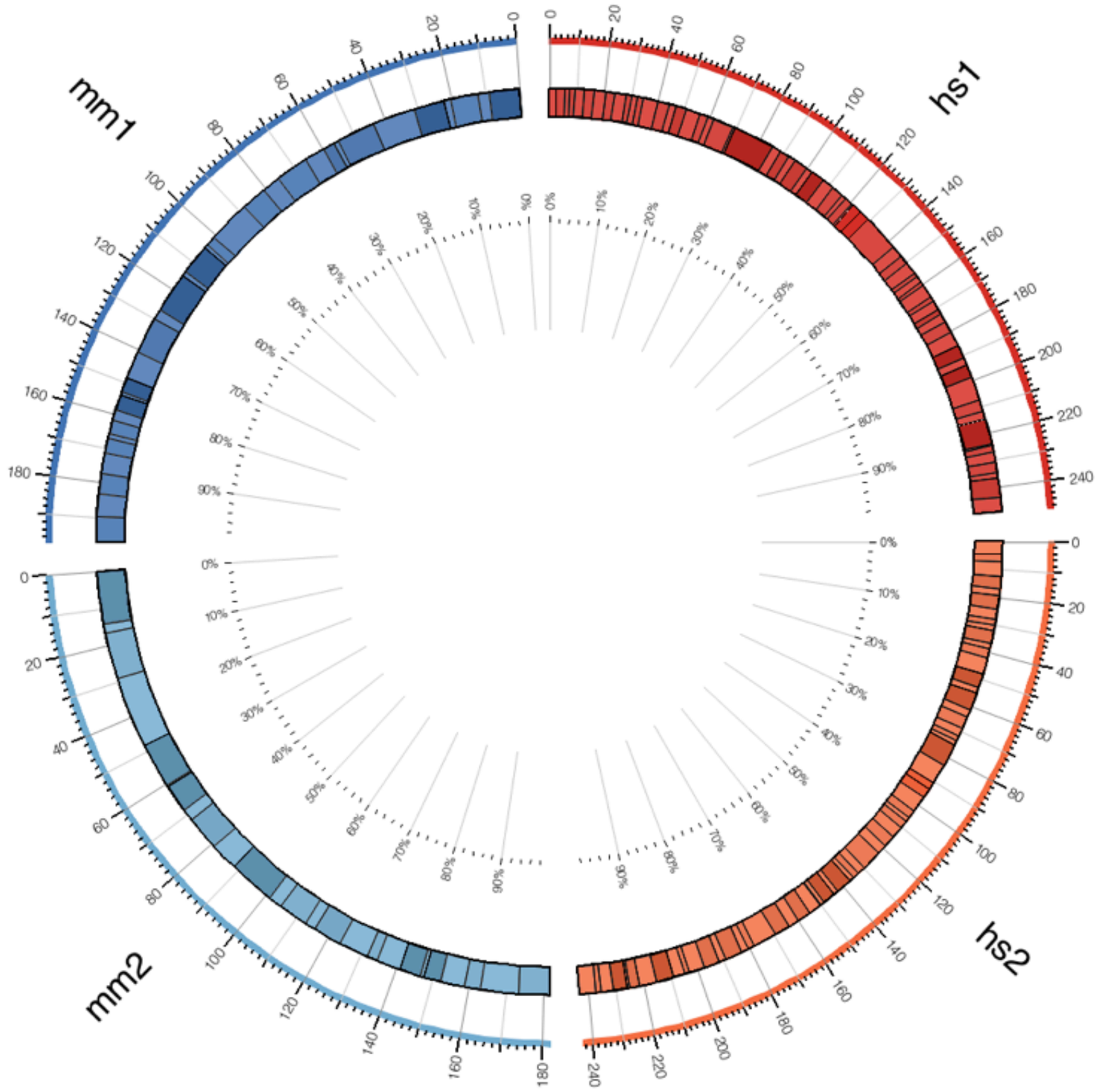

.

SESSION 2—DATA TRACKS

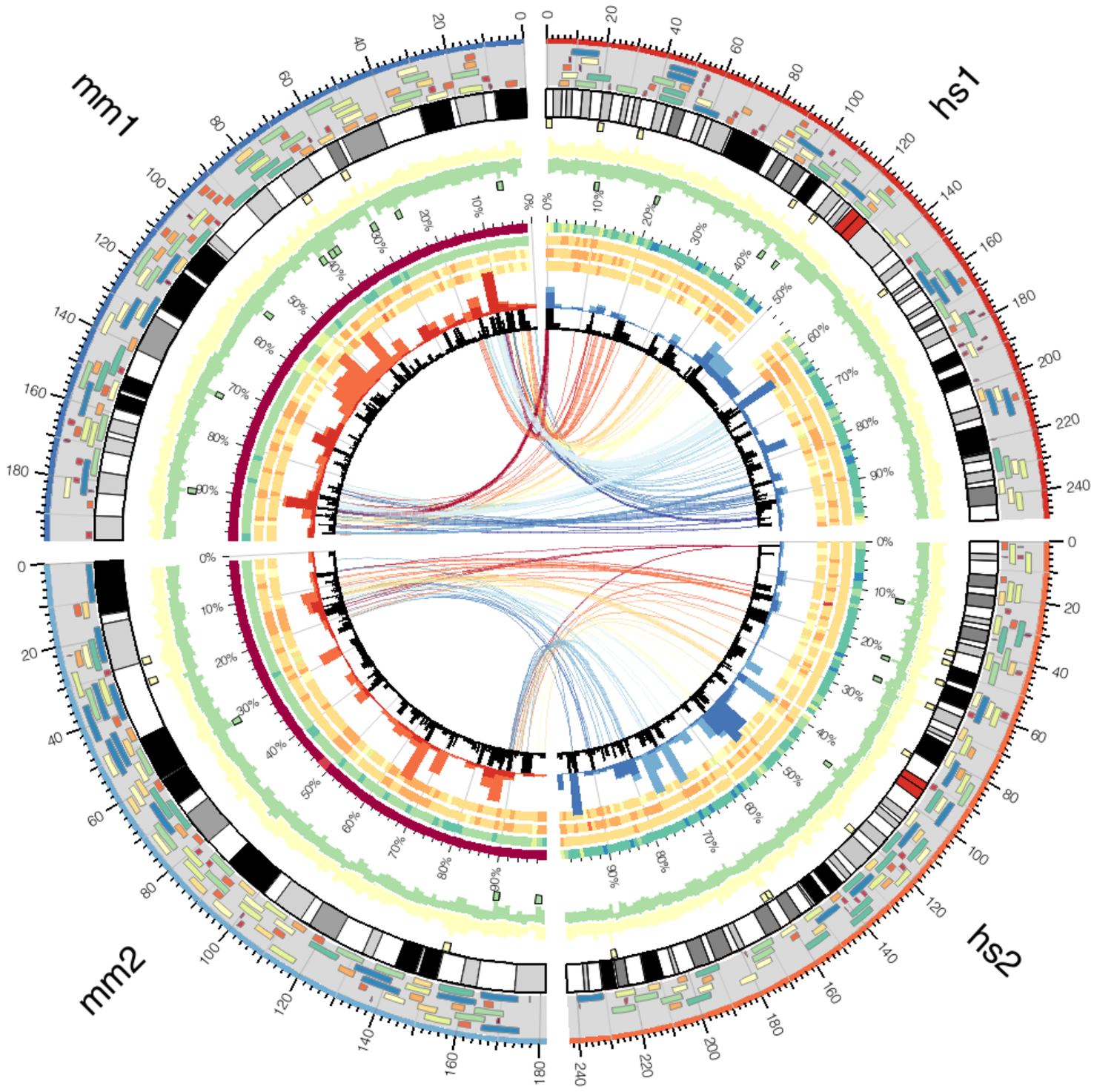

.

SESSION 3—BUNDLES AND AUTOMATION

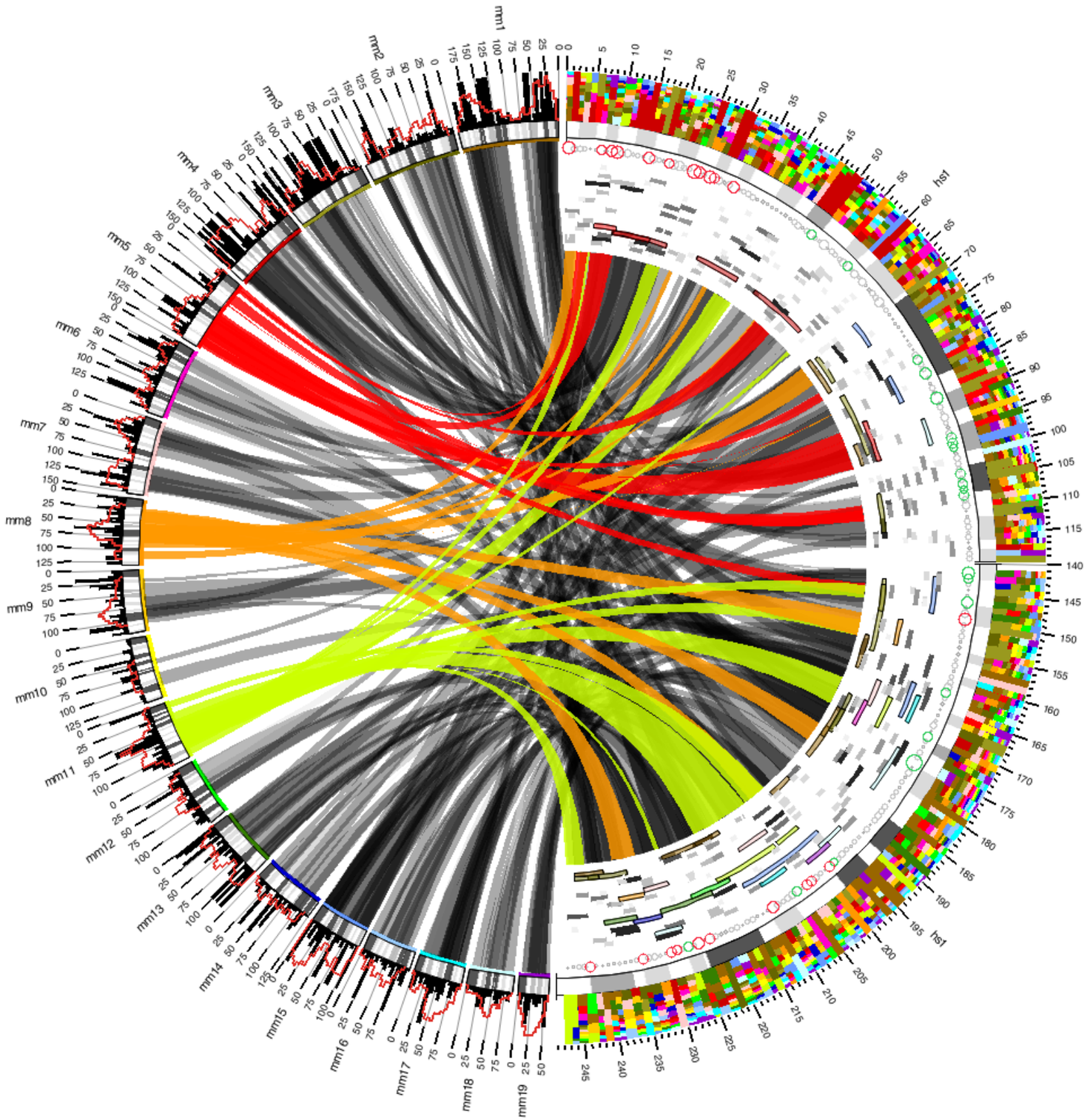

.

SESSION 5—CIRCOS CHALLENGE

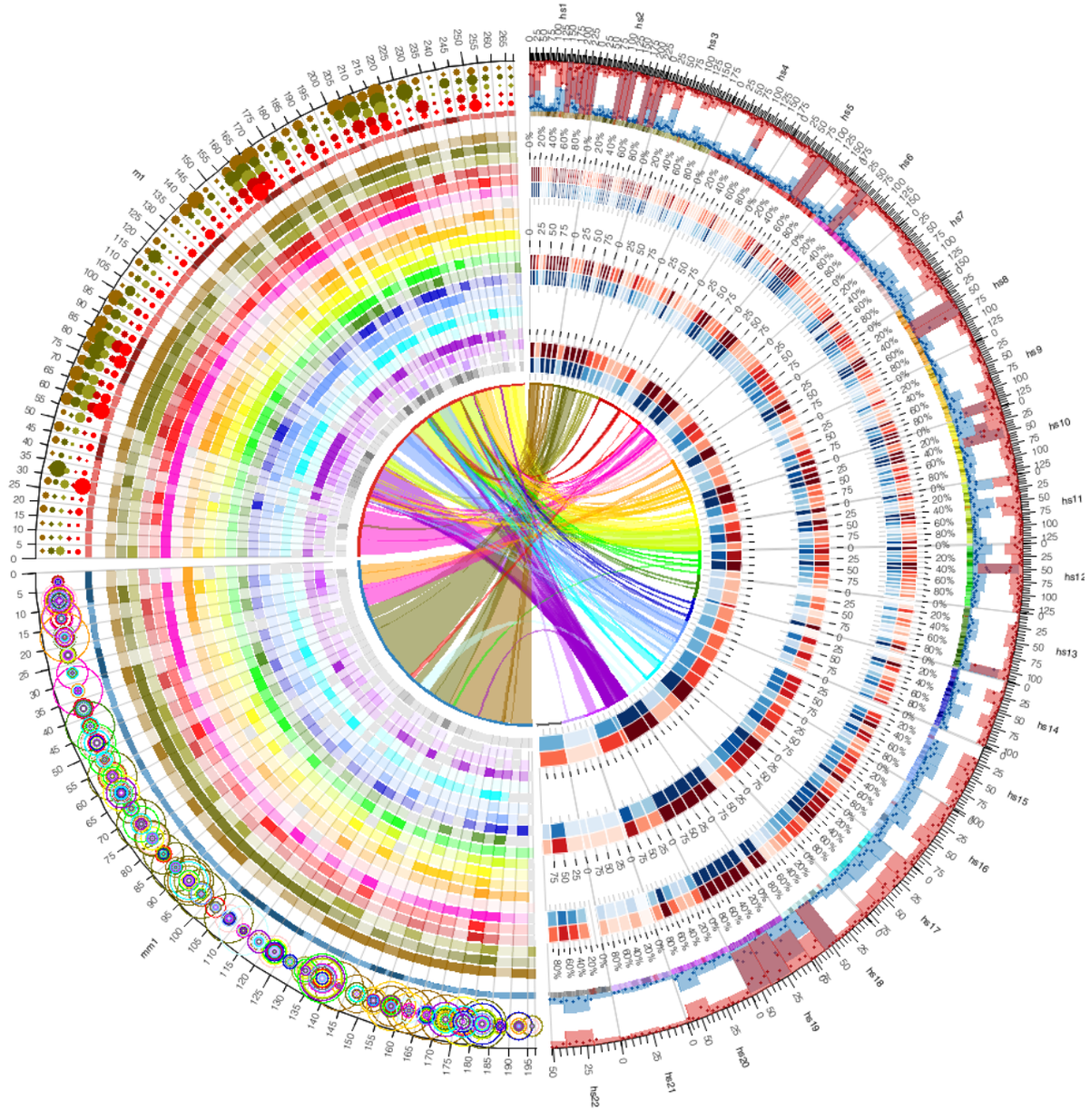

.

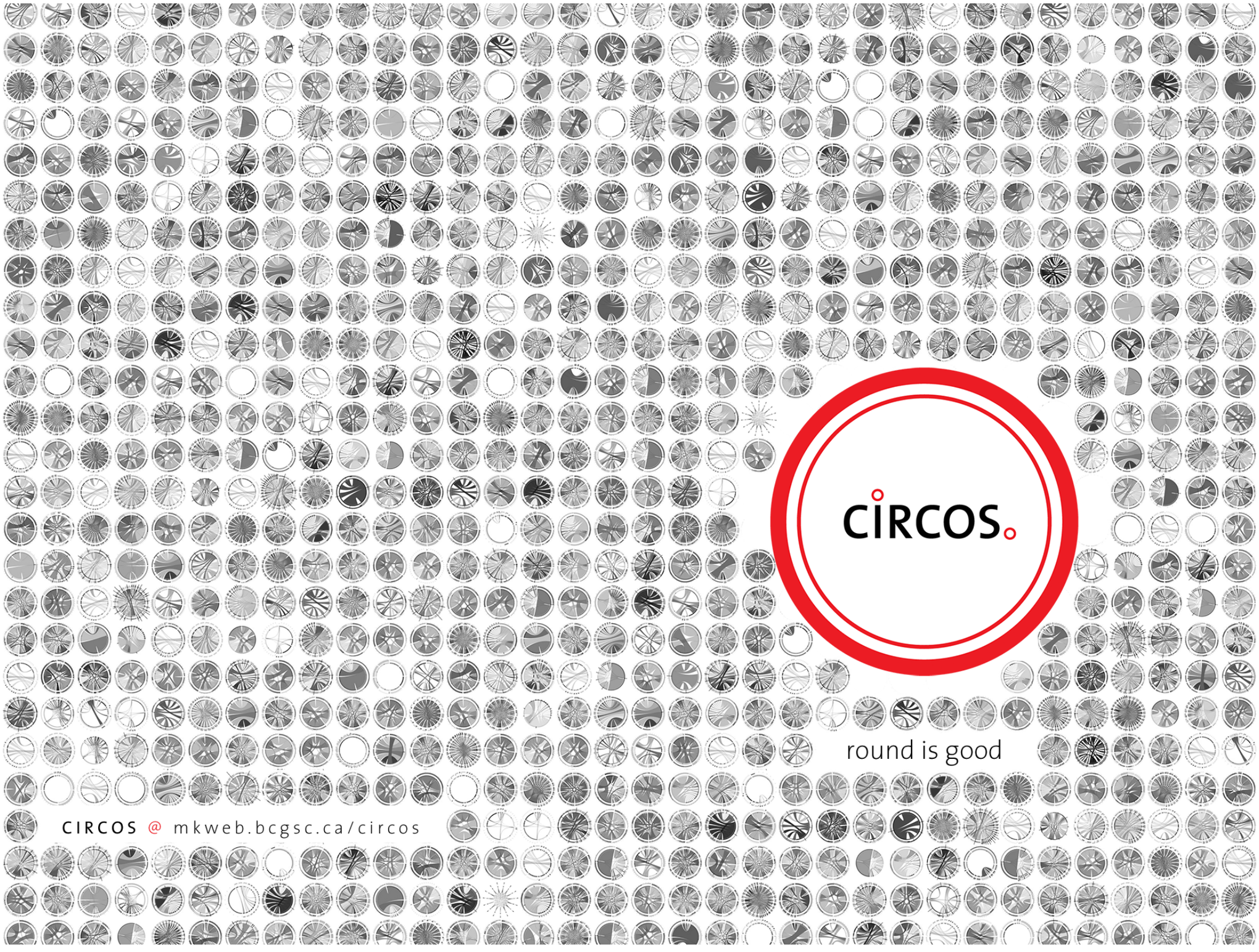
CIRCOS.
round is good
CIRCOS @ mkweb.bcgsc.ca/circos

Gordon Andrews (designer)
Gazelle chair (c. 1950) designed, 1957 manufactured
plywood, aluminium, wool
74.0 x 48.0 x 55.0 cm
Museum of Applied Arts and Sciences, Sydney
Purchased, 1989 (89/499)